Blockchain Based Secure Message Dissemination in Vehicular Networks

Ferheen Ayaz

Submitted for the degree of Doctor of Philosophy

University of Sussex

April 2022

Declaration

I hereby declare that this thesis has not been and will not be submitted in whole or in part to another University for the award of any other degree.

Signature:

Ferheen Ayaz

Abstract

Vehicular ad-hoc networks (VANETs) are one of the key elements in Intelligent Transportation System (ITS) to enable information exchange among vehicles and Roadside Units (RSUs) via vehicle-to-vehicle (V2V) and vehicle-to-infrastructure (V2I) communications. With continuously increasing number of vehicles on road, there are numerous security and privacy challenges associated with VANETs. Communication among vehicles is needed to be secure and bandwidth efficient. Also, the messages exchanged between vehicles must be authentic so as to maintain a trusted network in a privacy-preserving manner. Furthermore, a sustainable economic model is required to incentivise honest and cooperative vehicles. Traditional security and privacy solutions in centralised networks are not applicable to VANETs due to its distributed nature, heterogeneity, high mobility and low latency requirements. Meanwhile, the new development of blockchain has been attracting significant interests due to its key features including consensus to evaluate message credibility and immutable storage in distributed ledger, which provides an alternative solution to the security and privacy challenges in VANETs.

This thesis aims to present blockchain solutions for the security and privacy of VANETs meeting the stringent requirements of low latency and bandwidth-efficient message dissemination. VANETs are simulated in OMNeT++ to validate the proposed solutions. Specifically, two novel blockchain consensus algorithms have been developed for message authentication and relay selection in presence of malicious vehicles. The first employs a voting based message validation and relay selection, which reduces the failure rate in message validation by 11% as compared to reputation based consensus. The second utilises federated learning supported by blockchain as a better privacy-preserving solution, which is 65.2% faster than the first voting based solution. Both approaches include blockchain-based incentive mechanisms and game theory analysis to observe strategic behaviour of honest and malicious vehicles. To further study the privacy aspect of vehicular networks, the integration of blockchain with physical layer security is also theoretically analysed in Vehicle-to-Everything (V2X) communications scenarios. The integration results in 8.2 Mbps increased goodput as compared to the blockchain solution alone.

In essence, our research work shows that blockchain can offer better control and security, as compared to centralised solutions, if properly adjusted according to the application and network requirements. Thus, the proposed solutions can provide guidelines for practically feasible application of blockchain in vehicular networks.

Acknowledgments

First and foremost, I would like to express my gratitude to my supervisor Dr. Zhengguo Sheng, for actually teaching me how to carry out a research project and his painstaking attention to detail throughout my PhD. The research would not have been possible without his constructive advice and thorough guidance. I would also like to thank my second supervisor, Prof. Maziar Nekovee for his kind support and encouragement to present my research on multiple occasions.

I greatly acknowledge the appreciation I received during my industrial placement at Kinseed, which has given me motivation to excel in future. Thanks to IEEE for funding the industrial placement and providing various opportunities of networking with research community.

I cannot forget the unwavering support of my family over the past four years, right from finding a PhD position until the end of the journey. Thank you, mom and dad, for making me who I am today. Special thanks go to my husband Raheel Jamil for always being on my side during good and bad times. I am also grateful to my brother Saqib Ayaz, for not only his constant care and support but also for facilitating me multiple times during technical difficulties and simulations. Thanks to Hina, Sineen and Yousuf for always making me smile.

Contents

List of Acronyms

5G	Fifth-generation
A2A	Air-to-Air
A2G	Air-to-Ground
AI	Artificial Intelligence
AV	Autonomous Vehicle
AWGN	Additive White Gaussian Noise
C-V2X	Cellular Vehicle-to-Everything
CA	Central Authority
CDF	Cumulative Distribution Function
DAG	Direct Acyclic Graph
DCF	Distributed Coordination Function
DIFS	DCF Interframe Space
DR	Data rate
DSRC	Dedicated Short Range Communications
FD-NOMA	Full Duplex Non-Orthogonal Multiple Access
FL	Federated Learning
FV	Failure in Validation
GPS	Global Positioning System
IoT	Internet-of-Things
IoV	Internet-of-Vehicles
ITS	Intelligent Transportation System
LB	Lower Bound
MAC	Medium Access Control
MANET	Mobile Ad-hoc Network
MSE	Mean Squared Error
NOMA	Non-Orthogonal Multiple Access
OBU	On-Board Unit
P2P	Peer-to-peer
PBFT	Practical Byzantine Fault Tolerant Algorithm

PDF	Probability Density Function
PLS	Physical Layer Security
PoET	Proof-of-Elapsed-Time
PoFL	Proof-of-Federated-Learning
PoQF	Proof-of-Quality-Factor
PoS	Proof-of-Stake
PoW	Proof-of-Work
QoS	Quality of Service
RSU	Road Side Unit
SIC	Successive Interference Cancellation
SIFS	Short Interframe Space
SINR	Signal to Interference and Noise Ratio
SUMO	Simulation of Urban Mobility
UAV	Unmanned Aerial Vehicle
UB	Upper Bound
V2I	Vehicle-to-Infrastructure
V2N	Vehicle-to-Network
V2P	Vehicle-to-Pedestrian
V2V	Vehicle-to-Vehicle
V2X	Vehicle-to-Everything
VANET	Vehicular Ad-hoc Network
VeINS	Vehicles In Network Simulation
WAVE	Wireless Access in Vehicular Environment

List of Notations

Distances and speed

$d_{i,j}$	Distance between node i and node j
$dir_{i,s}$	Direction of node i with respect to sender s
d_{neigh}^{min}	Minimum distance between neighbour nodes
d_{hop}^{min}	Minimum hop distance
DF_i	Distance Factor of node i
R	Transmission range
λ_V	Node/vehicle density (nodes/m^2)
v_i	Speed of node i
σ_i^2	Variance of v_i

Numbers and means

n_{hop}	Hop number
n_{th}	Threshold number of votes
n_{tr}	Number of simultaneous transmissions
n_{itf}	Number of interference nodes
n_{neigh}	Number of neighbour nodes
n_{mn}	Number of mining nodes
n_m	Number of malicious nodes
n_h	Number of honest nodes
n_{cp}	Number of colluding players
n_e	Number of eavesdroppers
n_s	Number of senders
n_r	Number of receivers
n_{FL}	Number of nodes participating in FL
n_B	Number of nodes uploading local models via FL blockchain
n_{WB}	Number of nodes uploading local models without FL blockchain
n_V	Number of nodes (vehicles) with RSU in transmission range

n'_V	Number of moving nodes reaching RSU
n_{RLY}	Number of $RLYs$
n_A	Number of acknowledgement messages
n_Z	Number of possible data sizes
μ_m	Mean number of malicious nodes
μ_h	Mean number of honest nodes
μ_d	Mean distance between nodes and RSU
μ_v	Mean speed of nodes (vehicles)

Probabilities

p_m	Probability of malicious nodes
p_{cp}	Probability of collusion
p_t	Average transmission probability
p_{suc}	Probability of success transmission
p_{col}	Probability of collided transmission
p_{idle}	Probability of encountering idle slot
p_z	Probability of using data size s_z
p_{out}	Outage probability

Time

τ_i	Validation time of node i
a_{τ_i}, b_{τ_i}	Upper, lower limit of τ_i
t_{icd}	Time at which incident message is received
T_{delay}	Time delay to finalize consensus
T_{slot}	Time slot in MAC layer
T_{suc}	Time for success transmission
T_{col}	Time for collided transmission
T_{DIFS}, T_{SIFS}	Time intervals for DIFS, SIFS
$T_{CTS}, T_{ACK}, T_{RTS}$	Time intervals for DCF related operations
T_{avg}	Average length of a time slot in DCF
T_{MB}	Time to transmit a microblock

T_{eyp}	Time to encrypt a block
TS	Time slot to upload local models

Throughput

λ_B	Blockchain throughput (block/s)
λ_{KB}	Keyblock throughput (keyblock/s)
λ_{MB}	Microblock throughput (microblock/s)
DR	Data rate (bit/s)

Power and channel-related parameters

P_{noise}	Noise Power
P_i	Power of signal transmitted by node i
QF_i	Quality Factor of node i
$SINR_{i,j}$	SINR between node i and node *j*
$Q(SINR_i)$	Quality of node i's SINR
$g_{i,j}$	Channel gain between node i and node *j*
$h_{i,j}$	Channel coefficient between node i and node *j*
$C_{i,j}$	Secrecy rate between node i and node *j*
α	Path loss exponent
η	Coefficient of self-interference
β_1	Threshold of $SINR_{i,j}$
β_2	Threshold of $C_{i,j}$

Incentive Distribution

CC	Call Compensation
CC_{mn}	Call Compensation for mining nodes
CC_r	Call Compensation for $RLYs$
ω_1	Weight to distribute CC among mining nodes
ω_2	Weight to distribute CC among mining $RLYs$
U_i	Utility of node i
s_i	Data size of node i

$Cost(s_i)$	Cost of training s_i
I	Incentive in FL
TC	Transaction Charge
ρ_i	Cost coefficient of node i
Rep_i	Reputation of node i
Rep_T	Reputation Threshold
Rep_{Rew}	Reputation Reward

Federated Learning

$LF(\boldsymbol{w}_x^k)$	Loss function of model x (local or global) at k^{th} iteration
$\boldsymbol{w}_i^k$	Weights of local model by node i at k^{th} iteration
$\boldsymbol{w}_G^k$	Weights of global model at k^{th} iteration

Miscellaneous

B_i	Behaviour of node i
κ	Consensus parameter
L	Length of a packet
W	Window size
FV	Failure in Validation
ORG	Originator
RLY	Relay node

List of Tables

List of Figures

List of Publications

1. **F. Ayaz,** Z. Sheng, I. W. Ho, D. Tian, and Z. Ding, “Blockchain-enabled FD-NOMA based Vehicular Network with Physical Layer Security,” Accepted for *IEEE 95th Vehicular Technology Conference*, Helsinki, Finland, June 2022.
2. **F. Ayaz**, Z. Sheng, D. Tian, M. Nekovee, and N, Saeed “Blockchain and Artificial Intelligence Based Security and Privacy for Internet of Vehicles,” Submitted to *IEEE Internet of Things Magazine*, April 2022.
3. **F. Ayaz,** Z. Sheng, D. Tian, and Y. L. Guan, “A Blockchain based Federated Learning for Message Dissemination in Vehicular Networks,” *IEEE Transactions on Vehicular Technology*, vol. 71, no. 2, pp. 1927 – 1940, February 2022, doi: 10.1109/TVT.2021.3132226.
4. Z. Xue, Y. Liu, G. Han, **F. Ayaz**, Z. Sheng and Y. Wang, “Two-layer Distributed Content Caching for Infotainment Applications in VANETs,” *IEEE Internet of Things Journal*, vol. 9, no. 3, pp. 1696-1711, February 2022, doi: 10.1109/JIOT.2021.3089280.
5. **F. Ayaz**, Z. Sheng, D. Tian, and Y. L. Guan, "A Proof-of-Quality-Factor (PoQF) based Blockchain and Edge Computing for Vehicular Message Dissemination," *IEEE Internet of Things Journal,* vol. 8, no. 5, pp. 2468-2484, February 2021, doi: 10.1109/JIOT.2020.3026731.
6. **F. Ayaz**, Z. Sheng, D. Tian, and V. Leung, “Blockchain-enabled Security and Privacy for Internet of Vehicles,” *Internet of Vehicles and its Applications in Autonomous Driving*, *Springer*, pp. 123-148, September 2020, doi: https://doi.org/10.1007/978-3-030-46335-9_9.
7. **F. Ayaz**, Z. Sheng, D. Tian, Y. L. Guan, and V. Leung, “A Voting Blockchain based Message Dissemination in Vehicular Ad-Hoc Networks (VANETs),” *Proc. of IEEE International Conference on Communications (ICC)*, Dublin, Ireland, pp. 1-6, June 2020, doi: 10.1109/ICC40277.2020.9148823.

Significant Participations

1. Industrial Placement at *Kinseed, UK*, **funded by IEEE Electron Device Society**, 16 August – 22 October 2021.
2. “A Voting Blockchain-Enabled Incentivised Message Dissemination in Vehicular Ad-hoc Networks,” poster presentation in *N2Women Workshop ACM SIGCOMM*, 10 August 2020. **Received N2Women Fellowship**.
3. “Blockchain-Enabled Vehicle-to-Vehicle (V2V) Communications,” Research Poster Competition in *Festival of Doctoral Research, University of Sussex*, 15 June 2020. **Received Runner-up prize**.

Chapter 1 - Introduction

1.1 Overview

The extensive use of digital technologies and multiple forms of interactions, (e.g., human-to-human, human-to-device, device-to-device) have led to the development of Internet-of-Things (IoT) into a global network connecting diverse devices, for example, smartphones, TV and vehicles. Internet-of-Vehicles (IoV) is one particular vertical domain of IoT incorporating communications between vehicles and other objects, using various communication models and approaches, for example, vehicle-to-vehicle (V2V), vehicle-to-infrastructure (V2I) and vehicle-to-everything (V2X), etc. IoV offers multiple services including resource-sharing, task-offloading and infotainment, etc. However, it can be considered as an advanced form of Vehicular-Ad-hoc-Network (VANET), and its primary objective is real-time sharing of information for a safe journey and smooth traffic flow [1]. Disruptions in traffic flow and congestions have been very common with increasing vehicle density on road, leading to a high risk of accidents and a serious threat to road safety [2]. Safe driving conditions can be achieved by VANET in which a vehicle can initiate reliable and efficient message dissemination in emergency situations, such as a road accident [3]. The oncoming vehicles may re-route themselves to avoid traffic congestion by receiving an alert prior to entering into an affected area. Thus, timely exchange of messages about an incident or traffic jam can lead to a better journey for the oncoming vehicles.

Nevertheless, due to massive growth in the number of connected vehicles, VANET comes across several challenges which are yet to be addressed for its secure implementation. A VANET encompasses large number of untrusted nodes, including vehicles and Road Side Unit (RSU), some of which may be malicious and tend to disrupt message exchange during emergency. Privacy is also an essential requirement in communications among untrusted nodes. Furthermore, it is not feasible for a Central Authority (CA) to be in-charge of the entire network, as it may become a single point of failure affecting the whole network. Therefore, decentralisation is recommended for VANETs [4]. Considering decentralisation, blockchain is seen as a promising solution to some of the challenges in VANETs. Blockchain is originally a distributed ledger to record history of financial transactions in the form of immutable and cryptographic blocks [5]. However, its robust architecture and application of its framework outside finance can potentially support VANETs. This thesis explores blockchain as a solution to distributed message dissemination in VANETs and utilises its features for resolving security, privacy and trust issues.

Despite the complementing features of blockchain, such as decentralisation, immutability and privacy support in an infrastructure-less environment, the integration of conventional blockchain in a dynamic and heterogenous vehicular network is yet another challenge. It is mainly due to latency constraints in emergency message dissemination and high speed of mobile nodes. This thesis investigates blockchain-based solutions particularly suited to a VANET environment.

1.2 Motivation

There are two main aims behind this research. First is to resolve security, privacy and trust related issues of VANETs through blockchain. Second is to address challenges of existing blockchain approaches and propose practically feasible solutions specifically for VANETs. The motivations behind utilising blockchain and proposing specific solution for VANETs are described below.

One of the security challenges of VANETs is credible message dissemination, i.e., to verify that a message is true before it is forwarded. Blockchain can be utilised to verify messages as it is conventionally used to record history of verified transactions only. Nodes undergo a mutual agreement called consensus to verify a transaction. Similarly, consensus can be utilised for message validation. Also, decentralised relay selection for efficient multi-hop communications in VANETs is another challenge. Nodes undergoing a blockchain consensus can mutually select an appropriate relay among themselves for timely dissemination of message in a distributed and trusted manner. Furthermore, blockchain-based transactions can support secure and immutable distribution of incentives among nodes. Since blockchain stores information in the form of encrypted blocks, it can also ensure privacy preservation in VANETs.

If blockchain is employed for emergency message dissemination in VANETs, it must support high throughput and low latency. Famous blockchain, such as bitcoin, uses Proof-of-Work (PoW) consensus which has a latency of around ten minutes [6]. Due to short-lived connectivity among high-speed nodes, PoW is not appropriate for VANETs. In addition, the high computation complexity and power requirements of PoW are also not suitable for On-Board Unit (OBU) on vehicles. Alternatives to PoW are proposed for achieving better throughput. For example, Proof-of-Stake (PoS) is commonly used in vehicular communications, where stakes are considered as reputation or trust ratings of nodes [7]. However, PoS is considered biased towards nodes with high stakes. The consensus algorithms with their strength, weaknesses and their suitability in VANETs are further discussed in Chapter 2. Due to limitations of existing consensus algorithms, this thesis proposes novel consensus algorithms specifically designed for VANET applications.

1.3 Objectives

This thesis mainly answers two research questions:

1) How to design an efficient message dissemination solution for vehicular networks using blockchain?
2) How blockchain can ensure the security, privacy and trust in vehicular networks?

The detailed objectives of the thesis are as follows

1.3.1 Understanding blockchain and its applications in vehicular networks

The first objective of the thesis is to gain a better understanding of blockchain, its structure, variations, consensus algorithms, features and applications in wireless networks. Next is to identify security, privacy and trust requirements of vehicular communications and analyse advantages and limitations of existing solutions, particularly focusing on why and how blockchain can be a better solution. Later, it is aimed to thoroughly analyse blockchain's performance and suitability in vehicular networks. Therefore, the performance of blockchain-enabled vehicular networks is investigated under different conditions, i.e., varying percentage of malicious nodes, various speeds and traffic densities of nodes on road and different strategic behaviour.

1.3.2 Proposing blockchain solutions suitable to VANETs

One of the main objectives is to investigate the limitations of existing blockchain consensus algorithms and propose new solutions which are particularly appropriate to message dissemination in VANETs. The proposed consensus algorithms aim to validate a message, i.e., evaluate its credibility and select relay node in a distributed manner. The latency in message dissemination and blockchain throughput are considered as key parameters to analyse performance of the proposed consensus algorithms. Complete blockchain-based message dissemination solutions are proposed, as shown in Figure 1.1, which can validate a message initiated in case of incident or emergency and select the most appropriate relay node in a decentralised fashion. The solutions also include a sustainable economic model, in which the originator of incident pays virtual credits or cryptocurrency to the affected nodes on road, as a compensation of causing an incident.

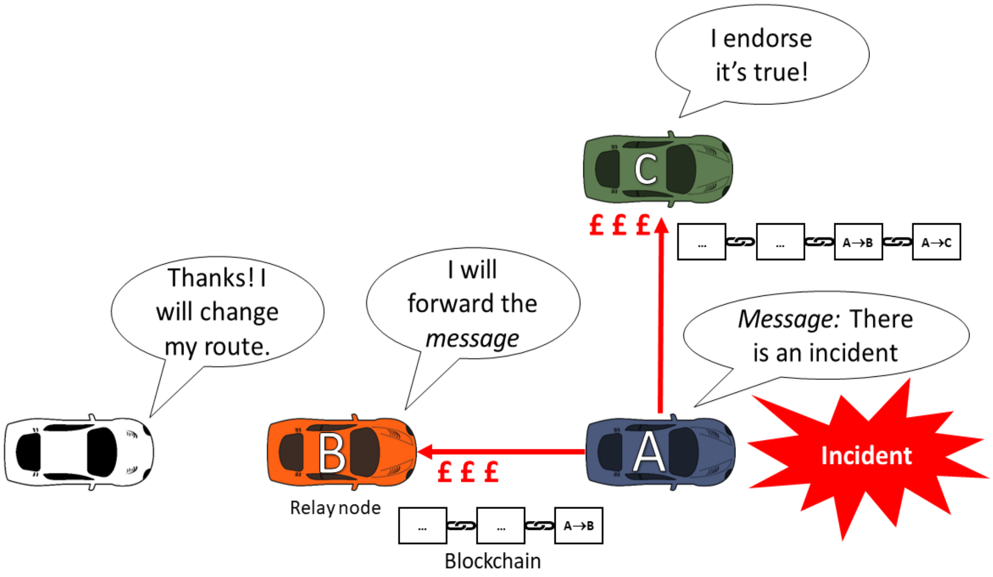

Figure 1.1: A blockchain-based message dissemination solution.

1.3.3 Integrating blockchain with other security and privacy solutions

Another objective is to investigate how blockchain can support other security and privacy approaches of vehicular networks, e.g., Federated Learning (FL) and Physical Layer Security (PLS). Integrated solutions are proposed aiming for higher security and privacy.

Detailed theoretical and simulated analysis are conducted for performance evaluation of integrated approaches and practical feasibility of their co-existence.

1.4 Statement of Originality

The original contribution of the thesis includes substantial blockchain solutions and consensus algorithms specifically for message dissemination in VANETs. The following chapters of the thesis are believed to be containing significant and original contributions

- The first contribution of the thesis is the proposed message validation by voting and competitive relay selection on the basis of its distance from sender and other channel quality parameters. Chapter 3 theoretically analyses the performance bounds of failure and latency in message validation. An incentive mechanism to promote honest voting and relay selection is also proposed and analysed using game theory.
- As an alternative to voting, Chapter 4 proposes a faster relay selection method by using blockchain-enabled FL. An incentive mechanism is presented to motivate nodes for a cooperative FL process and is analysed using Stackelberg game model. FL also enhances privacy of the proposed solution.
- To further study privacy in blockchain-enabled vehicular networks, the last contribution of this thesis is to analyse possible integration of PLS with blockchain. Chapter 5 theoretically analyses blockchain implementation on application layer with respect to physical layer characteristics, i.e., Signal to Interference Noise Ratio (SINR) and secrecy rate.

1.5 Organisation of the Thesis

The remainder of the thesis is outlined as follows. Chapter 2 discusses the technical background of vehicular communications, security, privacy and trust in VANETs. It also provides detailed introduction to blockchain and reviews blockchain-based solutions. Important and original contributions are presented in Chapter 3, Chapter 4 and Chapter 5, including a voting based blockchain solution, a blockchain-enabled FL approach and security analysis of blockchain integrated with PLS against jamming and eavesdropping attack, respectively. A conclusive summary of contributions and possible future research directions from this thesis are highlighted in Chapter 6. A description of tools used to obtain simulated results is present in Appendix A.

Chapter 2 – Background

This chapter consists of two main sections. First is vehicular communications, which briefly introduces different interfaces through which vehicles can communicate, describes VANET system model and discusses its security, privacy and trust requirements. Second is blockchain, which introduces blockchain structure, its features, consensus and current variations. The applications of blockchain to meet security, privacy and trust requirements are also discussed.

2.1 Vehicular Communications

Broadly, vehicular communications in IoV aims to attain full connectivity of a vehicle with not only other vehicles on road but also with every other object including passengers' smart phones, external management platform, navigation systems and other road users for both infotainment and entertainment purposes. An IoV network is composed of an environment consisting of humans, vehicles and things exploiting vehicle-to-everything (V2X) communications. The evolution of fifth-generation (5G) has led to the introduction of Cellular V2X (C-V2X) communications, which exploits Long Term Evolution direct device-to-device communications and allows vehicle-to-vehicle (V2V), vehicle-to-infrastructure (V2I) and vehicle-to-pedestrian (V2P) communications without network coverage. When in coverage, the communications can be augmented by Vehicle-to-Network's (V2N's) extended range and assistance, as shown in Figure 2.1 [8].

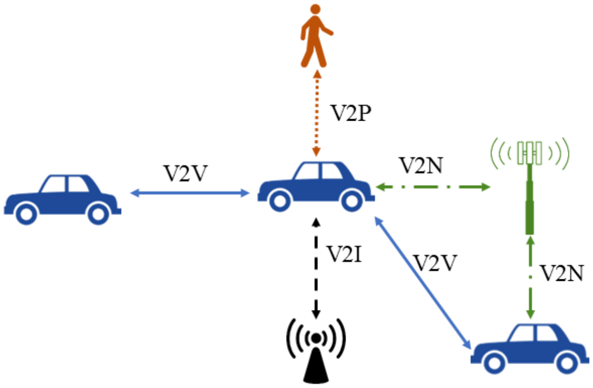

Figure 2.1: IoV in C-V2X communications.

The major aim of Intelligent Transportation System (ITS) is to improve road safety, driving conditions and traffic flow through vehicular communications. It relies primarily on V2V and V2I communications for sharing critical messages related to road and driving conditions [9]. A VANET consists of only two types of communications, V2V and V2I [10]. VANET predominately exploits Dedicated Short Range Communications (DSRC) for V2V, V2I and hybrid communications in a single hop or multi-hop fashion [11]. DSRC is standardised as IEEE 802.11p and IEEE 1069.x, combinedly called as Wireless Access in Vehicular Environment (WAVE) [12]. A VANET is a special class of Mobile Ad-hoc Networks (MANETs) with pre-defined routes (roads). As shown in Figure 2.2, vehicles exchange messages with nearby vehicles in a particular transmission range via V2V communications and communicate with RSU via V2I interface. Vehicles and RSUs are termed as 'nodes' in a VANET.

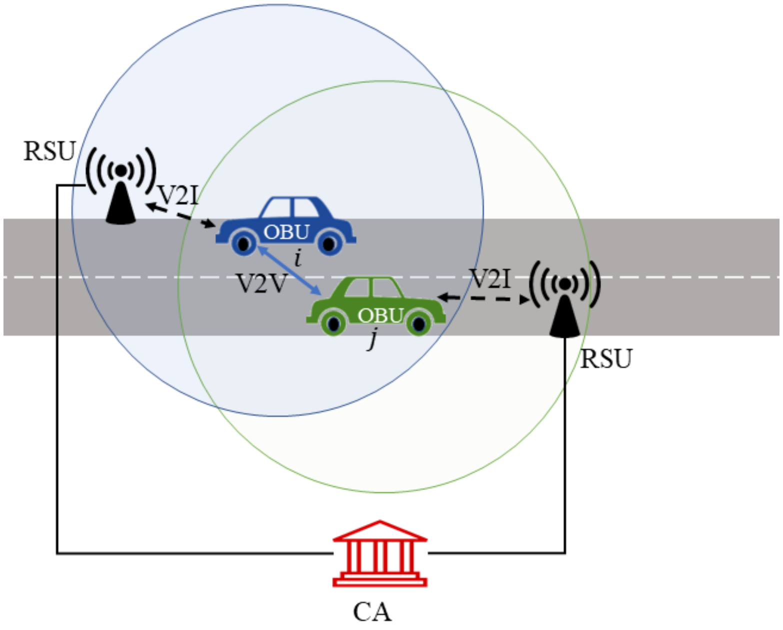

Figure 2.2: System model of a VANET.

Road safety is ensured in VANETs by exchanging appropriate messages among vehicles. Any alteration to these messages may lead to network failure and posing a serious threat to safety. Regardless of the technology, securing information is of utmost importance in V2V and V2I communications. Three main concerns in the design of secure VANETs are: security, privacy and trust. Security is defined as the approach to make the system free from danger or threat and the measures taken to be protected [13]. For example, security in VANET can refer to a solution to prevent an attack by malicious nodes. Privacy deals with rights to access or hide identities, messages and protection of personal information such as position or heading direction of a node. Trust deals with how nodes perceive each other (such as honest or adversarial) and received messages (such as true or false) [10]. There are two types of adversarial nodes in VANETs. One is malicious node, which tends to damage the network, for example, sharing false messages or attempting to validate false messages. The other is selfish node, which tends to save its energy by not cooperating in forwarding messages in multi-hop communications [14].

2.1.1 System Model of VANET

As shown in Figure 2.2, a VANET consists of the following major components:

- *Vehicles*: The vehicles are mobile nodes containing OBUs equipped with sensors, such as Global Positioning System (GPS) and camera, processors, storage, network devices and transceivers. The vehicles can communicate with its neighbour nodes via DSRC in a particular transmission range.
- *Road Side Unit (RSU)*: RSUs are immobile nodes on the road edges dedicated to communicate with vehicles via DSRC as well as with other RSUs and CA via infrastructural network. RSUs can facilitate in emergency message dissemination and provide internet connection to vehicles.
- *Central Authority (CA)*: A CA performs administrative roles in VANET including node registration, maintaining trust, managing incentive distribution schemes and assigning or revoking cryptographic keys and certificates. CA usually communicates with RSU only via wired connection.

2.1.2 Message types in VANET

The two major types of messages broadcasted in VANET are:

- *Beacon messages*: They are single hop periodic messages regularly initiated by mobile nodes to share their status on road with their neighbours. The information exchanged in beacon messages is usually position, speed, acceleration and vehicle type. The interval between two beacon messages generation by a same node is usually 100 ms to 1000 ms [15].

- *Emergency messages*: These messages are event-triggered and can be initiated by any node in case of unusual or emergency situations such as an incident or traffic jam. An emergency message is usually generated by vehicle if it detects a situation via camera or any other sensor equipped in OBU [16]. Because of the strict time constraint in case of emergency, an efficient routing protocol is required to transmit a message securely via multi-hop V2V or V2I communications. The issue of high dynamicity of nodes and scalability is also considered while designing routing protocol of messages. The allowable latency in communicating emergency messages depends on the type of emergency and is upper bounded by 1000 ms [3].

2.1.3 Security, Privacy and Trust in VANETs

Figure 2.3 illustrates the relationship among security, privacy and trust requirements and solutions in VANETs. This subsection discusses key attributes of each domain and reviews some solutions existing in literature.

A. Security

Security refers to the condition that VANET is protected from threats and attacks by adversary. The key attributes of security in VANETs include

- *Credibility:* It is essential for nodes in VANET to assess credibility of a message before dissemination. A message initiated by a node may not always be true. This is because a malicious node can affect the credibility of a message in the following ways [17]
    - generate a false message
    - validate a false message
    - deny a true message
    - collude with other nodes to perform any of the above actions

  The credibility of a generated message is assessed by three approaches. The first is pre-event, where each node has its trust rating based on which its originated message is considered true or false. If its trust rating falls below a certain threshold, the message generated by the node is ignored. This approach can be centralised where a CA stores trust ratings [18] or cluster-based where a cluster head manages trust rating [19]. The second is post-event, in which a message is validated on the basis of a threshold number of endorsements or votes from the neighbouring nodes [20]. The third is hybrid, where only trusted nodes take part in evaluation of message credibility [21]. The metrics to evaluate a message validation or credibility approach in vehicular communications include the speed of reaching a decision, communication overhead and tolerance rate of malicious nodes.

- *Availability:* It is the assurance that a network remains operational in presence of malicious nodes. In case of emergency on road, a VANET must be able to independently disseminate the message up to a required number of hops, desired area or time limit, so that the information is available to all relevant nodes. Therefore, a swift and reliable message dissemination solution is required in VANETs. The receiving nodes must be able to select the most appropriate relay node among themselves, which can effectively forward a message to a large number of other nodes [22]. Relay selection in vehicular communications plays a crucial role in message broadcasting. An inappropriate relay may cause unacceptable latency or sometimes failure in delivering a message to a desired number of vehicles or area. A central node such as RSU can be used for message dissemination. However, it requires a large infrastructure investment [23] and its volume and placement positions are crucial for system performance [24]. Moreover, RSU assisted routing protocol may result in higher latency because of an increased route discovery time [25]. Relay node selection depends on a number of factors, such as, distance between sender and receiver, and some physical and Medium Access Control (MAC) layer properties including channel quality, collision probability and SINR. Prior to relay node selection, probabilistic estimations predict the optimal node with the most suitable combination of its distance and link stability at the time of transmission [26] - [27]. However, probabilistic predictions rely on certain approximations, for example, number of nodes within a transmission range, which may not be highly accurate when varying traffic and speed limits are imposed in a vehicular network. A cross-layer approach integrating both MAC and physical layer for optimum bandwidth utilisation is presented in [28]. The weighted combination of distance and channel quality are used to determine link stability for relay node selection in [29]. To make relay selection more adaptive to network changes, Artificial Intelligence (AI) based mechanisms are designed. Fuzzy logic has been used in [30] - [31], which makes decision according to distance, moving direction and speed of nodes. However, fuzzy logic is also dependent on thresholds and weights to be set in the rule base for making inferences. In [32], satellite images are used to detect buildings and obstacles to enable machine learning driven channel characterisation. The path with lowest propagation loss is used for message dissemination in [32]. RSU assisted deep learning based technique is developed for relay selection in [33]. It is pointed out that machine learning and deep learning algorithms require large processing power to handle huge amount of data and therefore they must require infrastructure support for implementation.

A security attack against availability is called jamming, in which an attacker causes interference to reduce SINR between sender and receiver to a level that an originated message is unable to reach its desired receiver and hence the information remains unavailable [10]. Therefore, selecting an appropriate relay node with least interference is desirable to ensure availability [27]. Availability aligns with the integrity protection attribute of 5G security requirements identified by 3GPP, i.e., a message should be protected from jammers and interferers to prevent degradation in SINR while it is being transmitted [34].

B. Privacy

Privacy means that only designated nodes in VANETs have permission to view other nodes' original identities and control over granting access rights to nodes for viewing, sharing or originating messages [10]. The two attributes of privacy are as follows

- *Anonymity:* According to 3GPP requirement of privacy, anonymity is authenticating a node in a network without revealing its original identity [35]. One of the most commonly used approaches for anonymity in VANETs is public key cryptography [36], where public/private key pairs and digital certificates are used for pseudonymous communications. A third trusted party or CA is responsible for issuance of key pairs and a digital certificate for authentication. Another approach is identity based and combined public key cryptography, which reduces the burden of CA as it uses private key for authentication instead of additional digital certificate by CA [37]. In both approaches, timely updates of key pairs are required for sustainable privacy preservation.

- *Confidentiality:* It implies that information contained in a message is secret and only a legitimate receiver should be able to access it. Eavesdropping attack attempts to break in confidentiality and retrieve information from messages without access rights [10]. PLS offers secrecy as a physical layer's protection from eavesdropping. Secrecy rate of vehicular networks is analysed in [38] considering double Rayleigh fading environment. Only one legitimate receiver and one eavesdropper is assumed to be presented within the transmission range of sender, which is not very practical in high dense scenarios. In [39], the impact of eavesdropping is studied on various speeds and transmission ranges of nodes. It is concluded that secrecy rate can be maintained in presence of eavesdroppers at the cost of high transmission power and bandwidth. Cryptographic schemes are also used to protect confidentiality. As a trade-off they result in increased message size and additional computational and delay [39]. Confidentiality corresponds to 'Access' feature of 3GPP privacy requirement, i.e., only legitimate nodes are allowed to access a message [35].

C. Trust

Trust is used to support security in VANETs. For example, trust ratings are used to evaluate message credibility. Also, an increase in trust or reputation score is served as an incentive to motivate nodes to cooperate and actively participate in message dissemination.

- *Incentive Distribution Mechanisms:* Incentive distribution mechanisms fall under the category of trust management models as they propose schemes to update trust ratings or reputation. However, there are two common types of incentive mechanisms: price-based and reputation based. In price-based strategy, messages are treated as commodities which are exchanged for virtual credits [40] - [41]. On the contrary, reputation-based strategies use measurement of trustworthiness to enforce cooperation. A threshold of reputation is set to distinguish malicious behaviour from honest. A punishment scheme is applied for malicious behaviour [42] - [43]. Game theoretical analysis [44] is usually used to predict honest, selfish or malicious actions of nodes according to a designed incentive strategy. It is suggested that an integrated strategy of both price-based and reputation-based schemes is more effective in promoting cooperation and detecting malicious behaviour in MANETs [45]. A joint price and reputation based opportunistic routing solution for vehicular networks is presented in [46], where the originator pays a price to contributing nodes for successful delivery of message to a destination. The participating nodes are selected on the basis of their reputation. CA also receives a fraction of price for offering management services. A price-based approach in [47] claims to establish trust in VANETs by imposing price for initiating a message. The price is considered as a guarantee of message's truthfulness.

Incentive mechanisms are not only effective to encourage selfish nodes to cooperate but also discourage cheating attempts by malicious nodes. Discouraging malicious and selfish behaviour is of crucial importance in VANETs, as they may hinder emergency message dissemination and risk road safety. A Payment Punishment scheme is proposed in [48] to demotivate malicious nodes to disseminate false messages.

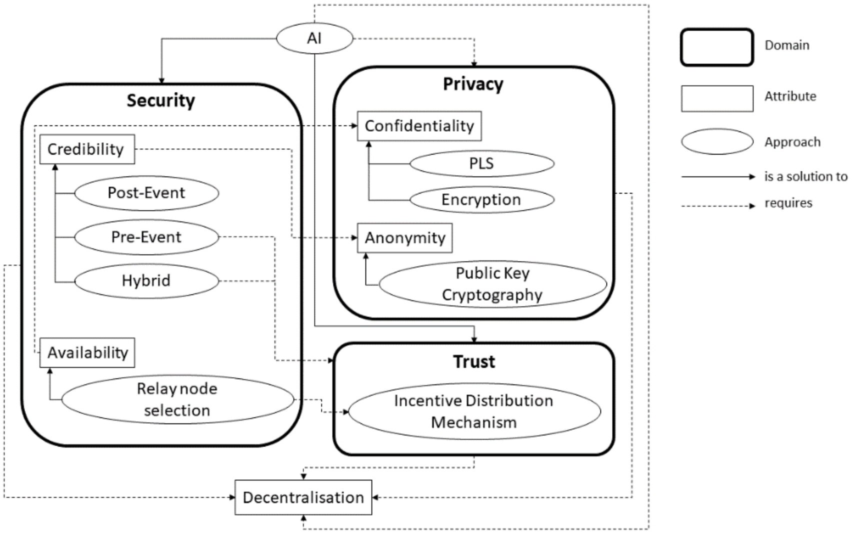

Figure 2.3: Relationship between security, privacy, and trust in VANETs.

D. *Decentralisation requirement for security, privacy and trust*

Due to high dynamic and distributed nature of VANETs, decentralisation is an essential requirement for security, privacy and trust. VANETs must be able to independently make decisions, even when CA is out of reach. Since low latency is an important criterion when propagating messages to fast moving vehicles, a decentralised network in which nodes can select relay nodes among themselves independently without any CA is desired as a scalable and cost-effective approach [49]. Also, privacy and trust management would be compromised if CA is attacked or untrusted. Decentralization and third-party independence eliminate the possibility of single point failure in a network.

E. *AI for security, privacy and trust*

AI and machine learning algorithms are commonly integrated with a number of security and trust solutions, for example, misbehaviour detection by Support Vector Machine [50] and relay selection by deep learning [33]. There can be two approaches to perform machine learning or deep learning: on-device or off-device. In on-device learning, an inference model is trained on a node with its own private data without being shared with any other node [51]. It is considered as an effective solution for VANETs because of its privacy and low communication overhead, as it does not require data transfer to a cloud [52]. However, it is usually an uncooperative approach and an inefficient utilization of computation resource. It is because no knowledge of an on-device trained model is shared with other nodes and therefore, one node cannot utilize the benefits of a trained model produced by another. On the contrary, in a centralised solution or off-device learning, data from all connected nodes is gathered on a cloud or a central node, which produces inference model for all nodes [53]. Transmitting big data to a central node in VANETs is susceptible to propagation loss due to channel fading and is both bandwidth and time inefficient. Connectivity time among nodes is also limited. Furthermore, it is essential that the central node employs secure and privacy-preserving techniques for managing and storing big data.

- *Federated Learning (FL):* To manage the diverse nature of big data and also its privacy preserving requirements, FL is suggested as a suitable AI technique for various cooperative applications in vehicular communications [54]. In FL, nodes train local models individually on their own private data. Instead of whole data, they share only local models with a central node or aggregator, which combines all local models to form a global model. Since FL relies on a central aggregator and VANETs require decentralization, it is challenging to implement conventional FL in VANETs. Also, an incentive mechanism is required to motivate nodes for contributing towards FL and discourage inaccurate local models. Furthermore, a malicious node can use false data or deliberately produce an inaccurate local model. Therefore, FL needs some means to detect malicious behaviour. It can be concluded that although FL is suitable for VANETs, it must be incorporated with solutions to offer decentralisation, security against malicious behaviour and a robust incentive distribution mechanism, all of which can be enabled by blockchain [55].

The next section of this chapter defines blockchain and its features and also discusses how blockchain can potentially be a solution to security, privacy and trust while offering decentralisation.

2.2 Blockchain

2.2.1 Introduction

A blockchain is a peer-to-peer electronic cash system in which transaction history is maintained in the form of immutable timestamped blocks. As shown in Figure 2.4, each block in a blockchain contains a cryptographic link to the previous block known as hash [56]. Blockchain based cryptocurrency, bitcoin, was first introduced by Satoshi Nakamoto in 2008 [5]. Since then, multiple variations of blockchain and cryptocurrencies have been released.

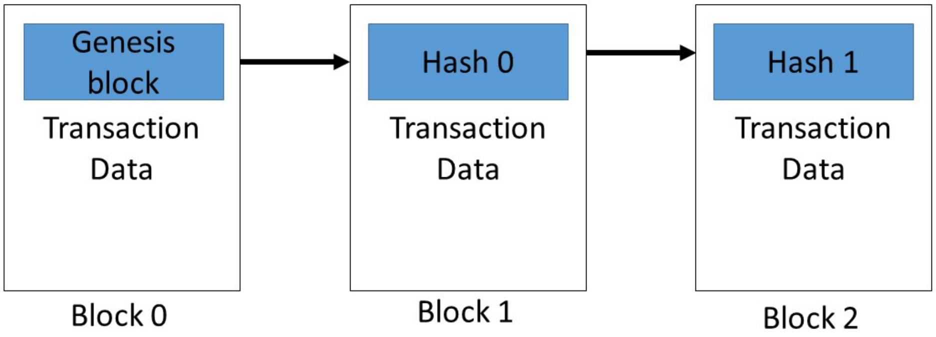

Figure 2.4: The blockchain structure.

A conventional blockchain inherently possesses a network of nodes. Whenever a transaction request is made, it is broadcasted across the network. Nodes have the right to validate a transaction and mine the validated transaction into a block containing an encrypted hash of previous block, thereby making it cryptographically secure. Nodes which append a block to the blockchain after validation and broadcast it in the network are known as miners. Miners have to go through a mutual agreement called consensus algorithm to create a block which makes it fraud-proof [57]. For each mined block, a miner earns reward in relevant cryptocurrency, which is usually paid by the proposer of a validated transaction [58]. All nodes are responsible to update their copy of blockchains regularly to ensure consistency in the entire distributed ledger [59].

2.2.2 Features

A blockchain-enabled network offers the following features

- *Decentralisation:* The methodology of validating and recording transactions in a blockchain is decentralised and independent of CA. This feature makes it suitable for distributed networks, for example in VANETs [60] - [61]. Also, blockchain is not stored in a central server or node. All nodes possess a copy of blockchain. If a malicious node attempts to modify contents of a block, it must do it in every copy, which can be difficult [62] - [63].
- *Credibility*: Nodes go through a consensus algorithm to validate a transaction in a block. If a malicious node attempts to propose a fake transaction, it cannot be included in a block without being validated by a consensus algorithm [64] - [65]. The consensus algorithm can be used to validate a message instead of a financial transaction in VANET thus ensuring credibility of a message.
- *Privacy*: The transactions are made in blockchain using private keys. A key can also be changed for different transactions. This feature introduces anonymity in the network [66]. The blocks are also encrypted and can be accessed with correct pair of keys, ensuring confidentiality of data [67]. Similarly, messages or transactions of incentives in VANET can also be anonymously recorded and kept confidential in blockchain.

- *Automation:* Blockchain can enforce a set of rules and allow automation of multi-step processes and interaction among nodes using smart contract. Smart contracts are self-executing scripts residing on the blockchain, which run independently in a prescribed manner [68]. Nodes can store a set of agreed rules to validate a transaction in smart contract. It executes on receiving transaction proposals and automatically reaches consensuses in less time without the need of third party [69]. Recent works have utilised smart contract to automate secure charging of electric vehicles [70] - [71].

2.2.3 Consensus Algorithms

The consensus algorithm of a blockchain is designed to solve Byzantine general's problem [72] - [73]. This problem considers the presence of faulty or malicious nodes in a network. These nodes can behave differently to other nodes. For examples, they may ignore a valid transaction or propose a fake transaction [74]. A consensus algorithm works in two ways, i.e., it either elects a miner in a network which validates a block through a competition or eligibility criteria, or it defines a set of rules run by smart contract to validate a transaction. The consensus is finalised in a distributed manner and is intended to work without errors in the presence of faulty nodes. The performance of a consensus algorithm is evaluated by the following metrics

- *Tolerance:* Number of malicious nodes it can control without altering the original validity status of a transaction and its ability to resolve forks and prevent cheating.
- *Latency:* Time required to validate and propagate a transaction.
- *Throughput*: Number of blocks generated per second.

Some of the common consensus algorithms are:

- *Proof-of-Work (PoW):* In PoW, the nodes solve a complex cryptographic challenge which typically takes around 10 minutes to complete. The node which solves the challenge first is elected as miner. PoW can tolerate around 50% malicious nodes in a network [75]. However, due to its complexity and huge time consumption, it is not considered appropriate for mobile networks with short-lived connectivity span, such as, VANETs [76].

- *Proof-of-Stake (PoS)**:*** It is an alternative to PoW which can save computational energy and time. It works under the assumption that the node with the highest number of stakes is less likely to be faulty [77]. The nodes prove the amount of credit or stakes owned. The node with largest number of stakes becomes miner. It takes considerably less time than PoW. However, it is unfair to nodes owning less stakes and therefore promotes oligarchy in the network. Only nodes with high stakes are able to be active in the network, which demotivates other nodes to participate. Therefore, it is not suitable to applications where positive cooperation is required from every node, for example, sharing resources, information exchange and emergency message dissemination.
- *Proof-of-Elapsed-Time (PoET)**:*** In PoET, each node generates a random number, following a probability distribution, to determine how long it needs to wait before generating a block. The node with shortest waiting time is elected as miner. Generating a random number requires significantly less energy as compared to solving a cryptographic challenge. However, it is proved to be less secure in theory because malicious nodes can easily generate the shortest time to become miner [78].
- *Practical Byzantine Fault Tolerant (PBFT) algorithm**:*** It is a voting-based consensus algorithm aimed to achieve high throughput and low computation cost. As shown in Figure 2.5, it consists of the following stages [79] - [80]:
    - An originator initiates a transaction proposal and requests nodes to vote for validation.
    - Nodes, also known as endorsers, vote if the transaction is valid.
    - If the transaction is validated by a threshold number of votes, it is added as a block into blockchain.

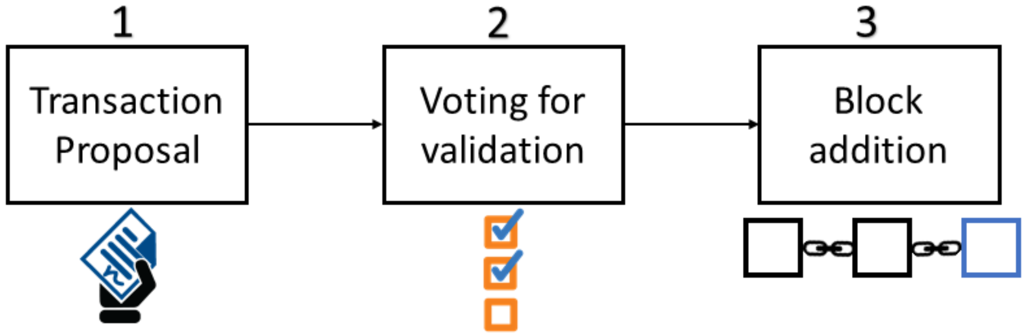

Figure 2.5: The stages of PBFT algorithm.

A comparison of the above discussed consensus algorithms is presented in Table 2.1.

Consensus	**Energy saving**	**Time saving**	**Discriminatory**	**Secure**
PoW [5]	No	No	Yes (towards computational power)	Yes
PoS [77]	Yes	Yes	Yes (towards amount owned)	Yes
PoET [78]	Yes	Yes	No	No
PBFT [79] - [80]	Yes	Partial	No	Partial

Table 2.1: Comparison of consensus algorithms.

2.2.4 Blockchain Variations

Due to increasing applications of blockchain outside finance, many variations in its framework and structure are now proposed and widely practised. Initially, a blockchain was designed to store transactions of cryptocurrency. When cryptocurrency is managed by blockchain, each block contains a set of verified transactions and a cryptographic hash linked with previous block, as shown in Figure 2.4: The blockchain structure.Figure 2.4. However, a block can be used to store a verified record of any item according to required application, for example, update in reputation rating of a node or message exchanged at each hop, as shown in Figure 2.6.

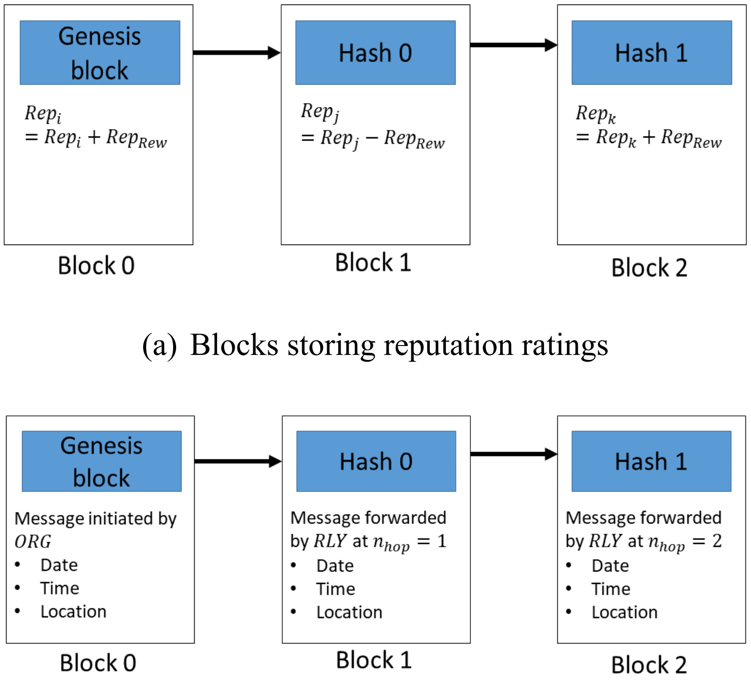
Genesis block
$Rep_i = Rep_i + Rep_{Rew}$
Block 0
Hash 0
$Rep_j = Rep_j - Rep_{Rew}$
Block 1
Hash 1
$Rep_k = Rep_k + Rep_{Rew}$
Block 2
Genesis block
Message initiated by ORG
Date
Time
Location
Block 0
Hash 0
Message forwarded by RLY at $n_{hop} = 1$
Date
Time
Location
Block 1
Hash 1
Message forwarded by RLY at $n_{hop} = 2$
Date
Time
Location
Block 2

(a) Blocks storing reputation ratings

(b) Blocks storing message details at each hop

Figure 2.6: Variations in block contents.

A. Permissioned and Permissionless Blockchains

Blockchains were conventionally designed to be permissionless. Nowadays, blockchains are broadly classified into the following two categories [81]:

- *Permissionless blockchain:* In permissionless blockchain, all nodes have equal rights to access and generate blocks, thus ensuring transparency in the network. PoW and PoS are mostly used with permissionless blockchain [56].
- *Permissioned blockchain:* In a permissioned blockchain, specific roles and access limitation can be associated to certain nodes. Permissioned blockchain usually employs limited number of nodes in a consensus. PBFT algorithm is common for achieving consensus among a group of nodes in permissioned blockchain [82]. Considering different roles in ITS, such as automotive manufacturers, government

and transportation authorities, a permissioned blockchain is considered appropriate for vehicular applications [16].

B. Hierarchical Blockchains

Variations are also present in distributed ledger of blockchain to ensure high throughput. A conventional blockchain ledger is horizontal, where each block is only linked with the previous block, as shown in Figure 2.4. However, several hierarchical structures of blockchain have now been proposed to improve throughput and latency of block generation. Such solutions contain parallel tiers of off-chain blocks, all connected to a main block, as shown in Figure 2.7. Miner is usually considered as a leader in hierarchical blockchain. The subordinates of miner are used to validate transactions at the same time and generate blocks containing the hash of a previous block [83]. In this way, multiple blocks containing one hash are added in parallel.

In a conventional (non-hierarchical) blockchain, parallel blockchain extension is called fork, as shown in Figure 2.8. As a common practice, blockchain picks one of the parallel blocks to continue, and meanwhile, disqualifies other forking blocks by longest chain acceptance protocol [84]. Forks also lead to creation of malicious chains [75]. On the contrary, in a hierarchical structure, parallel blocks are not considered as forks. In a hierarchical blockchain, blocks are classified into two types: keyblock and microblock. Instead of a linear ledger, microblocks representing off-chain transactions are added in parallel, whereas keyblocks are main blocks which are appended horizontally in the blockchain by a leader or a central node, for example, RSU in vehicular networks. Practical implementation of a conventional blockchain in VANETs is challenging. Due to limited connectivity duration in V2V communications, moving nodes may not always have an updated blockchain ledger, which leads to a fork situation, as shown in Figure 2.9 (a). To address this issue, the hierarchical structure of blockchain is proposed for vehicles [85]. As shown in Figure 2.9 (b), parallel addition of microblocks does not disturb the main linear ledger and forks are not disqualified but accepted as off-chain micro-transactions recorded in a decentralised manner.

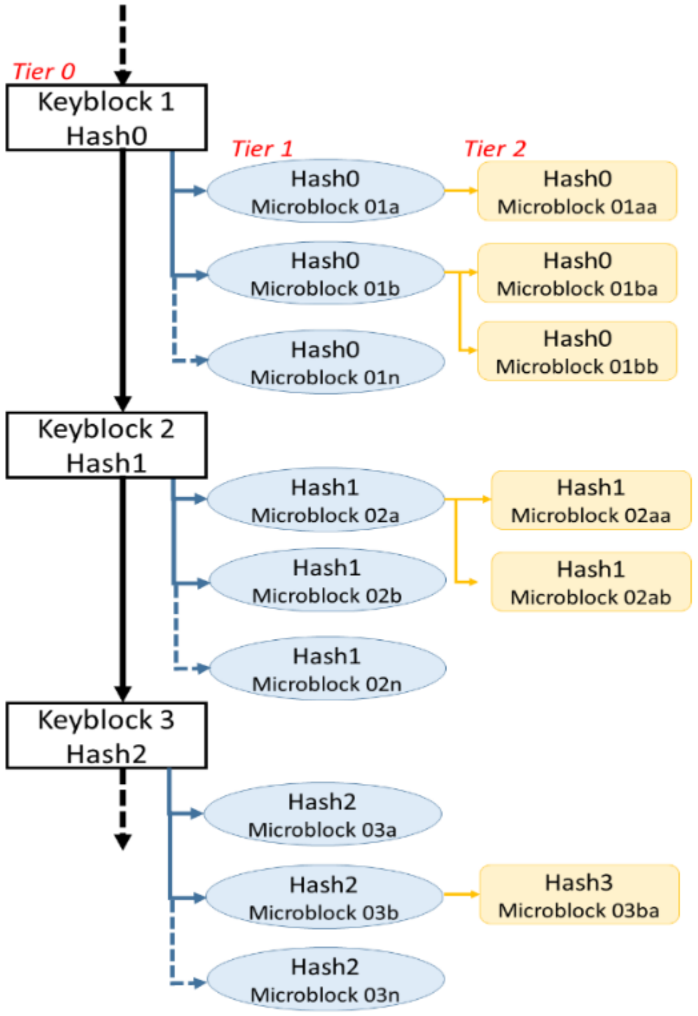

Figure 2.7: A hierarchical blockchain structure.

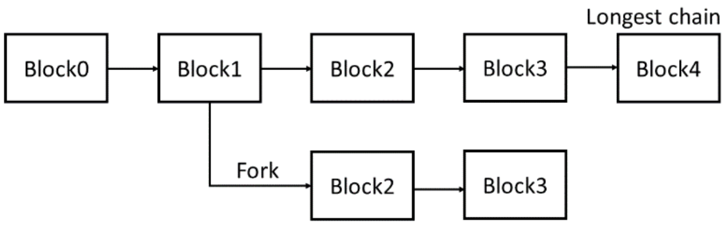

Figure 2.8: Fork occurrence in conventional blockchain.

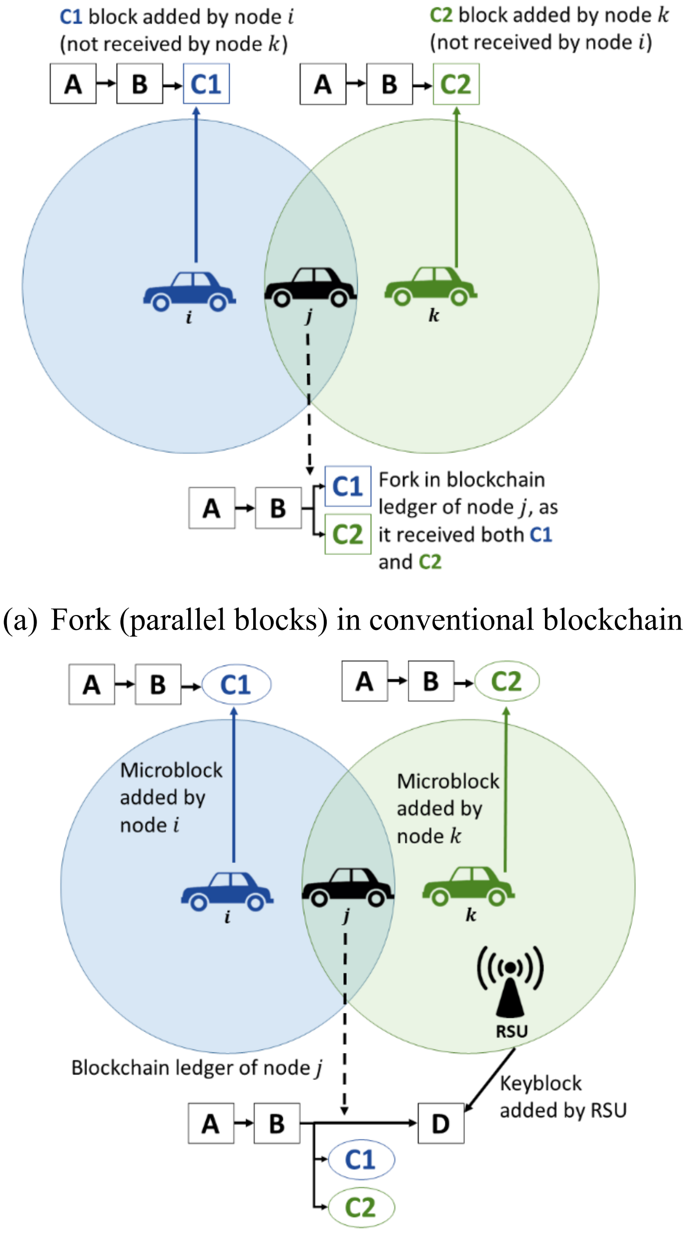

(a) Fork (parallel blocks) in conventional blockchain.

(b) Parallel microblocks and linear keyblocks

Figure 2.9: Parallel addition of microblocks to resolve forks in blockchain in vehicular networks.

2.2.5 Blockchain for Security, Privacy and Trust

The prospect of blockchain as a security, privacy and trust solution has drawn increasing interests in communications research community. This subsection reviews some of the existing approaches of blockchain implementation in ad-hoc networks, particularly in VANETs. Table 2.2 summarises the advantages and challenges of discussed applications.

Domain	Applications	Advantages	Challenges
Security	Credibility Evaluation [86] - [87]	Decentralisation	Choice of suitable consensus is necessary for low latency
Privacy	Certificate / Key management [88] - [89]	Automation	Often needs CA and complete decentralisation is difficult to achieve
	Confidentiality Protection [90]	Private blockchain with access control	Possibility of eavesdropping
Trust	Reputation Management [7], [91] - [92]	Decentralisation and immutability	Difficult to find suitable consensus: PoW is time consuming, PoS does not motivate nodes with low reputation
	Incentive Mechanism [37] , [93] - [94]	Privacy and immutability	Additional cryptographic computations

Table 2.2: Advantages and challenges of blockchain applications.

A. Security

- *Credibility:* The distributed ledger of blockchain storing trust ratings or consensus to reach a mutual agreement provides solutions to assess message credibility. Trust or reputation ratings based blockchain solutions are commonly used as decentralised pre-event approaches to evaluate message credibility in VANETs. A permissioned blockchain of reputation using PoW consensus is proposed in [86], which is used to validate messages on the basis of sender's reputation. In [95], smart contract is utilised to update trust ratings of nodes, which are then used to classify honest or malicious message originator. Blockchain can also be used to validate a message by post-event approach. A blockchain-based solution can achieve consensus if satisfactory endorsements are received as a proof-of-event [96]. PBFT based voting is used in [37] and [87] to collect endorsements for message credibility. Also, as a hybrid approach in [7], Delegated PoS consensus only allows selected nodes take part in post-event validation. These nodes are selected on the basis of their trust ratings.

- *Availability:* To ensure availability of message in VANETs, a relay selection Stackelberg game model considering trust ratings of nodes stored in blockchain is proposed in [97]. However, it is worth noting that formulating a blockchain consensus exclusively for enabling distributed relay selection is a novel contribution of this thesis.

B. Privacy

- *Anonymity:* As discussed in Section 2.1, public key cryptography is used to ensure anonymity in VANETs. In large scale networks, it may result in running several cryptographic operation requests at the same time which is not a feasible solution [98]. Blockchain based solutions are proposed in literature for third party independence and dynamic key management [88]- [99]. A blockchain managed by CA to assign or revoke encrypted keys in VANET is proposed in [88]. However, when a CA is responsible for issuing or revoking certificates for private vehicular communications, there is a risk of single point of failure affecting the whole system. Therefore, distributed ledger of blockchain is recommended in [100], where multiple nodes keep the record of issued or revoked certificates. A similar approach is presented in [101], where blockchain is used for key management and RSUs are assigned as validators. Specific nodes or validators perform the role of CA in [100]-[101]. Therefore, they can be considered as partially decentralised solutions. Key management through blockchain as a potential research area for future has also been discussed in [89].
- *Confidentiality:* The confidentiality of VANETs can be protected by implementing encrypted blocks and access control schemes. However, there still remains a possibility of eavesdropping even when blockchain is used because of the broadcasting nature of both VANETs and block announcement procedure [102]. In [90], the nodes are allowed to register into a private blockchain only when the secrecy rate of physical layer exceeds a certain threshold. A blockchain based

federated learning mechanism is proposed in [103]. Despite the privacy preserving nature of both federated learning and blockchain, an additional technique is applied to protect location confidentiality of nodes.

C. Trust

- *Reputation Management:* The distributed ledger of blockchain is commonly utilised as a decentralised storage medium for recording trust ratings or reputation scores [91] - [104]. In [7], a blockchain based reputation management solution is proposed with PoS consensus, where reputation is considered as the stake of nodes. The nodes report their reputation opinions of other nodes to a nearby RSU. To carry out consensus protocol, the reputation values are downloaded from RSU and a mining node is elected on the basis of highest reputation. A node is considered malicious if its reputation value falls below a certain threshold. A similar approach is presented in [92], where RSUs store reputation of nodes and maintain blockchain. To carry out the consensus, mining RSUs undergo a joint PoW and PoS algorithm, where reputation is regarded as a stake. Both mechanisms rely on RSUs for blockchain management.
- *Incentive Distribution Mechanisms:* Blockchain also manages distribution of incentives by recording them in the form of transactions involving cryptocurrency or virtual credit. Secure blockchain-based incentive mechanisms are proposed in the literature to encourage cooperative message delivery and data sharing in distributed peer-to-peer (P2P) applications. In [93], data storage among nodes in wireless sensor networks is incentivised and proof of stored data is proposed as the consensus algorithm. An example of incentivized caching for content delivery based on blockchain is presented in [105]. In [106], an incentive strategy is proposed for crowdsensing applications where privacy is preserved by cryptographic signatures. In [107], a pricing strategy to ensure successful message delivery using blockchain is presented and proved to be secure against the collusion of intermediate nodes and receiver using the game theory. Similarly, in [108], P2P data sharing using permissionless blockchain is proposed. In both [107] and [108], the incentive mechanism is proved to encourage cooperation among nodes by including a mandatory charge paid by transmitting nodes. Incentive-based message

relaying in distributed P2P applications using the blockchain is also proposed in [109] and proved to be secure against selfish behaviour. In VANETs, a blockchain based incentive mechanism which uses virtual credits, known as CreditCoin, as a reward for forwarding the message is proposed in [37]. The transactions of CreditCoins are managed by blockchain, which is independent to V2V communications. The message dissemination solution is not completely decentralised because it relies on RSUs or official public vehicles as servers to conduct consensus. A decentralised solution of incentive distribution through blockchain is proposed in [61]. It is suggested to automatically punish negative behaviour in an ITS. For example, behaviours of over-speeding and ignoring traffic lights are punished by imposing fine, recalculating tax or insurance, which can be implemented by the use of smart contract without requiring a CA. In [94], the incentive-based message delivery in wireless ad hoc networks for smart cities and ITS is presented, where the message is validated using PBFT, and the incentives and privacy are controlled using blockchain.

2.3 Summary

This chapter first introduces VANET and discusses requirements and approaches for security, privacy and trust for message dissemination. Secondly, blockchain, its consensus algorithms, variations and promising solutions to security, privacy and trust are reviewed. It can be concluded that the features of blockchain can offer solutions to many challenges in VANETs. Specifically for message dissemination, blockchain is a potential approach to provide decentralisation, security and trust. Table 2.3 summarises challenges associated with message dissemination in VANET and corresponding solutions provided by the blockchain.

Some of the existing approaches to implement blockchain in VANETs are discussed in this chapter. However, it is crucially important that technical challenges, such as dynamic nature of VANETs, short-lived connectivity, broadcast storm, packet collision, and computing complexity are addressed while implementing the blockchain. Therefore, current blockchain solutions may not be fully compatible with vehicular networks in practice and new approaches are in need for VANETs. It is well-acknowledged that security, privacy and trust solutions are widely discussed in literature, but for a message dissemination solution in VANETs, there is a need to establish an integrated approach in which efficient and trusted communications in a vehicular network can be managed in a decentralised fashion. Also, a detailed performance analysis is required to evaluate the practical feasibility of blockchain in VANETs.

Issues in VANET	**Blockchain based solutions**
Message validation	Consensus algorithm
Trust without third party dependence	Decentralised ledger
Privacy requirement	Cryptographic hashes
Broadcasting storm / relay selection	Miner election by consensus
Incentive distribution	Miner incentives

Table 2.3: VANET issues and opportunities using blockchain.

Chapter 3 – Voting based Blockchain for Message Validation and Relay Selection

Some existing blockchain consensus and their limitations are discussed in Chapter 2. This chapter introduces a novel voting-based Proof-of-Quality-Factor (PoQF) consensus as a solution appropriate to VANETs. PoQF incorporates message validation and a decentralised relay selection mechanism. The motivation and challenges in conventional voting based PBFT are discussed in section 3.1. The rest of the chapter consists of three main sections. In section 3.2, we explain the formulated model and approach, and propose two ways of incentive distribution mechanisms for message validation and multi-hop relaying. In section 3.3, we theoretically analyse the proposed solution. The simulation results of the proposed solution are discussed in section 3.4.

3.1 Overview

3.1.1 Motivation

As discussed in previous chapters, blockchain applications in vehicular networks can offer many advantages including decentralisation and improved security. However, one of the challenges to implement blockchain in VANETs is to select an appropriate consensus algorithm particularly satisfying vehicular application requirements. The large latency and high computation costs of PoW and unfairness of PoS are already discussed. If PoW is employed in VANETs, it must be run by RSU [110] or computation offloading to edge devices is required [111]. PoS, the alternative to PoW, usually finds its applications in reputation management [7], [92]. Another consensus algorithm, PoET, offers the fairness with less computation workload but its weakness in security and vulnerability in the presence of malicious nodes is proved in literature [78]. Selection of consensus for blockchain applications in VANETs is widely discussed in literature and the voting based PBFT is one the most recommended approaches for connected vehicles [37], [94], [112]-[113], which offers high throughput and has the ability to negotiate message validity [94], [112].

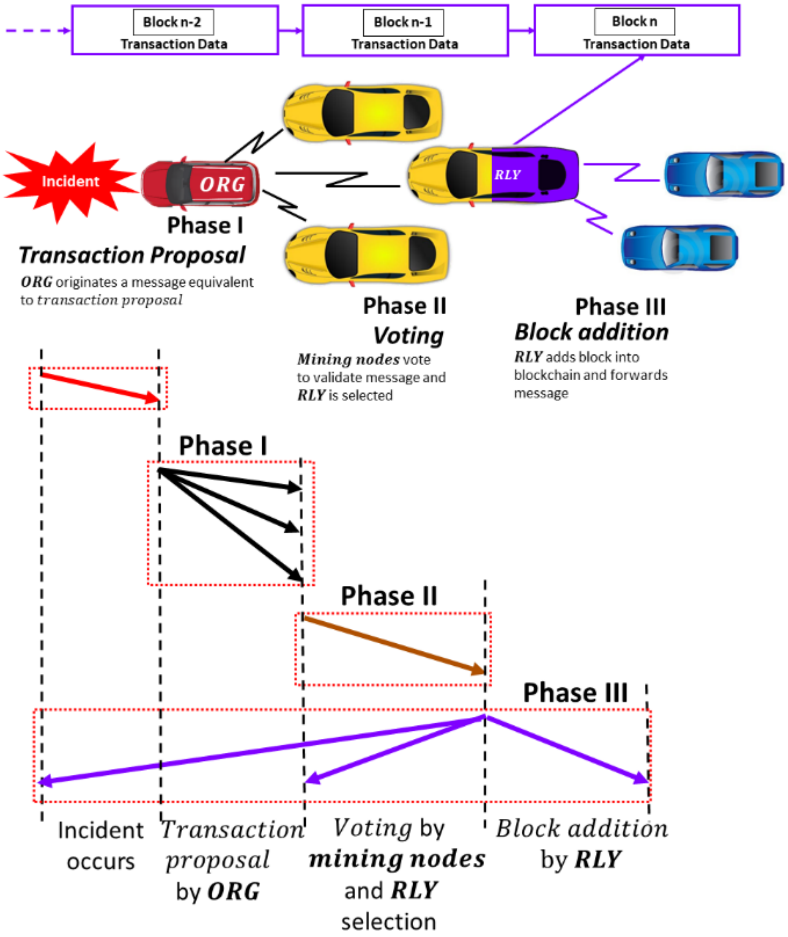
Block n-2
Transaction Data
Block n-1
Transaction Data
Block n
Transaction Data
Incident
ORG
RLY
Phase I
Transaction Proposal
ORG originates a message equivalent to transaction proposal
Phase II
Voting
Mining nodes vote to validate message and RLY is selected
Phase III
Block addition
RLY adds block into blockchain and forwards message
Phase I
Phase II
Phase III
Incident occurs
Transaction proposal by ORG
Voting by mining nodes and RLY selection
Block addition by RLY

Figure 3.1: Voting based message validation and dissemination.

Consensus	Applications
PBFT	Message validation [37], [113], high throughput [94], [112]
PoS	Trust or reputation management [7]
PoW	Consensus run by RSUs [110] or edge computing servers [111]

Table 3.1: Consensus Algorithms used in VANETs.

As shown in Figure 3.1, the voting-based consensus in VANETs is basically analogous to threshold-based message validation in which a message is considered valid only if it is confirmed by a threshold number of nodes located in a close proximity of an originator (ORG) [37]. Based on existing literature, Table 3.1 summarises consensus algorithms used for VANETs and indicates several usages of PBFT including message validation by voting, high throughput and ability to finalize transactions independently without RSU reliance.

3.1.2 Contributions

a) Threshold number of votes

In a voting-based consensus, the threshold value to finalise a validation is crucial. A low threshold value may lead to false validation, whereas a high threshold value can result in an increased latency. This chapter identifies a range of threshold values with varying percentage of malicious nodes which result in a decreased percentage of failure in validating a message by the proposed PoQF. The detailed derivations are presented in Proposition 3.4 and Assuming that $p_m^2 e^{-\frac{(n_{th}-\mu_m)^2}{\mu_m+n_{th}}} \approx (1-p_m)^2 \left(1-e^{-\frac{(\mu_h-n_{th}-1)^2}{2\mu_h}}\right) \approx 0$, (3.29)

leads towards the condition, $p_m > 0.5$. It shows that the condition in (3.28) is fulfilled when $p_m > 0.5$ and therefore, according to (3.26), minimum FV^{UB} is obtained when $n_{th} > \max(\mu_m, \mu_h)$. Since $\mu_m > \mu_h$only when $p_m > 0.5$, it means that minimum FV^{UB}at $p_m > 0.5$ is attained when $n_{th} > \mu_m$. ■

Proposition 3.5.

b) Security against malicious nodes

In a conventional PBFT, the nodes broadcast their votes only for a true transaction. The transaction is automatically marked as false if the threshold number of votes are not received. As a novel contribution, this chapter proposes a consensus algorithm which receives both true and false votes. Certain rules described in section 3.2.2 decide message validity if threshold number of votes are not received in either case or if there is a tie. These features enhance the security of the proposed PoQF.

c) Relay node selection

Traditionally, voting based consensus is used to verify credibility of a message. This chapter incorporates a relay selection mechanism in voting. Along with the votes to validate message, each node also computes and broadcasts its score, i.e., Quality Factor to become a relay. Similar to the miner election in a blockchain consensus, the node with the highest Quality Factor is elected as relay for message dissemination.

3.2 System Modelling and the Proposed Blockchain Design

3.2.1 Components

The proposed solution consists of following components:

- *Originator (ORG):* It is the node which is involved in an incident. ORG is the sender s of the message at first hop, i.e., when $n_{hop} = 1$, where n_{hop} is the hop number.
- *Mining node:* A node i which receives and responds to the message from sender s by broadcasting its vote for message validity and Quality Factor (QF_{i}) to become a relay node.
- *Quality Factor of node i (QF_i):* It is the parameter on the basis of which a node i qualifies to become a relay node. The calculations to compute QF_{i} are explained later in this section.
- *Relay node (RLY):* A node i with highest QF_i becomes RLY at a particular n_{hop}.
- *Proof-of-Quality-Factor (PoQF):* It is the voting and QF_i based consensus algorithm carried out in a decentralised manner by nodes in VANET to validate and disseminate a message via blockchain.
- *Microblock:* It is the block generated by mining node i recording its QF_i and vote towards validity of a message. Microblocks are appended in parallel in a blockchain at each hop.
- *Keyblock:* It is the block generated by RLY and records final validity status of a message after voting.
- *Waiting Time (τ_i):* It is a random waiting time for which node i waits before generating a microblock.
- *Failure in Validation (FV):* It is the probability that the original validity of a message is inverted after PoQF consensus at $n_{hop} = 1$.
- *Transaction Charge (TC):* $TC > 0$ is paid by mining node i while voting. The motivation behind introducing TC is to discourage malicious false votes.
- *Call Compensation (CC):* As a compensation of causing an incident, CC is the amount paid by ORG. It is distributed as an incentive to cooperative nodes, i.e., honest mining nodes and RLY at each hop.

3.2.2 The Proposed PoQF Consensus

The proposed PoQF consists of four stages, as illustrated in Figure 3.2. At the first stage, an incident occurs and a message is initiated by ORG involved in the incident. The message is analogous to a transaction proposal in a consensus that requires validation.

At the second stage, each mining node i generates a microblock, in which it records its vote towards validity of the message and QF_i, to become a potential RLY. A node i waits for time τ_i before it announces a microblock. τ_i is a randomly generated number following uniform distribution, i.e., $\tau_i \sim \mathcal{U}(a_{\tau_i}, b_{\tau_i})$, where a_{τ_i} and b_{τ_i} are lower and upper limits of τ_i, respectively, which are dependent on QF_i. The motivation behind using τ_i is three-fold: one is to prevent all nodes from transmitting at the same time and causing packet collision, second is to introduce fairness by giving less waiting time to nodes with higher QF_i and the third is to ensure randomization if node i and node j have $QF_i = QF_j$. Using uniform distribution to randomize scheduling of messages so as to avoid packet collision has been previously used in literature [114].

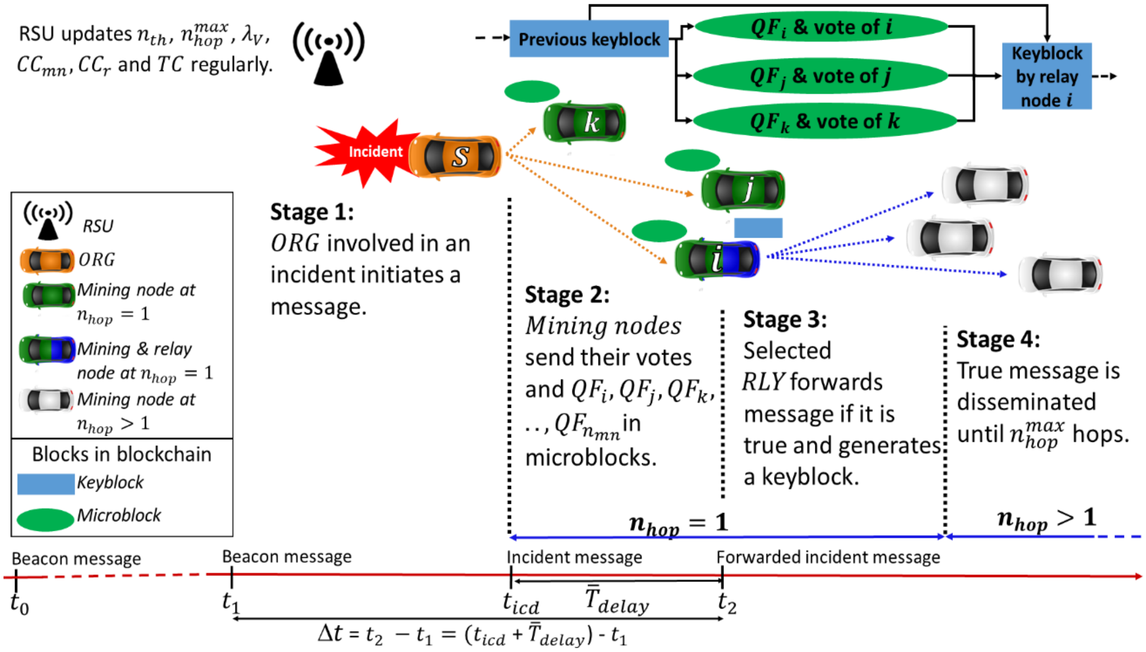
RSU updates n_{th}, n_{hop}^{max}, λ_V, CC_{mn}, CC_r and TC regularly.
Previous keyblock
QF_i & vote of i
QF_j & vote of j
QF_k & vote of k
Keyblock by relay node i
Incident
S
k
j
i
RSU
ORG
Mining node at $n_{hop} = 1$
Mining & relay node at $n_{hop} = 1$
Mining node at $n_{hop} > 1$
Blocks in blockchain
Keyblock
Microblock
Stage 1: ORG involved in an incident initiates a message.
Stage 2: Mining nodes send their votes and QF_i, QF_j, QF_k, .., $QF_{n_{mn}}$ in microblocks.
Stage 3: Selected RLY forwards message if it is true and generates a keyblock.
Stage 4: True message is disseminated until n_{hop}^{max} hops.
$n_{hop} = 1$
$n_{hop} > 1$
Beacon message
Beacon message
Incident message
Forwarded incident message
t_0
t_1
t_{icd}
$\overline{T}_{delay}$
t_2
$\Delta t = t_2 - t_1 = (t_{icd} + \overline{T}_{delay}) - t_1$

Figure 3.2: The proposed PoQF consensus.

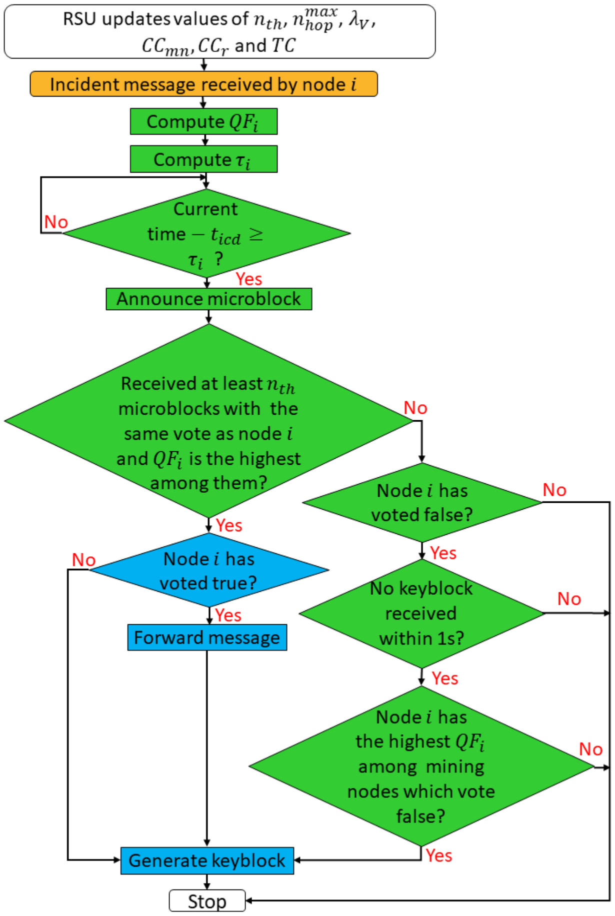
RSU updates values of n_{th}, n_{hop}^{max}, λ_V, CC_{mn}, CC_r and TC
Incident message received by node i
Compute QF_i
Compute τ_i
Current time $- t_{icd} \geq \tau_i$?
No
Yes
Announce microblock
Received at least n_{th} microblocks with the same vote as node i and QF_i is the highest among them?
No
Yes
Node i has voted false?
No
Yes
Node i has voted true?
No
Yes
Forward message
No keyblock received within 1s?
No
Yes
Node i has the highest QF_i among mining nodes which vote false?
No
Yes
Generate keyblock
Stop

Figure 3.3: Flowchart of actions by mining node at $n_{hop} = 1$.

At the third stage, node i is selected as a RLY if it fulfills two conditions. First, it has received at least n_{th} microblocks with the same votes as its own. Second, its QF_i is the highest among all microblocks with the same votes as its own. The motivation behind these two conditions instead of QF_i only is to enhance security of PoQF. For example, if a malicious node i with the highest QF_i among all mining nodes votes false for an originally true message and receives n_{th} microblocks with true votes, it cannot become RLY and earn incentive. Similarly, if an honest node i with the highest QF_i votes false for an originally false message but receives n_{th} microblocks with true votes, it cannot become a RLY to forward a false message. RLY will forward the message only if it is validated as true but always generate a keyblock to record message validity after PoQF and transactions, which are related to incentive distribution. As shown in Figure 3.3, if no node receives at least n_{th} microblocks with the same votes as its own until 1s, i.e. the maximum allowable latency for emergency message dissemination [3], the message is considered as false and a keyblock to record such transaction will be generated by the mining node i with highest QF_i, which voted false. If two $RLYs$ with opposing votes are selected (one with true vote and another with false vote), the message is considered true so that the cooperation may not be stopped in case of a true incident. The value of n_{th} corresponding to real traffic conditions is communicated to nodes by RSU.

The fourth stage is continuation of message dissemination. If the message is validated as true, it is disseminated after a new RLY selection by PoQF at each hop until it reaches a maximum specified distance or until $n_{hop} \leq n_{hop}^{max}$, where n_{hop}^{max} is the maximum number of hops up to which a message is required to be forwarded. It is noted that votes to validate a message are not required for $n_{hop} > 1$. It is simply because the validation of message has been done by adjacent witness nodes (mining nodes at $n_{hop} > 1$) through a camera or location/speed verification [16]. All other nodes beyond the first hop may not have access to validate the ORG.

3.2.3 QF_i Calculations

QF_i determines the quality of mining node i at the time when it forwards the message as RLY. Each node regularly shares its position and velocity via beacon message. As shown in Figure 3.2, two consecutive beacons messages are exchanged at t_0 and t_1 before the occurrence of incident. To compute QF_i, node i makes probability based predictions of distances with its neighbour nodes at time $t_2 = t_{icd} + \overline{T}_{delay}$, where t_{icd} is the time at which the incident message is received from the sender s (ORG or previous RLY) and $\overline{T}_{delay}$ is the mean time delay to finalize consensus and is described in details in Section 3.4.33.3.2. As QF_i decides the RLY, it is governed by two factors [115]: the probability of success that a node's transmission can reach to all of its neighbour nodes, i.e., Quality of SINR at t_2, $Q(SINR_i^{t_2})$, and the probability that its distance to the sender s is larger than a threshold for ensuring successful transmission over longer distances, i.e., Distance Factor at t_2, $DF_i^{t_2}$. Hence, $QF_i = Q(SINR_i^{t_2}) \cdot DF_i^{t_2}$.

a) $\underline{Q\left(SINR_i^{t_2}\right)}$

If mining node i becomes RLY, the SINR of a signal received at receiving node j from node i at t_2 is

$$SINR_{i,j} = \frac{\left(d_{i,j}\right)^{-\alpha}}{P_{noise}+\Sigma_{k=1,k\neq i}^{n_{itf}}\left(d_{j,k}\right)^{-\alpha}} \ , \tag{3.1}$$

where α is the path loss exponent and its value depends on fading environment [27], $d_{i,j}$ is the distance between node i and node j, $d_{j,k}$ is the distance between node j and interfering node k, n_{itf} is the number of interference nodes and P_{noise} is the noise power. For a successful message transmission, it is required that the SINR exceeds a certain threshold β_1, i.e., $SINR_{i,j} \geq \beta_1$. The probability that $SINR_{i,j} \geq \beta_1$ at t_2, i.e., $Pr\left(SINR_{i,j}^{t_2} \geq \beta_1\right)$ is given as

$$\begin{aligned} Pr\left(SINR_{i,j}^{t_2} \geq \beta_1\right) &= Pr\left(\frac{\left(d_{i,j}^{t_2}\right)^{-\alpha}}{P_{noise} + \Sigma_{k=1,k\neq i}^{n_{itf}}\left(d_{j,k}^{t_2}\right)^{-\alpha}} \geq \beta_1\right) \\ &= Pr\left(d_{i,j}^{t_2} \leq \left(\beta_1\left(P_{noise} + \Sigma_{k=1,k\neq i}^{n_{itf}}\left(d_{j,k}^{t_2}\right)^{-\alpha}\right)\right)^{-\frac{1}{\alpha}}\right), \end{aligned} \tag{3.2}$$

where $d_{i,j}^{t_2} = d_{i,j}^{t_1} + \Delta d_{i,j}^{\Delta t}$ is the distance between node i and node j at t_2 and $\Delta d_{i,j}^{\Delta t}$ is the relative distance change between node i and node j during $\Delta t = t_2 - t_1$. $d_{i,j}^{t_1}$ can be obtained from the beacon message received at t_1 and the expected value of $\Delta d_{i,j}^{\Delta t}$ can be found using Probability Density Function (PDF) of standard Gaussian distribution. Referring to the results in [27] and [116], the velocity of a node i follows a standard Gaussian distribution, i.e., $v_i \sim \mathcal{N}(0, \sigma_i^2 t)$, where $\sigma_i^2 = \frac{\left(v_i^{t_1} - v_i^{t_0}\right)^2}{t_1 - t_0}$ is variance of v_i and $v_i^{t_0}$ and $v_i^{t_1}$ denote v_i at t_0 and t_1, respectively, which are shared by node i via beacon messages. $\Delta d_{i,j}^{\Delta t}$ is defined as

$$\Delta d_{i,j}^{\Delta t} = \left(v_i^{t_1} - v_j^{t_1} + \Delta v_i^{\Delta t} - \Delta v_j^{\Delta t}\right)\Delta t \ , \tag{3.3}$$

where $\Delta v_i^{\Delta t}$ is the change in v_i during Δt. By the principle of linear combination of Gaussian variables, $\Delta v_i^{\Delta t} \sim \mathcal{N}(0, \sigma_i^2 \Delta t)$, $\Delta v_i^{\Delta t} - \Delta v_j^{\Delta t} \sim \mathcal{N}\left(0, \left(\sigma_i^2 + \sigma_j^2\right)\Delta t\right)$ and hence, $\Delta d_{i,j}^{\Delta t} \sim \mathcal{N}\left(0, \left(\sigma_i^2 + \sigma_j^2\right)\Delta t^3\right)$. If $v_i^{t_2}$ is not known, (3.2) can be calculated by assuming $\Delta d_{i,j}^{\Delta t}$ as a standard Gaussian variable.

Each node i calculates (3.2) as per Theorem 3.1. with respect to all its neighbour nodes. As n_{itf} is the number of neighbours of node j except node i, n_{itf} and $d_{j,k}^{t_2}$ are unknown to node i . It can estimate the expected values to find $Pr\left(SINR_{i,j}^{t_2} \geq \beta_1\right)$. Hence $\left(\beta_1\left(P_{noise} + \Sigma_{k=1,k\neq i}^{n_{itf}}\left(d_{j,k}^{t_2}\right)^{-\alpha}\right)\right)^{-\frac{1}{\alpha}}$ in (3.2) can be rewritten as $\left(\beta_1\left(P_{noise} + E\left(n_{itf}\right)E\left(d_{j,k}^{t_2}\right)^{-\alpha}\right)\right)^{-\frac{1}{\alpha}}$, where $E(.)$ denotes expected value. The location of nodes (vehicles) on road is assumed to follow an independent homogeneous spatial Poisson distribution with density parameter λ_V nodes/m^2 on a two-dimensional road segment with no separation of lanes in order to make it general and allow dynamic movement of nodes [117]. Therefore, $E\left(n_{itf}\right)$ can be estimated as the number of nodes within the transmission range of node j. Assuming that transmission range of each node is a uniform circular area with radius R, $E\left(n_{itf}\right)$ can be calculated as the number of nodes inside the area excluding node i, i.e., $E\left(n_{itf}\right) = \Sigma_{k=1}^{\pi R^2 \lambda_V}\left(k.\frac{\left(\pi R^2 \lambda_V\right)^k}{k!} e^{-\pi R^2 \lambda_V}\right) - 1$, where λ_V corresponding to real traffic conditions is communicated to nodes via RSU. It is noted that an adaptive λ_V corresponding to real traffic conditions is out of the scope of this chapter but can be locally estimated by calculating the number of received beacons [118] or with the use of edge computing servers [119].

- *Lemma 3.1:* $E\left(d_{j,k}^{t_2}\right) = \frac{2}{3R^2}\left(R^3 - {d_{neigh}^{min}}^3\right)$, where d_{neigh}^{min} is the minimum allowed distance between two neighbour nodes.

  Proof: The PDF of interference nodes at location (X, Y) within the area πR^2 is defined in [120] as $1/\pi R^2$. Therefore, $E\left(d_{j,k}^{t_2}\right)$ can be calculated as

$$E\left(d_{j,k}^{t_2}\right) = \int (X^2 + Y^2) f_{(X,Y)} dX dY. \tag{3.4}$$

Assuming transmission range is a uniform circle with radius R, then $X = Rcos\phi$ and $Y = Rsin\phi$. Therefore, (3.4) becomes

$$\begin{aligned} E\left(d_{j,k}^{t_2}\right) &= \int_{d_{neigh}^{min}}^{R} \int_{0}^{2\pi} \frac{z^2}{\pi R^2} d\phi dr \\ &= \frac{2}{3R^2}\left(R^3 - {d_{neigh}^{min}}^3\right). \end{aligned} \tag{3.5}$$

■

- *Theorem 3.1:* $Pr\left(SINR_{i,j}^{t_2} \geq \beta_1\right) =$

$$\begin{cases} \frac{1}{2}\left(erf\left(\frac{\Delta d_{i,j}^{\Delta t}}{\sqrt{2\left(\sigma_i^2+\sigma_j^2\right)\Delta t^3}}\right) - erf\left(\frac{-\Delta d_{i,j}^{\Delta t}}{\sqrt{2\left(\sigma_i^2+\sigma_j^2\right)\Delta t^3}}\right)\right), \; d_{i,j}^{t_1} \leq d_x \\ 1-\frac{1}{2}\left(erf\left(\frac{\Delta d_{i,j}^{\Delta t}}{\sqrt{2\left(\sigma_i^2+\sigma_j^2\right)\Delta t^3}}\right) - erf\left(\frac{-\Delta d_{i,j}^{\Delta t}}{\sqrt{2\left(\sigma_i^2+\sigma_j^2\right)\Delta t^3}}\right)\right), \; otherwise, \end{cases}$$

where $d_x = \left(\beta_1 \left(P_{noise} + E\left(n_{itf}\right) E\left(d_{j,k}^{t_2}\right)^{-\alpha}\right)\right)^{-\frac{1}{\alpha}}$ and $E\left(d_{j,k}^{t_2}\right)$ is defined in Lemma 3.1.

Proof: Since $d_{i,j}^{t_2} = d_{i,j}^{t_1} + \Delta d_{i,j}^{\Delta t}$, it is essential to first find the probability of $\Delta d_{i,j}^{\Delta t} \leq d_x - d_{i,j}^{t_1}$. If $d_{i,j}^{t_1} \leq d_x$, the actual required communication distance, $\Delta d_{i,j}^{\Delta t}$ can be calculated as in [116]

$$\Delta d_{i,j}^{\Delta t} = \begin{cases} d_x + d_{i,j}^{t_1}, & Case\ 1, \\ d_x - d_{i,j}^{t_1}, & Case\ 2, \end{cases} \tag{3.6}$$

where $Case$ 1 is either of the following

- node i and node j are moving towards each other
- node i is in front of node j, both moving in same direction, and $v_i < v_j$
- node j is in front of node i, both moving in same direction, and $v_i > v_j$

and $Case$ 2 is either of the following

- node i and node j are moving away from each other
- node i is in front of node j, both moving in same direction, and $v_i > v_j$
- node j is in front of node i, both moving in same direction, and $v_i < v_j$.

Therefore, PDF of $\Delta d_{i,j}^{\Delta t}$ can be defined as

$$f\left(\Delta d_{i,j}^{\Delta t}\right) = \frac{1}{\sqrt{2\pi\left(\sigma_i^2 + \sigma_j^2\right)\Delta t^3}} e^{-\frac{\left(\Delta d_{i,j}^{\Delta t}\right)^2}{2\left(\sigma_i^2+\sigma_j^2\right)\Delta t^3}}. \tag{3.7}$$

Consider both acceleration and deceleration, the Cumulative Distribution Function (CDF) can be calculated as

$$F\left(\Delta d_{i,j}^{\Delta t}\right) = \int_{-\Delta d_{i,j}^{\Delta t}}^{\Delta d_{i,j}^{\Delta t}} f\left(\Delta d_{i,j}^{\Delta t}\right) d\left(\Delta d_{i,j}^{\Delta t}\right). \tag{3.8}$$

As $F\left(\Delta d_{i,j}^{\Delta t}\right) = Pr\left(d_{i,j}^{t_2} \leq d_x\right) = Pr\left(SINR_{i,j}^{t_2} \geq \beta_1\right)$,

$$Pr\left(SINR_{i,j}^{t_2} \geq \beta_1\right) = \frac{1}{2}\left(erf\left(\frac{\Delta d_{i,j}^{\Delta t}}{2\left(\sigma_i^2+\sigma_j^2\right)\Delta t^3}\right) - erf\left(\frac{-\Delta d_{i,j}^{\Delta t}}{2\left(\sigma_i^2+\sigma_j^2\right)\Delta t^3}\right)\right). \tag{3.9}$$

Otherwise, if $d_{i,j}^{t_1} > d_x$, the actual required communication distance $\Delta d_{i,j}^{\Delta t}$ can be calculated as

$$\Delta d_{i,j}^{\Delta t} = \begin{cases} d_x - d_{i,j}^{t_1}, & Case\ 1, \\ d_x + d_{i,j}^{t_1}, & Case\ 2, \end{cases} \tag{3.10}$$

where $Case$ 1 and $Case$ 2 are the same as defined in above. As $d_{i,j}^{t1} > d_x$, for $d_{i,j}^{t_2} \leq d_x$, it is required that $\Delta d_{i,j}^{\Delta t} < 0$. Therefore, $1 - f\left(\Delta d_{i,j}^{\Delta t}\right)$ is calculated and ultimately $Pr\left(d_{i,j}^{t_2} \leq d_x\right) = Pr\left(SINR_{i,j}^{t_2} \geq \beta_1\right)$ is expressed as

$$Pr\left(SINR_{i,j}^{t_2} \geq \beta_1\right) = 1 - \frac{1}{2}\left(erf\left(\frac{\Delta d_{i,j}^{\Delta t}}{2\left(\sigma_i^2+\sigma_j^2\right)\Delta t^3}\right) - erf\left(\frac{-\Delta d_{i,j}^{\Delta t}}{2\left(\sigma_i^2+\sigma_j^2\right)\Delta t^3}\right)\right). \tag{3.11}$$

■

$Q\left(SINR_i^{t_2}\right) = \sum_{j=1}^{j=n_{neigh}} Pr\left(SINR_{i,j}^{t_2} \geq \beta_1\right)$, where n_{neigh} is the number of neighbours of node i whose position and velocities are exchanged through beacon messages.

b) $\underline{DF_i^{t_2}}$

It is the probability that one hop distance between node i and the sender s is larger than a minimum threshold, d_{hop}^{min}, and is defined as

$$DF_i^{t_2} = Pr\left(d_{i,s}^{t_2} > d_{hop}^{min}\right) = 1 - Pr\left(d_{i,s}^{t_2} \leq d_{hop}^{min}\right), \tag{3.12}$$

where $Pr\left(d_{i,s}^{t_2} \leq d_{hop}^{min}\right)$ can be found by using the same calculation as described in proof of Theorem 3.1.

- *Proposition 3.1:* $0 \leq QF_i \leq n_{neigh}$.

  Proof: $Q\left(SINR_i^{t_2}\right)$ is a sum of $Pr\left(SINR_{i,j}^{t_2}\right)$, for all neighbor nodes of i. Therefore, the possible range of $Q\left(SINR_i^{t_2}\right)$ is $0 \leq Q\left(SINR_i^{t_2}\right) \leq n_{neigh}$. According to (3.12), the possible range of $DF_i^{t_2}$ is $0 \leq DF_i^{t_2} \leq 1$. As $QF_i = Q\left(SINR_i^{t_2}\right) \cdot DF_i^{t_2}$, it can be concluded that $0 \leq QF_i \leq n_{neigh}$. ■

3.2.4 Adversary Model

Let n_{mn} be the number of mining nodes in a PoQF consensus out of which n_m nodes are malicious and n_h nodes are honest when $n_{hop} = 1$. A malicious node in the proposed blockchain design is defined as the node voting against the original validity of a message, that is, if a message is true, the malicious node will vote false and vice-versa. Let B_i be the behavior of mining node i. $B_i = 1$ when it is malicious and $B_i = 0$ when it is honest and $n_m = \sum_{i=1}^{n_{mn}} B_i$. B_i follows Binomial distribution, i.e., $B_i \sim \mathcal{B}(n_{mn}, p_m)$, where $p_m \epsilon [0,1]$ is the probability that $B_i = 1$. The reason for considering Binomial distribution is because it has only two possible outcomes for a discrete random number. So, one of the outcomes can be defined as malicious and another as honest. $\mu_m = p_m n_{mn}$ and $\mu_h = (1 - p_m) n_{mn}$ represent the mean number of malicious and honest nodes, respectively.

3.2.5 Incentive Distribution Mechanism

Call Compensation ($CC = CC_{mn} + CC_r$) is the virtual credit paid by ORG as a penalty to cause incident and compensate affected nodes. As shown in Figure 3.4, assuming that a message is successfully validated, CC at each direction consists of CC_{mn}, which is equally distributed among honest mining nodes at $n_{hop} = 1$, and CC_r, which is equally distributed among $RLYs$ at $n_{hop} = \{1,2,..,n_{hop}^{max}\}$, in case a message is validated as true. Otherwise, CC_r is transferred to CA as a penalty charge. The values of CC_{mn}, CC_r and n_{hop}^{max} are specified by CA and communicated to nodes via RSU.

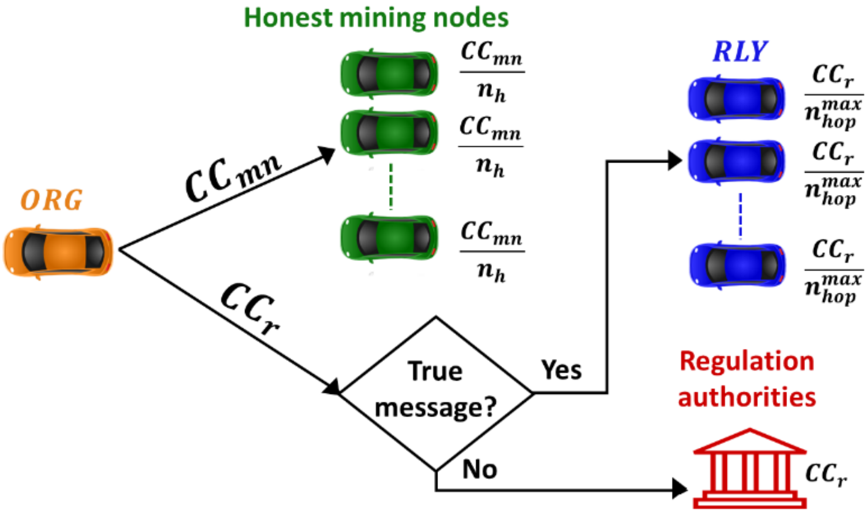

Figure 3.4: Distribution of Call Compensation.

a) *Reputation*

Let Rep_i be the reputation of node i. A node i is eligible to become a mining node and broadcast its vote if $Rep_i > Rep_T$, where Rep_T is a certain threshold. It is proposed that RLY is responsible to store updated Rep_i of each node i into the blockchain, whenever it performs block addition. Also, CC paid by ORG is inversely proportional to its reputation, i.e., $CC \propto \frac{1}{Rep_{ORG}}$.

Let Rep_{Rew} be the amount of reputation rewarded for honest behaviour and deducted for malicious behaviour. The updated reputation of mining node i after PoQF consensus at $n_{hop} = 1$ is

$$Rep_i = \begin{cases} Rep_i + Rep_{Rew}, & B_i = 0\,, \\ Rep_i - Rep_{Rew}, & B_i = 1\,. \end{cases} \tag{3.13}$$

At $n_{hop} > 1$, when message validation is not required, $Rep_i = Rep_i + Rep_{Rew}$ to encourage cooperation. The reputation of each RLY after PoQF consensus at every n_{hop} is updated as $Rep_{RLY} = Rep_{RLY} + Rep_{Rew}$.

b) Mechanism 1: TC for only voting towards false messages

If the message is successfully validated, the utility of a mining node i, U_i, after taking part in a PoQF consensus at $n_{hop} = 1$ is given as

$$U_i = \begin{cases} \dfrac{CC_{mn}}{n_h}, & B_i = 0 \; and\; message\; is\; true, \\ \dfrac{CC_{mn}}{n_h} - TC, & B_i = 0 \; and\; message\; is\; false, \\ -TC, & B_i = 1 \; and\; message\; is\; true, \\ 0, & B_i = 1 \; and\; message\; is\; false, \end{cases} \tag{3.14}$$

where $TC > 0$ is the Transaction Charge paid by mining node i only when it votes that a message is false. It is later paid to the RLY which generates the last keyblock related to a particular incident. The motivation of introducing TC is only to vote false is to promote fast dissemination of true message in case of emergency. The utility of RLY, U_{RLY}, is given as

$$U_{RLY} = \begin{cases} \dfrac{CC_r}{n_{hop}^{max}}, & n_{hop} \le n_{hop}^{max} \; and\; message\; is\; true, \\ n_m TC, & n_{hop} > n_{hop}^{max} \; and\; message\; is\; true, \\ n_h TC, & n_{hop} = 1 \; and\; message\; is\; false, \\ 0, & otherwise. \end{cases} \tag{3.15}$$

It is worth noting that a mining node i at $n_{hop} = 1$ selected as RLY will earn a cumulative utility of $U_i + U_{RLY}$. RLY records transactions related to U_i in the keyblock at $n_{hop} = 1$. For $n_{hop} > 1$, the corresponding RLY records transaction related to U_{RLY} of previous hop.

The message is disseminated until $n_{hop} \leq n_{hop}^{max}$ and PoQF is repeated until $n_{hop} \leq n_{hop}^{max} + 1$, because the last RLY at $n_{hop} \leq n_{hop}^{max} + 1$ records U_{RLY} of RLY at n_{hop}^{max}. As an incentive, it gains the reward of $n_m TC$ and records this transaction itself.

c) Mechanism 2: TC for all transmissions

Let TC be paid by every node which broadcasts a message or vote. The purpose of introducing TC for every transmission is to demotivate nodes to cast a fake vote or disseminate false message at the expense of their virtual credit. If the message is successfully validated, the utility of a mining node i, U_i, after taking part in a PoQF consensus at $n_{hop} = 1$ is given as

$$U_i = \begin{cases} \frac{CC_{mn}}{n_h} - TC, & B_i = 0\,, \\ -TC, & B_i = 1\,, \end{cases} \tag{3.16}$$

where CC_{mn} is the portion of CC distributed among mining nodes. Considering message dissemination in only one direction, let $CC = CC_{mn} + CC_r$, where $CC_{mn} = \omega_1 CC$, $CC_r = \omega_2 CC$, ω_1 and ω_2 are weights to divide CC among mining nodes and $RLYs$ respectively and $\omega_1 + \omega_2 = 1$. The utility of RLY is,

$$U_{RLY} = \begin{cases} \frac{CC_r}{n_{hop}^{max}} - TC, & message\ is\ true\,, \\ 0, & otherwise, \end{cases} \tag{3.17}$$

TC paid by every node is deposited to CA. CA regulates TC according to the incident recovery cost estimated at the location of incident and time of the day.

3.3 Theoretical Analysis

3.3.1 Security

a) Failure in Validation (FV)

In this chapter, the term FV is defined as the failure in determining the correct validity status of a message by PoQF consensus at $n_{hop} = 1$. Without loss of generality, it is assumed the probability that an ORG generates a false message, i.e., the ORG is malicious, is p_m and the probability of true message generation is $1 - p_m$. Therefore, FV can be expressed as

$$FV = p_m FV_{false} + (1 - p_m) FV_{true} \ , \tag{3.18}$$

where FV_{false} and FV_{true} denote FV of false and true message respectively. FV_{false} occurs when a malicious mining node receives at least n_{th} microblocks with malicious votes to mark an originally false message as true. Therefore, FV_{false} can be given as

$$FV_{false} = p_m Pr(n_m \geq n_{th}) \ . \tag{3.19}$$

FV_{true} occurs when an honest mining node does not receive n_{th} microblocks with honest votes to validate an originally true message and can be expressed as

$$FV_{true} = 1 - (1 - p_m) Pr(n_h \geq n_{th}) \ . \tag{3.20}$$

Bringing (3.19) and (3.20) into (3.18) gives

$$FV = 1 - p_m + p_m^2 Pr(n_m \geq n_{th}) - (1 - p_m)^2 Pr(n_h \geq n_{th}). \tag{3.21}$$

The following propositions are proved using tail inequalities for Binomial distribution [121].

- *Proposition* 3.2: The upper bound of $Pr(n_x \geq n_{th})$, where $x = m$ or h can be given as

$$Pr(n_x \geq n_{th})^{UB} = \begin{cases} e^{\frac{-(n_{th} - \mu_x)^2}{n_{th} + \mu_x}}, & n_{th} \geq \mu_x \\ \quad 1, & otherwise. \end{cases}$$

Proof: According to the multiplicative form of Chernoff bound [121], $Pr(X \geq (1 + \delta)\mu) \leq e^{-\frac{\delta^2 \mu}{2 + \delta}}$, where X is a sum of independent Binomial variables with mean μ and $\delta > 0$. Bringing $\mu = \mu_x$ and $(1 + \delta)\mu = n_{th}$ in Chernoff bound inequality gives

(3.22)

$$Pr(n_x \geq n_{th}) \leq \begin{cases} e^{\frac{-(n_{th}-\mu_x)^2}{n_{th}+\mu_x}}, & n_{th} \geq \mu_x\,, \\ 1, & otherwise. \end{cases}$$ ■

- *Proposition* 3.3: The lower bound of $Pr(n_x \geq n_{th})$, where $x = m$ or h can be given as

$$Pr(n_x \geq n_{th})^{LB} = \begin{cases} 1 - e^{\frac{-(\mu_x-n_{th})^2}{2\mu_x}}, & n_{th} \geq \mu_x \\ 0, & otherwise. \end{cases}$$

Proof: For $0 \leq \delta \leq 1$, Chernoff bound [121] states that $Pr(X \leq (1-\delta)\mu) \leq e^{-\frac{\delta^2\mu}{2}}$, which can be rewritten as $Pr(X \geq (1-\delta)\mu) \geq 1 - e^{-\frac{\delta^2\mu}{2}}$. Therefore, bringing $\mu = \mu_x$ and $(1-\delta)\mu = n_{th}$ in Chernoff bound inequality gives

$$Pr(n_x \geq n_{th}) \geq \begin{cases} 1 - e^{\frac{-(\mu_x-n_{th})^2}{2\mu_x}}, & n_{th} \geq \mu_x\,, \\ 1, & otherwise. \end{cases} \tag{3.23}$$ ■

By applying Proposition 3.2 and Proposition 3.3 in (3.21), the upper and lower bounds of FV, FV^{UB} and FV^{LB} can be derived as

$$FV^{UB} = 1 - p_m + p_m^2 Pr(n_m \geq n_{th})^{UB} - (1-p_m)^2 Pr(n_h \geq n_{th})^{LB}, \tag{3.24}$$

$$FV^{LB} = 1 - p_m + p_m^2 Pr(n_m \geq n_{th})^{LB} - (1-p_m)^2 Pr(n_h \geq n_{th})^{UB}. \tag{3.25}$$

The expanded forms of (3.24) and (3.25) under a varying range of n_{th} can be derived using (3.21), (3.22) and (3.23), as follows

$$FV \leq$$

$$\begin{cases} 1 - p_m + p_m^2 - (1-p_m)^2 \left(1 - e^{-\frac{(\mu_h-n_{th})^2}{2\mu_h}}\right), & n_{th} < min(\mu_m, \mu_h), \\ 1 - p_m + p_m^2 e^{-\frac{(n_{th}-\mu_m)^2}{\mu_m+n_{th}}} - (1-p_m)^2 \left(1 - e^{-\frac{(\mu_h-n_{th})^2}{2\mu_h}}\right), & \mu_m \leq n_{th} \leq \mu_h, \\ 1 - p_m + p_m^2, & \mu_h < n_{th} < \mu_m, \\ 1 - p_m + p_m^2 e^{-\frac{(n_{th}-\mu_m)^2}{\mu_m+n_{th}}}, & n_{th} > max(\mu_m, \mu_h), \end{cases}$$

(3.26)

and,

$$FV \geq$$

$$\begin{cases} 1 - p_m + p_m^2 \left(1 - e^{-\frac{(\mu_m - n_{th})^2}{2\mu_m}}\right) - (1 - p_m)^2, & n_{th} < min(\mu_m, \mu_h), \\ p_m - p_m^2, & \mu_m \leq n_{th} \leq \mu_h, \\ 1 - p_m + p_m^2 \left(1 - e^{-\frac{(\mu_m - n_{th})^2}{2\mu_m}}\right) - (1 - p_m)^2 e^{-\frac{(n_{th} - \mu_h)^2}{\mu_h + n_{th}}}, & \mu_h < n_{th} < \mu_m, \\ 1 - p_m - (1 - p_m)^2 e^{-\frac{(n_{th} - \mu_h)^2}{\mu_h + n_{th}}}, & n_{th} > max(\mu_m, \mu_h). \end{cases} \tag{3.27}$$

- *Proposition* 3.4: Minimum FV^{UB} at $p_m > 0.5$ can be obtained when $n_{th} > \mu_m$.

  Proof: To find the minimum FV^{UB}, we compare its value at two conditions of (3.26), i.e., $n_{th} > max(\mu_m, \mu_h)$ and $n_{th} < min(\mu_m, \mu_h)$, which are apparently less than others.

  $$\begin{aligned} &1 - p_m + p_m^2 e^{-\frac{(n_{th} - \mu_m)^2}{\mu_m + n_{th}}} \\ &< 1 - p_m + p_m^2 - (1 - p_m)^2 \left(1 - e^{-\frac{(\mu_h - n_{th} - 1)^2}{2\mu_h}}\right), \end{aligned} \tag{3.28}$$

  which can be simplified as

  $$p_m^2 e^{-\frac{(n_{th} - \mu_m)^2}{\mu_m + n_{th}}} < 2p_m - 1 - (1 - p_m)^2 \left(1 - e^{-\frac{(\mu_h - n_{th} - 1)^2}{2\mu_h}}\right). \tag{3.29}$$

  Assuming that $p_m^2 e^{-\frac{(n_{th} - \mu_m)^2}{\mu_m + n_{th}}} \approx (1 - p_m)^2 \left(1 - e^{-\frac{(\mu_h - n_{th} - 1)^2}{2\mu_h}}\right) \approx 0$, (3.29) leads towards the condition, $p_m > 0.5$. It shows that the condition in (3.32) is fulfilled when $p_m > 0.5$ and therefore, according to (3.26), minimum FV^{UB} is obtained when $n_{th} > max(\mu_m, \mu_h)$. Since $\mu_m > \mu_h$ only when $p_m > 0.5$, it means that minimum FV^{UB} at $p_m > 0.5$ is attained when $n_{th} > \mu_m$. ■

- *Proposition* 3.5: Minimum FV^{LB} can be obtained when $\mu_m \leq n_{th} \leq \mu_h$ at $p_m \leq 0.5$ and when $n_{th} > \mu_m$ at $p_m > 0.5$.

Proof: As we know that, $0 < e^{-x} \leq 1$ for any real valued x and $p_m \epsilon [0,1]$, it can be deduced from (3.27) that FV^{LB} is the minimum when $\mu_m \leq n_{th} \leq \mu_h$, which is only possible for $p_m \leq 0.5$. For $p_m > 0.5$, the minimum FV^{LB} can be obtained when $n_{th} > \mu_m$. ■

b) *Forks*

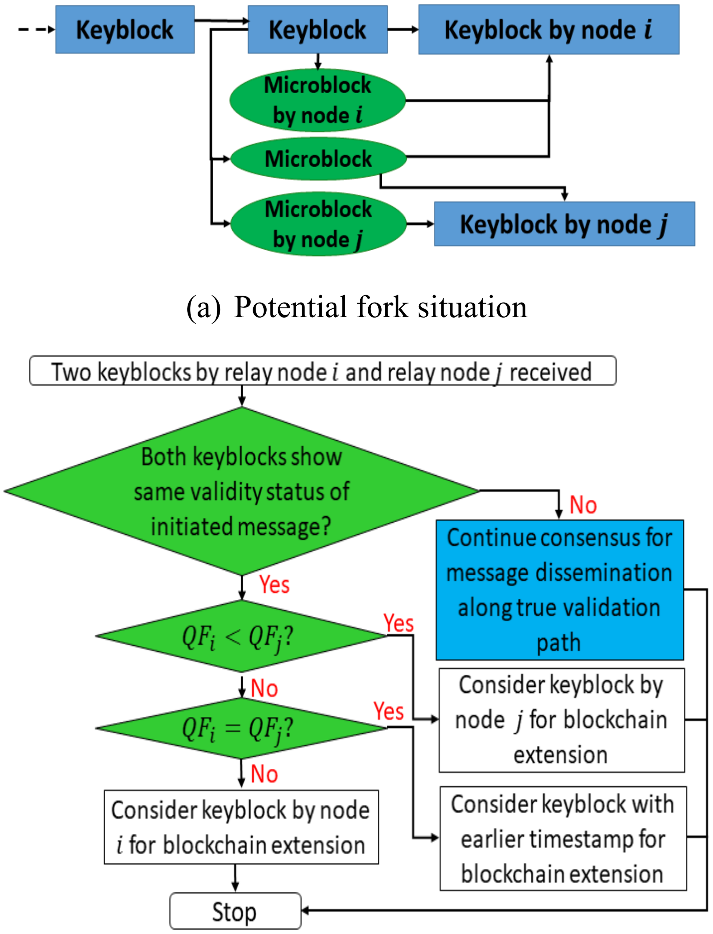
Keyblock
Keyblock
Keyblock by node *i*
Microblock by node *i*
Microblock
Microblock by node *j*
Keyblock by node *j*
Two keyblocks by relay node *i* and relay node *j* received
Both keyblocks show same validity status of initiated message?
No
Continue consensus for message dissemination along true validation path
Yes
$QF_i < QF_j$?
Yes
No
$QF_i = QF_j$?
Yes
Consider keyblock by node *j* for blockchain extension
No
Consider keyblock by node *i* for blockchain extension
Consider keyblock with earlier timestamp for blockchain extension
Stop

(a) Potential fork situation

(b) Flowchart of actions to resolve forks

Figure 3.5: Resolving forks in the proposed PoQF consensus.

In the proposed blockchain, a fork may be created as shown in Figure 3.5 (a) when two keyblocks are generated by different $RLYs$ at the same hop. Forks occur when two or more nodes fulfil both conditions of becoming a RLY, which are defined in Section 3.2. The flowchart of actions by a node in case of fork occurrence is shown in Figure 3.5 (b). If the keyblock by $RLY\ i$ marks the message as false and the keyblock by $RLY\ j$ marks the message as true, then the message dissemination is continued and new blocks are linked with the keyblock generated by $RLY\ j$. If both nodes show the same validity and $QF_i = QF_j$, the timestamps of both keyblocks are checked and the keyblock with the earlier timestamp is considered valid. However, if $QF_i > QF_j$, then new blocks are added in continuation with the keyblock generated by $RLY\ i$, regardless of the timestamp of $RLY\ j$. The motivation behind selecting the keyblock on the basis of QF_i instead of timestamp for blockchain extension is to discourage a possible cheating attempt by mining node j to become a RLY despite having $QF_i < QF_j$. Cheating by manipulating QF_i is difficult, as it is based on position and velocity of nodes which are shared through regular beacon message exchange and a cheating attempt can be easily detected and reported to concerned authority. In presence of forks, only the longest chain is stored.

c) *Game Theory Analysis of Incentive Distribution Mechanism 1: TC for only voting towards false messages*

We apply the game theory to analyse the impact of the proposed incentive distribution mechanism on actions of mining nodes at $n_{hop} = 1$ and evaluate the security of PoQF against colluding attack by mining nodes.

- *Players:* This game has n_{mn} players out of which n_h are honest and n_m are malicious. All players follow PoQF consensus as mining nodes and are located at $n_{hop} = 1$.
- *Actions:* Every player has two possible actions, honest, H, or malicious, M.
- *Utilities:* The payoff matrix in Table 3.2 shows (U_i, U_y), if FV does not occur after PoQF at $n_{hop} = 1$.

The analysis of the proposed incentive distribution mechanism is as follows.

- *Lemma 3.2:* Playing honest is the best response action of a mining node, if $CC_{mn} \geq n_h TC$.

  Proof: As shown in Table 3.2, if $TC \geq \frac{CC_{mn}}{n_h}$ and the message is false, playing honest will result in $U_y \leq 0$ which will be motivated to play maliciously. On the contrary, if $TC \leq \frac{CC_{mn}}{n_h}$, it makes $U_y \geq 0$ which will motivate the mining nodes to play honestly.

Therefore, to make honest as the best response action of mining nodes, it is required that $TC \leq \frac{CC_{mn}}{n_h}$ or $CC_{mn} \geq n_h TC$. ■

		Any other mining node	
		H	M
Mining node $\boldsymbol{i}$ with the highest $\boldsymbol{QF_i}$	H	$\left(\frac{CC_{mn}}{n_h}+\frac{CC_r}{n_{hop}^{max}},\frac{CC_{mn}}{n_h}\right)$	$\left(\frac{CC_{mn}}{n_h}+\frac{CC_r}{n_{hop}^{max}},-TC\right)$
	M	$\left(-TC,\frac{CC_{mn}}{n_h}\right)$	$(-TC,-TC)$

(a) True Message

		Any other mining node	
		H	M
Mining node $\boldsymbol{i}$ with the highest $\boldsymbol{QF_i}$	H	$\left(\frac{CC_{mn}}{n_h}+(n_h-1)TC,\frac{CC_{mn}}{n_h}-TC\right)$	$((n_h-1)TC,0)$
	M	$\left(0,\frac{CC_{mn}}{n_h}-TC\right)$	$(0,0)$

(b) False Message

Table 3.2: Payoff Matrix (U_i, U_y), where U_i=Utility of mining node i with the highest QF_i and U_y=Utility of any other mining node at $n_{hop} = 1$.

- *Proposition 3.6:* The action set (H, H) is both Pareto-optimal and Nash equilibrium of this game.

  Proof: From the payoff matrix in Table 3.2, it can be seen that no player can get the maximum utility by deviating from the action set (H, H), provided that Lemma 3.2 is fulfilled. In both true and false message cases, all mining nodes can get the highest payoff by playing honestly only. Therefore, the action set (H, H) is both Pareto-optimal and Nash equilibrium of this game. ■

- *Theorem 3.2:* A mining node cannot increase its expected utility sum by colluding with its malicious neighbours if $n_h TC \le CC_{mn} \le \frac{n_m CC_r}{n_{hop}^{max}(n_h - n_m)}$ and $p_m \le 0.5$.

Proof: Let n_{cp} colluding players form a group to mark a true message as false or a false message as true with a probability p_{cp}. The expected utility sum of colluding players as mining nodes, $E(U_{cp})$, if they mark a true message as false is

$$E(U_{cp}) = p_{cp}\left(\frac{CC_{mn}}{n_m} n_{cp} - n_{cp} TC\right) + (1 - p_{cp})\left(\frac{CC_{mn}}{n_h} n_{cp}\right). \tag{3.30}$$

The probability that one of the colluding players is selected as a RLY if the colluding attack is successful is n_{cp}/n_m and if colluding players play honestly is n_{cp}/n_h. Therefore, the total expected utility sum $E(U_{cp})$ is given as

$$\begin{aligned} E(U_{cp}) = p_{cp}&\left(\frac{CC_{mn}}{n_m} n_{cp} - n_{cp} TC + \left(\frac{n_{cp}}{n_m}\right) n_m TC\right) \\ &+ (1 - p_{cp})\left(\frac{CC_{mn}}{n_h} n_{cp} + \left(\frac{n_{cp}}{n_h}\right)\frac{CC_r}{n_{hop}^{max}}\right). \end{aligned} \tag{3.31}$$

To prevent collusion, it is required that $E(U_{cp}) \le E(U'_{cp})$, where U'_{cp} represents the utility of colluding players playing honestly, i.e.,

$$\begin{aligned} &p_{cp}\left(\frac{CC_{mn}}{n_m} n_{cp}\right) + (1 - p_{cp})\left(\frac{CC_{mn}}{n_h} n_{cp} + \left(\frac{n_{cp}}{n_h}\right)\frac{CC_r}{n_{hop}^{max}}\right) \\ &\le \frac{CC_{mn}}{n_h} n_{cp} + \left(\frac{n_{cp}}{n_h}\right)\frac{CC_r}{n_{hop}^{max}}, \end{aligned} \tag{3.32}$$

which leads towards the condition, $CC_{mn} \le \frac{n_m CC_r}{n_{hop}^{max}(n_h - n_m)}$. If $CC_{mn} \ge 0$, this condition can only be fulfilled when $n_h \ge n_m$, i.e., when $p_m \le 0.5$. Similarly, if colluding players attempt to mark a false message as true, then $E(U_{cp})$ is given as,

$$E(U_{cp}) = p_{cp}\left(\frac{CC_{mn}}{n_m}n_{cp} + \left(\frac{n_{cp}}{n_m}\right)\frac{CC_r}{n_{hop}^{max}}\right)$$
$$+(1-p_{cp})\left(\frac{CC_{mn}}{n_h}n_{cp} - n_{cp}TC + \left(\frac{n_{cp}}{n_h}\right)n_hTC\right). \tag{3.33}$$

To prevent collusion, it is required that $E(U_{cp}) \leq E(U'_{cp})$, which leads towards the condition $CC_{mn} \geq \frac{n_hCC_r}{n_{hop}^{max}(n_m-n_h)}$. Combining the condition of Lemma 3.2, it is needed that, $CC_{mn} \geq max\left(n_hTC, \frac{n_hCC_r}{n_{hop}^{max}(n_m-n_h)}\right)$. For $p_m \leq 0.5$, $CC_r > 0$ and $n_{hop}^{max} > 0$, we always get $\frac{n_hCC_r}{n_{hop}^{max}(n_m-n_h)} \leq 0$ and $n_hTC \geq \frac{n_hCC_r}{n_{hop}^{max}(n_m-n_h)}$. Therefore, it is proved that the incentive distribution mechanism is collusion resistant if $n_hTC \leq CC_{mn} \leq \frac{n_mCC_r}{n_{hop}^{max}(n_h-n_m)}$ and $p_m \leq 0.5$. ■

Thus, the incentive distribution mechanism is collusion resistant if values of CC_{mn}, CC_r and n_{hop}^{max} are adjusted such that Theorem 3.2 is fulfilled.

d) *Game Theory Analysis of Incentive Distribution Mechanism 2: TC for all transmissions*

The following proposition and theorem are presented to prove security of the incentive distribution mechanism against collusion.

- *Lemma 3.3*: Playing honest is the best response action of all players if $TC < min\left(\frac{CC_{mn}}{n_h}, \frac{CC_r}{n_{hop}^{max}}\right)$.

  Proof: According to (3.16), if $TC < 0$, U_i would be positive if a mining node i plays maliciously. On the other hand, if $TC \geq \frac{CC_{mn}}{n_h}$, U_i will be zero or negative if it plays honestly. In either of these cases, the best response action of players would be to play maliciously or selfishly. Also, according to (3.17), if $TC \geq \frac{CC_r}{n_{hop}^{max}}$, U_{RLY} will be negative and RLY will be motivated to play selfishly. Therefore TC must be set such that the action results in positive U_i and U_{RLY} or profit gain of both mining node i and RLY.

■

- *Theorem 3.3:* The proposed solution motivates all players to play honestly and is resistant against collusion of $RLYs$ if $0 \leq TC < min\left(\frac{CC_{mn}}{n_h}, \frac{CC_r}{n_{hop}^{max}}\right)$.

Proof: Let us consider the case with one conspired RLY at n_{hop}, i.e., $RLY(n_{hop})$. Suppose $CP = \{RLY(n_{hop}), RLY(n_{hop}+1)\}$ is a group of colluding players. CP conspires to form a longer path with an additional hop, i.e., $ORG \rightarrow RLY(n_{hop}) \rightarrow RLY(n_{hop}+1)$ instead of the most appropriate path, i.e., $ORG \rightarrow RLY'(n_{hop}+1)$. In both cases, the message reaches a maximum specified distance. Let p_{cp} be the probability with which $RLY(n_{hop})$ encounters $RLY(n_{hop}+1)$, where $p_{cp} \in [0,1]$ and ${p_{cp}}^2$ to encounter both ORG and $RLY(n_{hop}+1)$. The expected utility sum of CG, $E(U_{cp})$ is

$$E(U_{cp}) = {p_{cp}}^2 \left(U_{RLY(n_{hop})} + U_{RLY(n_{hop}+1)}\right) + (1-{p_{cp}}^2)U_{RLY'(n_{hop}+1)}, \tag{3.34}$$

or,

$$E(U_{cp}) = {p_{cp}}^2 \left(\frac{2CC_r}{n_{hop}^{max}} - 2TC\right) + (1-{p_{cp}}^2)\left(\frac{CC_r}{n_{hop}^{max}} - TC\right), \tag{3.35}$$

Since $n_{hop}^{max} = 2$ for collusion case and $n_{hop}^{max} = 1$ for non-collusion, $E(U_{cp})$ becomes

$$E(U_{cp}) = CC_r - TC - {p_{cp}}^2 TC. \tag{3.36}$$

To avoid collusion of relay nodes, it is required that $E(U_{cp}) \leq U_{RLY'(n_{hop}+1)}$, that is,

$$CC_r - TC - {p_{cp}}^2 TC \leq CC_r - TC. \tag{3.37}$$

It follows that

$$-{p_{cp}}^2 TC \leq 0, \tag{3.38}$$

or $TC \geq 0$. Similarly, by generalizing cases when $n_{cp} > 2$, the collusion resistant condition can be derived, that is, ${p_{cp}}^{n_{cp}}TC \geq 0$. Hence, for any $p_{cp} \in [0,1]$, the proposed incentive distribution mechanism is relay node collusion resistant if $TC \geq 0$. The upper bound of TC required to motivate all players to play honestly, i.e., $TC < min\left(\frac{CC_{mn}}{n_h}, \frac{CC_r}{n_{hop}^{max}}\right)$ is proved in Lemma 3.3. Therefore, the proposed incentive mechanism is secure against malicious actions and collusion if $0 \leq TC < min\left(\frac{CC_{mn}}{n_h}, \frac{CC_r}{n_{hop}^{max}}\right)$. ■

3.3.2 Latency and Throughput

The MAC throughput in bit/second is defined in [122] as $\lambda_{MAC} = p_t \cdot p_{suc} \cdot \frac{L}{T_{avg}}$, where $p_t = \frac{2}{W+2}$ is the average transmission probability of a node, W is the contention window size, p_{suc} is the probability of success transmission, L is the average length of a packet and T_{avg} is the average length of a time slot in Distributed Coordination Function (DCF). $p_{suc} = n_{tr} \cdot p_t \cdot (1-p_t)^{n_{tr}-1}$, where n_{tr} is the number of nodes contending the channel for transmission. According to IEEE 802.11 standard [122], T_{avg} is

$$T_{avg} = p_{idle} \cdot T_{slot} + p_{suc} \cdot T_{suc} + p_{col} \cdot T_{col}, \tag{3.39}$$

where T_{slot} is the unit time slot in DCF scheme, $p_{idle} = (1-p_t)^{n_{tr}}$ and $p_{col} = 1 - p_{idle} - p_{suc}$ are the probabilities of a node encountering an idle slot and collided transmission respectively, T_{suc} and T_{col} are average time for success and collided transmission respectively and are given as $T_{col} = T_{RTS} + T_{DIFS} + T_{slot}$ and $T_{suc} = T_{RTS} + T_{DIFS} + T_{CTS} + T_{ACK} + 3T_{SIFS} + 4T_{slot} + \frac{L}{DR}$, where T_{DIFS} and T_{SIFS} are time intervals for DCF Interframe space (DIFS) and Short Interframe Space (SIFS) respectively, T_{RTS}, T_{CTS} and T_{ACK} are pre-specified time intervals reserved for DCF related operations and DR is the average data rate among nodes. As λ_{MAC} is defined in bit/second, the average time consumption, T_{MB}, to successfully transmit a vote in a microblock of length L bits is

$$T_{MB} = \frac{L(bits)}{\lambda_{MAC}(bit/second)} = \frac{T_{avg}}{p_t \cdot p_{suc}}. \tag{3.40}$$

T_{MB} varies with n_{tr} only if W, L, T_{slot}, T_{col} and T_{suc} are considered as fixed for all transmitting mining nodes. As $1 \leq n_{tr} \leq n_{mn}$ and $n_{mn} = n_{neigh}$ if all neighbour nodes of ORG take part in consensus. If n_{neigh} is estimated by the number of received beacons [118] or with the use of edge computing servers [119], a node i can find T_{MB}^{min} and T_{MB}^{max}. Considering a fixed transmission range and a homogeneous distribution for all nodes, it can be assumed that n_{neigh} is statistically the same for every node. According to Proposition 3.1, $n_{neigh} - QF_i$ can be considered as the ranking of mining node i to announce its microblock. In this way, node i with a large QF_i can have less validation time before announcing a microblock. Consider T_{MB} as the time required by a mining node to successfully transmit a microblock. The lower bound of τ_i is given as

$$a_{\tau_i} = T_{MB}^{min}\left(n_{neigh} - QF_i\right), \tag{3.41}$$

and the upper bound of τ_i is given as

$$b_{\tau_i} = T_{MB}^{max}\left(n_{neigh} - QF_i\right), \tag{3.42}$$

For n_{mn} microblocks, the total time consumption (or validation latency), T_{delay} can be in the range $T_{MB}^{min} \cdot n_{mn} \leq T_{delay} \leq T_{MB}^{max} \cdot n_{mn}$. A mining node i with the highest QF_i becomes RLY as soon as it receives at least n_{th} microblocks and does not need to wait for receiving all n_{mn} microblocks. Therefore, T_{delay} is reduced for small n_{th} and lower and upper bounds of T_{delay} when a message is successfully validated by an honest node at $n_{hop} = 1$ can be found.

- *Proposition* 3.7*:* $T_{delay}^{LB} = T_{MB}^{min} \cdot n_{th}$.

  Proof: T_{delay} is the minimum when RLY receives first n_{th} consecutive microblocks with same votes immediately following the incident message. ■

- *Proposition* 3.8*:* $T_{delay}^{UB} = T_{MB}^{max} \cdot (n_{th} + p_m n_{mn})$.

  Proof: The maximum number of microblocks with malicious votes is $p_m n_{mn}$. T_{delay} will be the maximum if an honest RLY receives all $p_m n_{mn}$ microblocks before receiving n_{th} honest microblocks. ■

A keyblock is generated by RLY after the message validation. Therefore, the throughput in terms of number of keyblocks generated per second can be estimated as

$$\lambda_{KB} = \frac{1}{T_{delay}+T_{eyp}}, \tag{3.43}$$

where T_{eyp} is the time required to encrypt a keyblock.

3.3.3 Asymptotic Complexities

Consensus	**Latency**	**Security**	**Communications**
PoW	$\Theta(\kappa)$ [123]	$\Omega\left(\frac{n_{mn}}{2}\right)$ [124]	$\Theta(1)$ [123]
PoS	$\Omega(\kappa)$ [123]	$\Omega\left(\frac{2n_{mn}}{3}\right)$ [125]	$\Theta(1)$ [123]
PoET	$\Omega(\kappa)$ [78]	$\Omega\left(\frac{log\ log\ n_{mn}}{log\ n_{mn}}\right)$ [78]	$\Theta(1)$ [78]
PBFT	$n_{mn}O(1)$ [123]	$\Omega\left(\frac{n_{mn}-1}{2}\right)$ [113]	$O(n_{mn}^2)$ [126]
PoQF	$\kappa O(1)$	$\Omega\left(\frac{n_{mn}}{2}\right)$	$O(n_{mn})$

Table 3.3: Comparison of asymptotic complexities.

In this subsection, the scalability of various consensus algorithms are compared by analysing latency complexity, i.e., the time consumption required to confirm a transaction, security complexity, i.e., the minimum number of malicious nodes to control consensus, and communication complexity, i.e., the number of exchange messages required to validate a transaction. Without loss of generality, the asymptotic latency, security and communication complexity of various consensus algorithms are identified in Table 3.3 in terms of number of nodes participating in mining competition, n_{mn} and consensus parameter, κ, which is unique to each algorithm. κ refers to the difficulty level of hash puzzle in PoW, synchronization level in PoS, waiting time in PoET and number of minimum votes required in voting based algorithms (PBFT and PoQF). Standard mathematical notations are used in Table 3.3, i.e., $\Omega(.)$, $O(.)$ and $\Theta(.)$ denote the order of *at least*, *at most* and *exactly* respectively.

Table 3.3 shows that κ affects the latency in PoW, PoS and PoET. Despite the fast consensus of PoS, a strong synchronization among edge computing resources is needed for efficient running [123]. Latency of PoET depends on the length of waiting time which follows a fixed probability distribution. PoQF has to wait for a threshold number of votes, which has an impact on latency but its scalability does not rely on large computation power or storage capacity of nodes. PoET offers the least security and can be controlled by only a small fraction of malicious nodes [78]. According to Theorem 3.2, PoQF is secure against the collusion attack when $p_m \leq 0.5$. It provides the same security as PoW which is better than PBFT but worse than PoS [125]. In communication complexity, PoW, PoS and PoET are more efficient than PoQF, since they do not require multiple message exchanges. Despite the voting nature of PoQF, it has lower communication complexity than PBFT. Moreover, in VANETs, n_{mn} cannot be increased beyond a certain threshold due to limited number of nodes within a transmission range R and d_{min}^{neigh}, which makes PoQF scalable and applicable in V2V communications.

3.4 Simulated Performance Analysis

3.4.1 Simulation Setup

In this section, the performance of the proposed blockchain and PoQF consensus is analysed using OMNeT++ and SUMO (Simulation of Urban Mobility). An open-source framework VeINS (Vehicles In Network Simulation) is used to integrate SUMO with OMNeT++[1]. The code of blockchain implementation in OMNeT++ is mentioned in Appendix B. The simulation parameters listed in Table 3.4. Since n_{mn} are neighbor nodes of a sender s, $n_{mn} \leq 40$ will be considered when nodes are homogeneously distributed with a maximum of 200 nodes/km^2 and it is a reasonable assumption of maximum number of vehicles within a transmission range when the safe distance between nodes are maintained on road. Evaluation results are averaged over 100 simulation runs.

[1] Source code is available at https://zenodo.org/record/5172646#.YW16F_rMKUl.

Parameters	**Values**	**Parameters**	**Values**
Simulation time	200 s	Protocol	IEEE 802.11p
Size of area	10 km × 10 km	Encryption	SHA-256
Beacon frequency	0.1 s	P_{noise}	-99 dBm
λ_V	[50, 200] nodes / km^2	R	250 m
α	3	β_1	8 dB
Mobility model	Krauss	d_{neigh}^{min}	12 m
Average velocity	40 km/hr	d_{hop}^{min}	100 m
L	756 bytes	W	32
T_{RTS}	53 μs	T_{CTS}	37 μs
T_{DIFS}	58 μs	T_{SIFS}	32 μs
T_{ACK}	37 μs	T_{slot}	13 μs
T_{eyp}	3332.11 μs	DR	6 Mbps

Table 3.4: Simulation parameters for PoQF message dissemination.

3.4.2 Security

Figure 3.6 shows FV with respect to n_{mn} at different p_m and n_{th}. Two different values of p_m are chosen to show the results at both low ($p_m < 0.5$) and high ($p_m > 0.5$) densities of malicious mining nodes presented in the network. As shown in Figure 3.6 (a), FV with $p_m = 0.3$ is lower than FV with $p_m = 0.7$ when $n_{th} = 3$, i.e., $n_{th} \leq \mu_m$. It shows that a low n_{th} is suitable only for low p_m when honest nodes are in majority. On the contrary, as shown in Figure 3.6 (b), FV with $p_m = 0.3$ is higher than FV with $p_m = 0.7$ when $n_{th} = n_{mn}$, i.e., $n_{th} > \mu_m$. This is because when $n_{th} = n_{mn}$ both malicious and honest mining nodes are unable to finalize consensus within the maximum allowable latency of 1s and the message is marked as false. With $p_m = 0.3$, the probability of false message occurrence is lower than that of true message occurrence and it is hard to collect $n_{th} = n_{mn}$ honest votes to validate a true message. In this case, $FV^{UB} \approx 1 - p_m$ depicts the worst-case scenario of maximum probability of true message generation which will be marked as false. With $p_m = 0.7$, the probability of true message occurrence is lower than that of false message occurrence. FV does not occur when both honest and malicious nodes are unable to collect votes for a false message. It only occurs when a true message is not validated. As shown in Figure 3.6 (b), $FV^{LB} \approx 1 - p_m$ with $p_m = 0.7$, depicts the percentage of true messages which are not validated by PoQF.

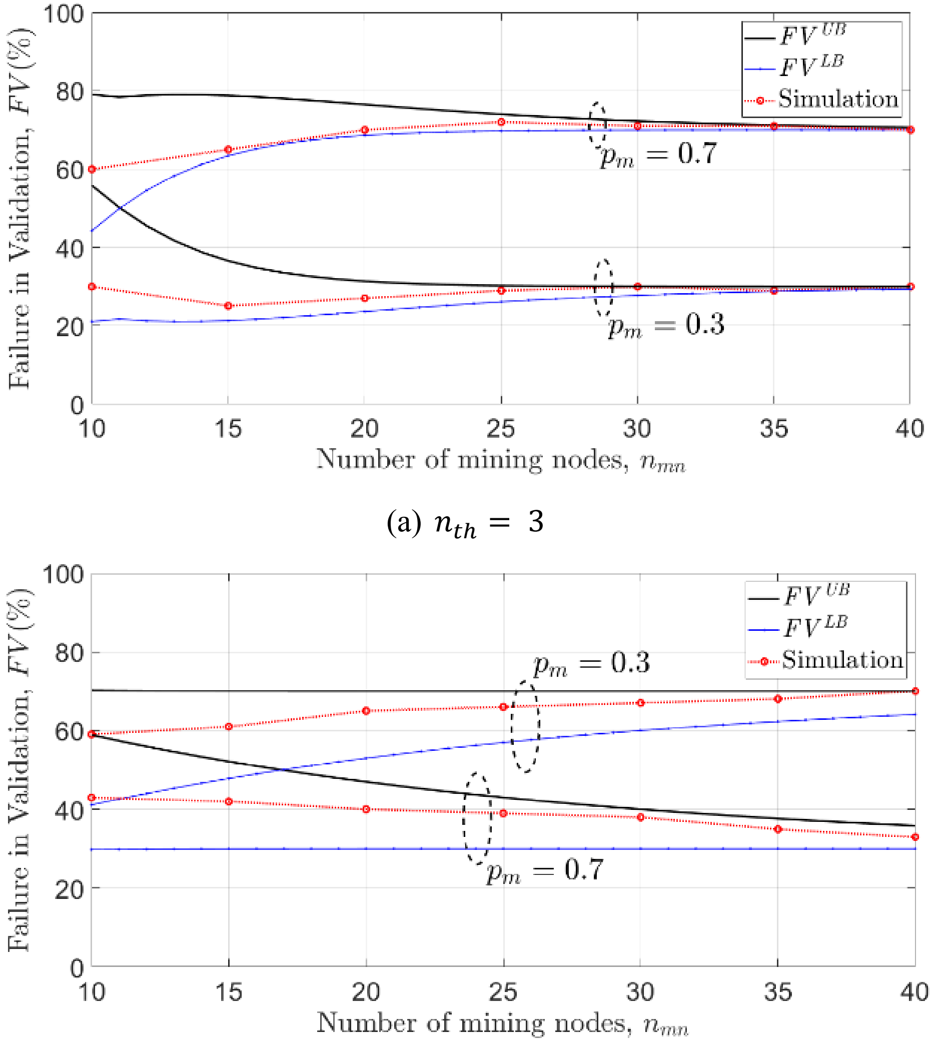

(a) $n_{th} = 3$

(b) $n_{th} = n_{mn}$

Figure 3.6: FV with respect to n_{mn}.

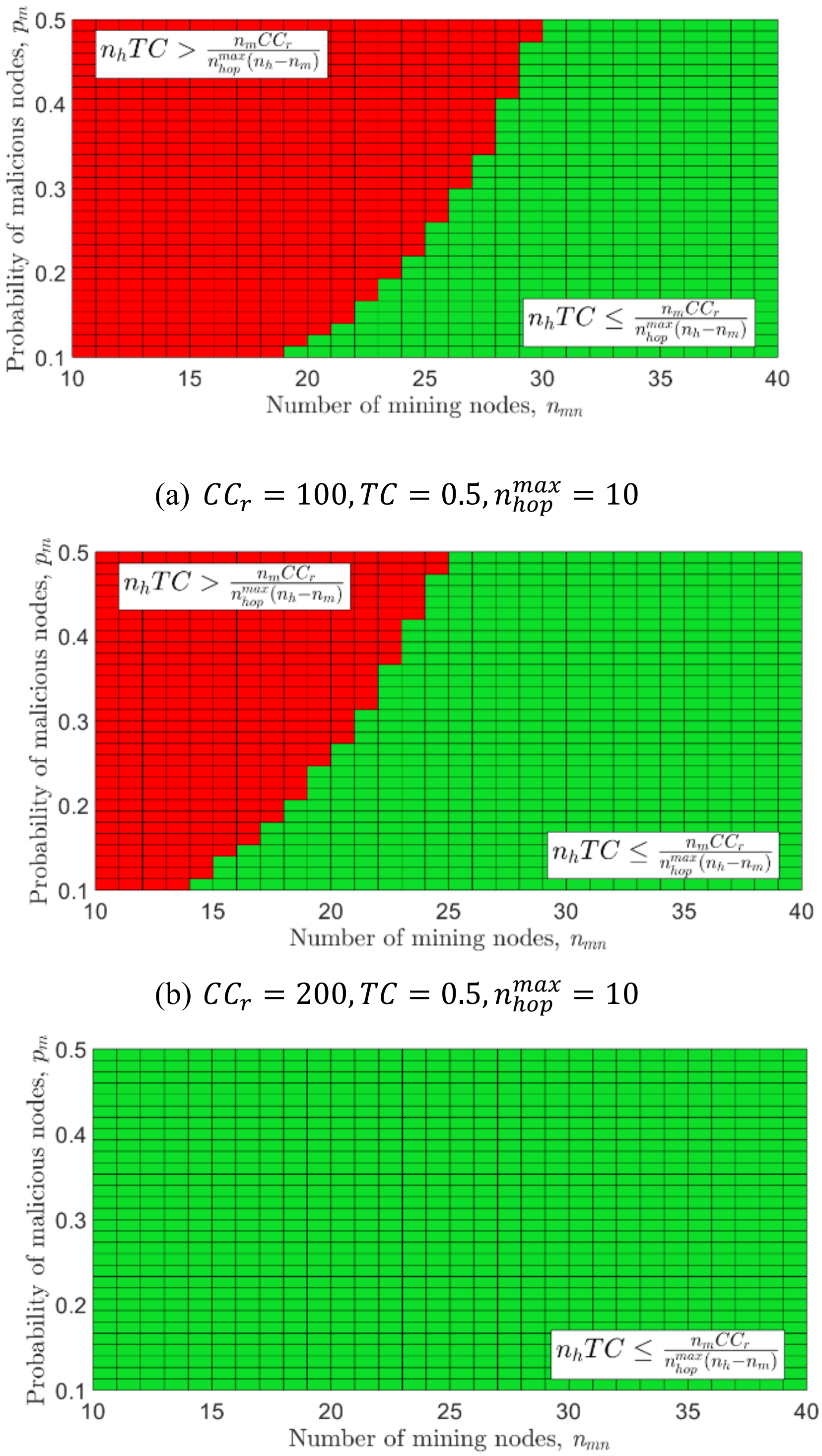

(a) $CC_r = 100, TC = 0.5, n_{hop}^{max} = 10$

(b) $CC_r = 200, TC = 0.5, n_{hop}^{max} = 10$

(c) $CC_r = 200, TC = 0.1, n_{hop}^{max} = 6$

Figure 3.7: Setting up CC_r, TC and n_{hop}^{max} for collusion resistant incentive distribution.

Figure 3.7 shows the impact of parameters: CC_r, TC and n_{hop}^{max}, on the collusion resistance feature of incentive distribution mechanism. According to Theorem 3.2, the incentive distribution mechanism is collusion resistant if $n_h TC \leq CC_{mn} \leq \frac{n_m CC_r}{n_{hop}^{max}(n_h - n_m)}$ and $p_m \leq 0.5$. As B_i follows Binomial distribution, it can be assumed that $n_m \approx \mu_m$ and $n_h \approx \mu_h$. Based on this assumption, Figure 3.7 (a) and (b) show that the incentive distribution mechanism cannot be collusion resistant for every n_{mn}, p_m under the fixed CC_r, TC and n_{hop}^{max}. However, in Figure 3.7 (c), when $CC_r = 200, TC = 0.1, n_{hop}^{max} = 6$, $n_h TC \leq \frac{n_m CC_r}{n_{hop}^{max}(n_h - n_m)}$ is satisfied for every $n_{mn} \in (10{,}40)$ and $p_m \in (0{,}0.5)$. Therefore, for a collusion resistant incentive distribution mechanism, it is required that the combination of CC_r, TC and n_{hop}^{max} are adjusted with varying n_{mn} and p_m, such that it is possible to choose CC_{mn} within the boundaries defined by Theorem 3.2. Apart from the security reason, a low n_{hop}^{max} is also favourable for successful message delivery, as the failure of multi-hop connectivity in VANETs increases with the number of hops.

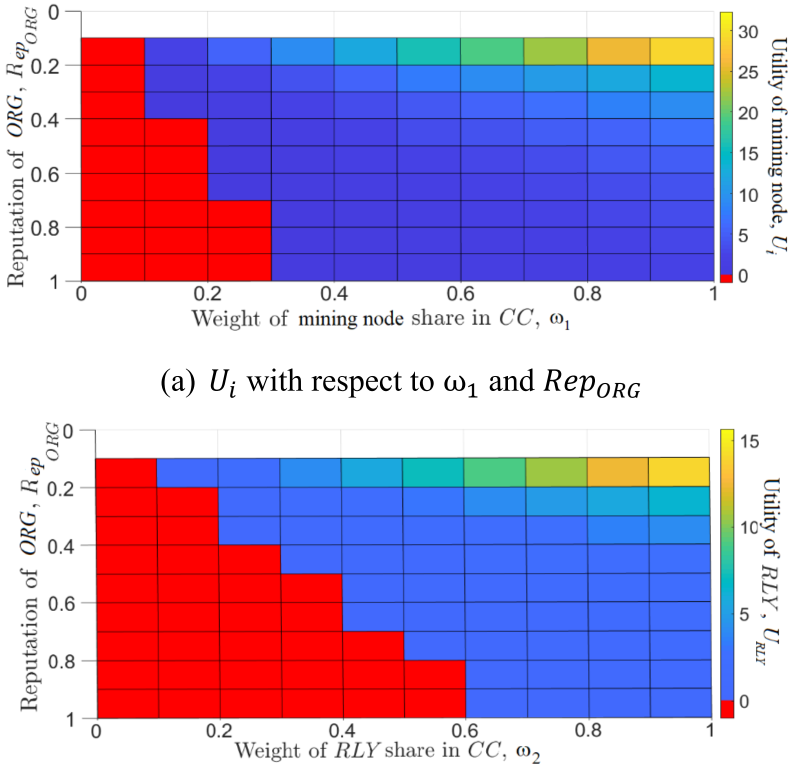

(a) U_i with respect to ω_1 and Rep_{ORG}

(b) U_{RLY} with respect to ω_2 and Rep_{ORG}

Figure 3.8: Setting up ω_1 and ω_2 for collusion resistant incentive distribution.

Figure 3.8 shows the combined effect of Rep_{ORG} and range of values of ω_1 and ω_2 resulting in different U_i and U_{RLY} according to incentive distribution mechanism 2 defined in Section 3.2.5 (c). In simulation, $CC = 10/Rep_{ORG}$ is arbitrarily set. Higher Rep_{ORG} leads to lower amount of CC, thereby resulting in less U_i and U_{RLY}. However, it must be ensured that blockchain-enabled message dissemination results in profit gain of all nodes, despite of deduction of TC. As shown in Figure 3.8, $\omega_1 > 0.3$ and $\omega_2 > 0.6$ would always result in positive U_i and U_{RLY}, irrespective of the value Rep_{ORG}. A positive expected utility motivates players to play honestly and discourages malicious actions, therefore resulting in a secure incentive distribution mechanism.

3.4.3 Latency and Throughput

Figure 3.9 shows T_{delay} of successful message validation with respect to n_{mn} at different values of p_m with $n_{th} = \mu_m + 1$. It can be seen that T_{delay} increases with p_m because of more frequent generation of microblocks by malicious nodes. Figure 3.9 (c) and (d) show that T_{delay}^{UB} exceeds the maximum allowable latency requirement of 1s [3] when $p_m \geq 0.6$ and $n_{mn} \geq 30$. At $p_m = 0.8$ and $n_{mn} \geq 35$, the mining nodes are unable to finalize consensus within 1s.

Figure 3.10 shows λ_{KB} of PoQF consensus at various n_{mn} and p_m. The highest λ_{KB} achieved is 11 keyblock/s at $p_m = 0.1$ and $n_{mn} = 15$ and the lowest is 0.9 keyblock/s at $p_m \geq 0.8$ and $n_{mn} = 35$, which means that at higher n_{mn} and p_m, PoQF with $\lambda_{KB} < 1$ keyblock/s may not be able to generate block within the limit of maximum allowable latency of 1s. This shows that the proposed blockchain exhibits better performance specifically at lower values of n_{mn} and p_m. λ_{KB} can be improved by offloading computations required for encrypting a keyblock to a nearby edge computing server which have high computation power, thereby reducing T_{eyp}.

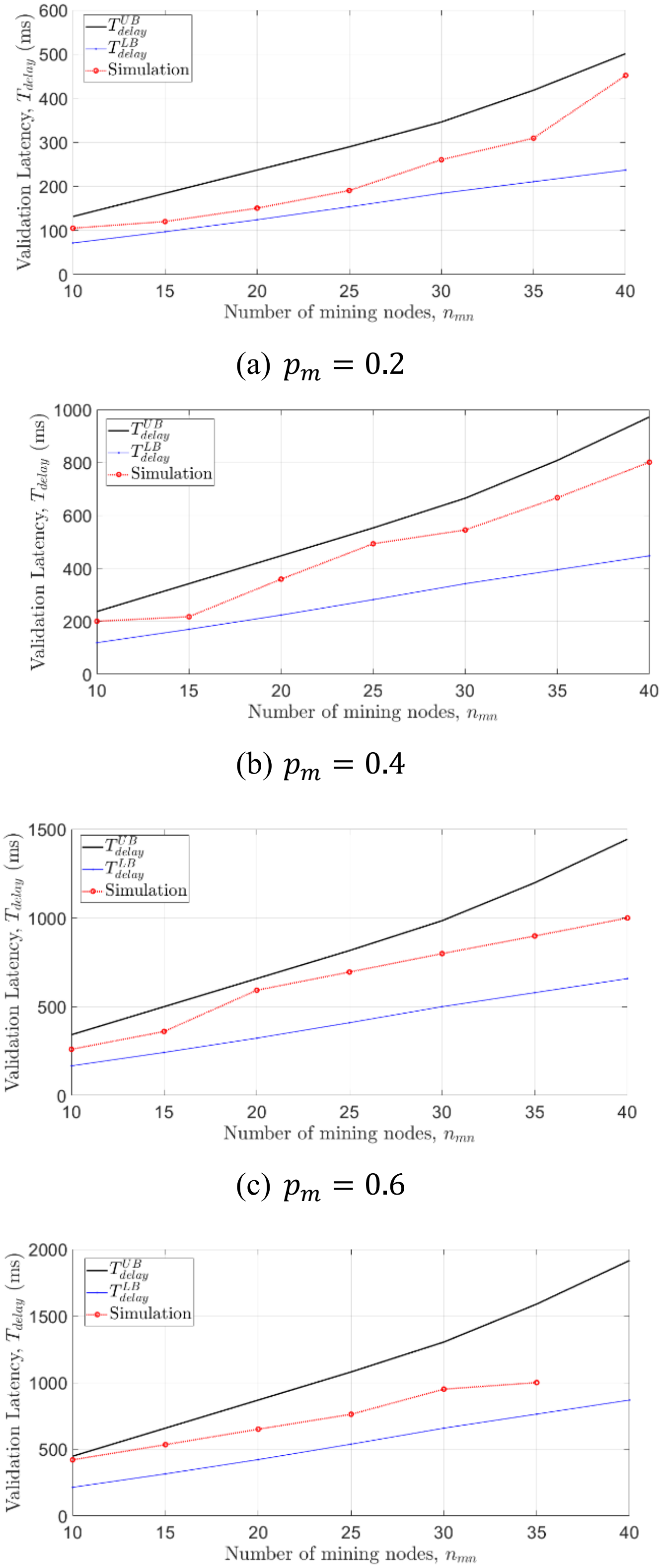

(a) $p_m = 0.2$

(b) $p_m = 0.4$

(c) $p_m = 0.6$

(d) $p_m = 0.8$

Figure 3.9: T_{delay} with respect to n_{mn}.

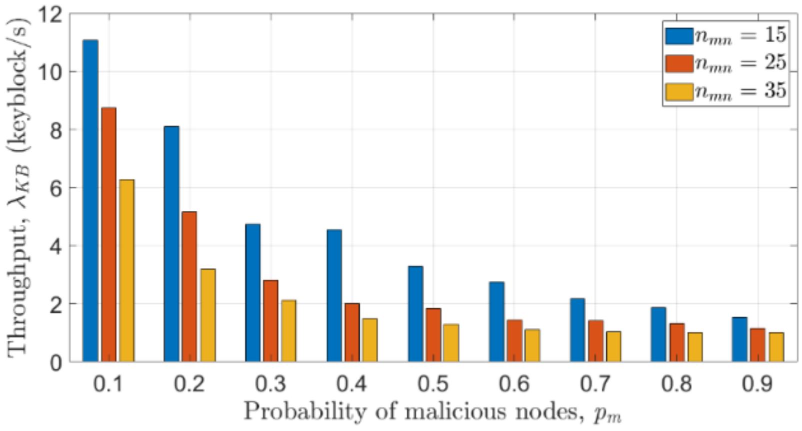

Figure 3.10: λ_{KB} with respect to p_m.

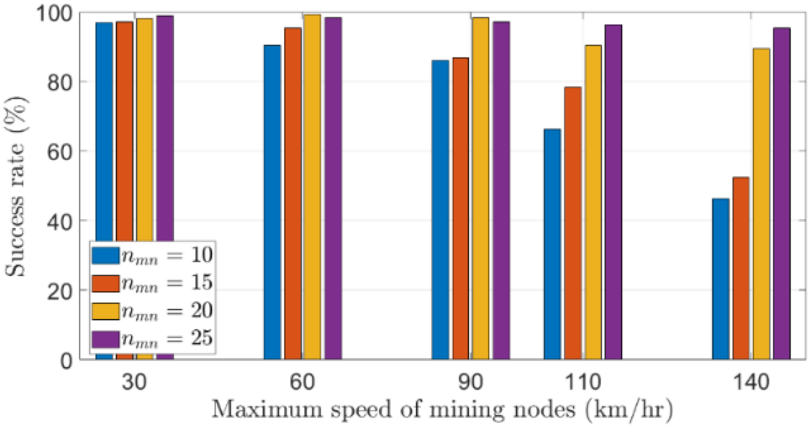

Figure 3.11: Average success rate with respect to speed.

Figure 3.11 shows the success rate of transmitting a true message under different maximum speeds of a mining node. For $n_{hop} > 1$, PoQF consensus is only used for RLY selection since the message is already validated at $n_{hop} = 1$, and therefore, the transmission success rate is independent of p_m. It shows that the success rate is falling with increasing speed, specifically for small n_{mn}. This is because a small n_{mn} depicts a low traffic density, so the nodes are likely to attain their maximum speeds and may lose connectivity before finalizing a consensus to select a RLY. In order to speed up consensus, a possible solution is that the RSUs reduce n_{th} when $n_{hop} > 1$. At $n_{hop} > 1$, the consensus only depends on the highest QF_i and does not require message validation. Since the mining node i sends its microblock earlier than the mining node j with $QF_j < QF_i$, it is not necessary for the mining node i to wait until QF_j is received. It is noted that in case of an incident or traffic jam, a high speed is not likely to be attained in the affected area and therefore, it is not recommended to reduce n_{th} at $n_{hop} = 1$, as it may result in large FV.

Figure 3.12 displays a_{τ_i} and b_{τ_i}, as the lower and upper limits of random τ_i generated by a mining node i. It shows that a_{τ_i} and b_{τ_i} reduce with an increasing QF_i and therefore τ_i leads to less waiting time for potential $RLYs$. Due to homogeneous distribution of nodes, n_{neigh} is the same for every node in a network. Therefore, deliberately reducing τ_i by node i is bounded by the lower limit of a_{τ_i}, which is known to every node in a network. Such attempt can be easily detected and reported to CA.

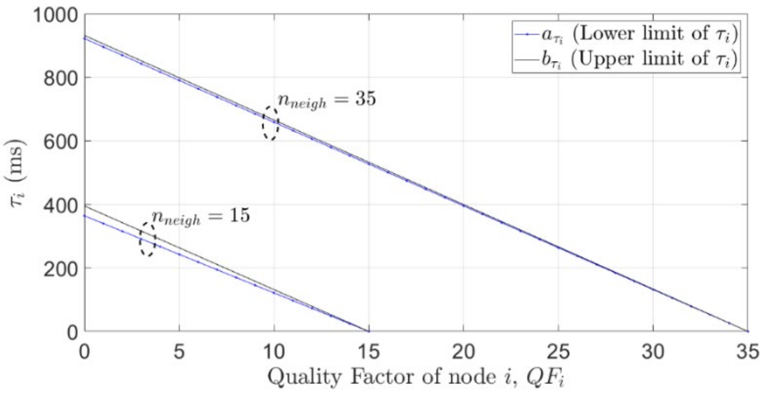

Figure 3.12: Values of a_{τ_i} and b_{τ_i}.

3.4.4 Comparison of PoQF with other Consensus Algorithms

Figure 3.13 compares the performance of PoQF with PoET and PoS. In Figure 3.13 (a), FV of PoQF is compared with PoET and PoS at different values of p_m and n_{mn}, while n_{th} is fixed at $\mu_m + 1$, as it results in low FV for all values of p_m. PoET is implemented such that each node generates a random number between 0 to 1s to determine its waiting time for collecting microblocks. It shows that FV of PoQF and PoET are closing to each other at low p_m. For high values of p_m, an honest node i with the highest QF_i is unable to collect sufficient microblocks from honest mining nodes within a random waiting time of PoET and therefore its FV rises with p_m at a higher rate than PoQF. In the reputation based PoS, a node is considered honest if its reputation exceeds a certain threshold. A reputation value is randomly assigned to each node on a scale of 0 to 100, thus the probability of reputation falling below a threshold of 50 is defined as p_m. PoS is implemented such that a malicious RLY only forwards the message from a malicious sender and an honest RLY only forwards the message from an honest sender. On an average, PoQF reduces FV by 11% and 15%, as compared to PoS and PoET, respectively.

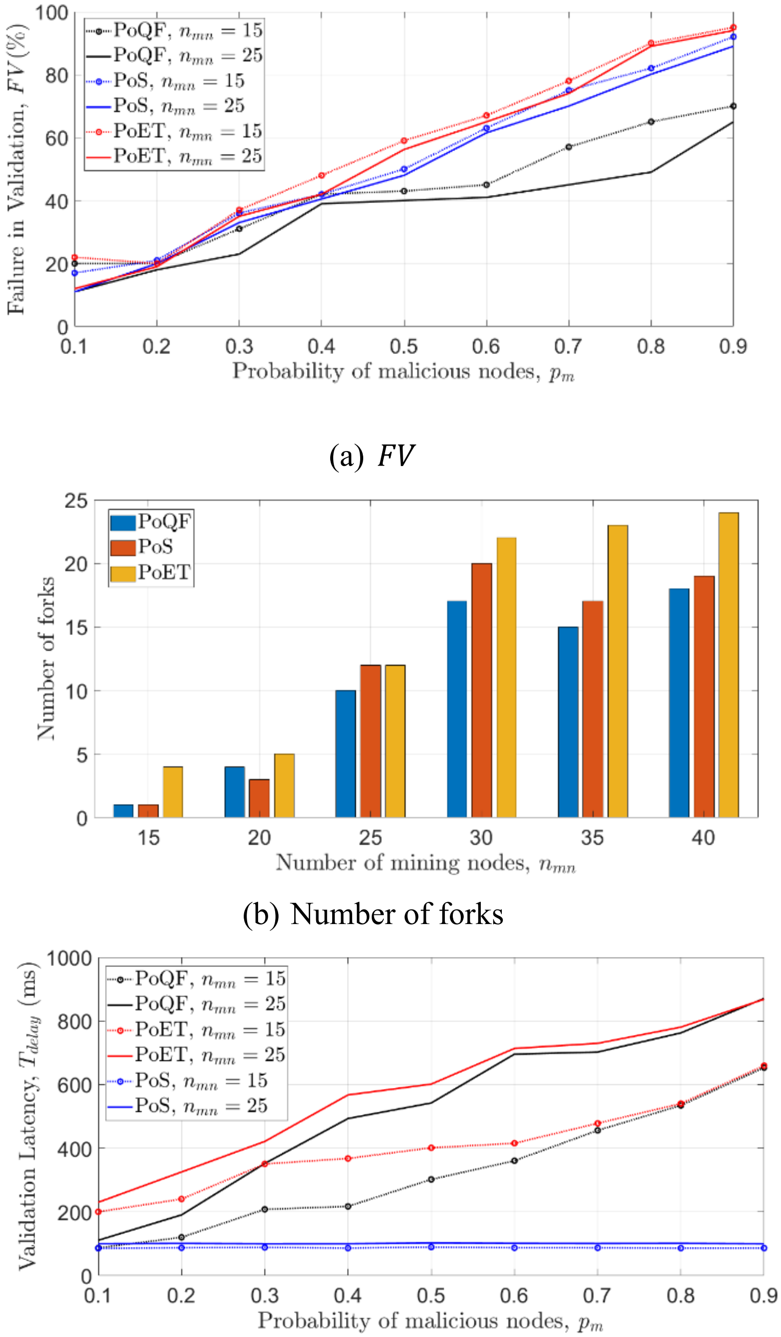

(a) FV

(b) Number of forks

(c) T_{delay}

Figure 3.13: Comparison of PoQF with PoS and PoET at $n_{th} = \mu_m + 1$.

Figure 3.13 (b) compares the number of forks created by PoQF, PoS and PoET consensus. A blockchain consensus should be able to avoid creation of forks in order to control discrepancies. In PoQF, node i with the highest QF_i is most likely to announce its microblock prior to other mining nodes. In this way, node j with $QF_j < QF_i$ cannot become RLY, if votes of both nodes are the same. This is how creation of forks is reduced in the proposed consensus. PoS is implemented by selecting RLY on the basis of the highest reputation which is randomly generated from 0 to 100 in the simulation. A fork appears when two nodes with same reputation simultaneously become RLY. In PoET, the time to announce microblock is not dependent upon QF. Therefore, node j with lower QF_j becomes RLY before receiving a microblock from node i even though $QF_i > QF_j$. In that case, a fork appears if both node i and node j generate keyblocks. It is noted that the number of forks in PoS is equal or lower than PoQF when $n_{mn} \leq 20$. Due to unreliable nature of vehicle connectivity, there remains a possibility of fork occurrence when an announced microblock by node i is not received by node j. It usually happens when mining nodes are in distance and beyond the transmission range of each other. This is why a low node density, ultimately leading to low n_{mn}, may result in a higher or equal number of forks created by PoQF as compared to PoS.

Figure 3.13 (c) compares T_{delay} of successful message validation consumed by PoQF, PoET and PoS. By using PoET, the mining node i is allowed to announce its microblock at a random time irrespective of its QF_i. On an average, T_{delay} of PoET is 68ms higher than PoQF. However, the difference is larger at lower p_m. Since τ_i is independent of QF_i in PoET, node j with lower QF_j may announce its microblock earlier than node i with $QF_i > QF_j$ and node i might have to wait longer. This waiting time is reduced in PoQF. However, with large p_m, an honest mining node i with the highest QF_i has to wait longer in PoQF for receiving n_{th} honest microblocks. It is because the frequency of malicious microblocks generation is increased with a large p_m. Hence the T_{delay} difference between PoQF and PoET becomes smaller. T_{delay} of PoS is independent of p_m and increases with n_{mn}. It is the smallest because it only consumes time in RLY selection, while the voting time is eliminated by the reputation-based message validation.

Consensus	Advantages	Limitations	Applications
PBFT [37]	• High throughput • Fair to all nodes	• Low adversary control	• Message validation
PoW [110]	• High security	• High power consumption • Low throughput	• Prevents security attacks
PoS [7]	• High throughput • Low power consumption	• Demotivating for nodes with low stakes	• Trust based data sharing
Joint PoW and PoS [92]	• Faster than PoW • Fairer than PoS	• High power consumption	• Reputation management
PoQF	• High adversary control • High throughput • Fair to all nodes	• Involves probabilistic predictions	• Message validation • Relay node selection

Table 3.5: Comparison of PoQF with other consensus algorithms for blockchain-enabled VANETs.

Table 3.5 compares performance of various consensus algorithms including PoQF and their potential applications in VANETs. It shows that PoQF can be employed for both message validation and relay selection.

3.5 Summary

In this chapter, a blockchain based PoQF consensus algorithm is proposed for message dissemination in vehicular networks. The theoretical performance of the proposed consensus is evaluated by deriving bounds on failure and latency in message validation, throughput of block generation and asymptotic latency, security and communication complexity. Moreover, two incentive distribution mechanisms have been presented to promote positive cooperation and discourage malicious behaviour of nodes and analysed using game theory. The proposed PoQF offers both high throughput and high adversary control and serves the dual purpose of message validation and relay selection. However, it relies on regular beacon message in which private information of nodes including its position and speed are shared.

Chapter 4 – Blockchain-enabled Federated Learning (FL) for Message Dissemination in Vehicular Networks

In this chapter, a decentralised message dissemination solution using a hierarchical blockchain based FL process is proposed, which is aimed to reduce latency and enhance privacy of a voting-based message dissemination. Section 4.1 introduces FL, the motivation of integrating FL with blockchain and challenges of FL in vehicular networks. Section 4.2 describes the proposed solution of blockchain-enabled FL for multi-hop relay selection. An incentive distribution mechanism to reward nodes participating in FL and message dissemination is also designed and analysed using Stackelberg game model. Both theoretical and simulated performance evaluation of the proposed approach are presented in section 4.3 and section 4.4 respectively.

4.1 Introduction

As discussed in Chapter 2, multi-hop relaying is one of the approaches in V2V communications to successfully deliver a message over a wide area. Optimal relay selection mechanisms result in better coverage, more reliable connectivity, and less communication overhead [127]. A voting based relay selection algorithm, such as the one described in Chapter 3 takes considerable time in waiting for votes, which increases with rising percentage of malicious nodes in the network. Furthermore, it relies heavily on probabilistic predictions and is prone to cheating attempts. For example, a malicious node may share false information in beacon messages. Alternatively, various intelligent relay selection schemes depending on a node's distance from predecessor, moving direction, speed and propagation loss in environment have been proposed using fuzzy logic [30] or machine learning algorithms [32]. Existing literature shows improved packet delivery ratio by machine learning algorithms in multi-hop V2V communications [128]. However, AI methods require huge processing power and are often not suitable for a fully distributed architecture [33]. In a traditional centralised architecture of machine learning, the data collected by mobile nodes is uploaded and processed in a cloud-based server to produce inference models [129]. With potentially large number of nodes in VANETs, where real-time decisions must be made within a restricted time, a cloud-centric approach is unable to offer acceptable latency and scalability. Also, a centralised architecture requires full connectivity which is challenging for VANETs. FL is an intermediary solution combining the advantages of both distributed learning and central aggregation.

4.1.1 Federated Learning (FL)

It is a distributed machine learning approach, in which nodes collect their own private data and train their individual machine learning or deep learning models, called local models, as shown in Figure 4.1. They do not share their collected data but only send self-trained local models to an aggregator. The aggregator combines all local models and produces a global model. The nodes further train the global model individually to create updated local models and submit them to aggregator. These steps are repeated in multiple iterations until a desired accuracy of global model is achieved [130]. FL is considered as a feasible solution for safety and time critical applications involving vehicles [54]. However, due to heterogeneity of data in vehicular networks, the performance of a global model may vary significantly across different nodes, environments, and traffic situations [131].

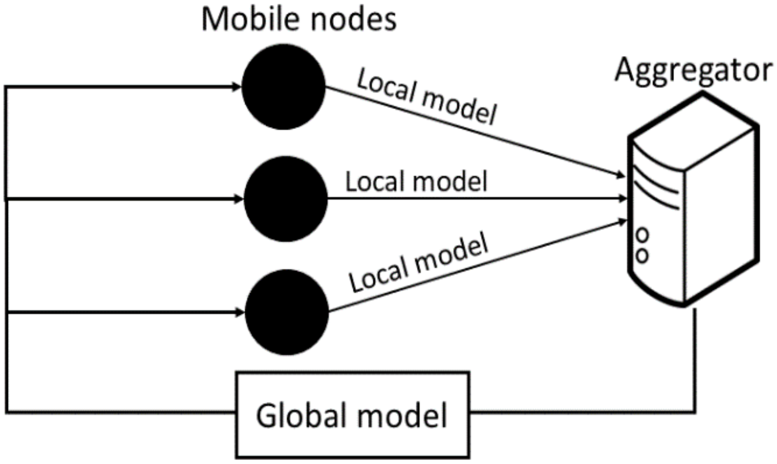

Figure 4.1: The FL process.

4.1.2 FL meets Blockchain

Despite offering a distributed approach, FL still relies on a central aggregator. Furthermore, it needs a sustainable incentive distribution mechanism to reward cooperative nodes based on their contributions and prevent adversary attacks. For example, a malicious node may deliberately modify data used for creating a local model, thereby causing poisoning attack

[132] or a selfish node may not cooperate in data collection resulting in inaccurate weights of a local model.

FL issues	Blockchain based solutions
Requires central aggregator	Independent of third party
Needs incentive strategy to motivate cooperative nodes	Manages cryptocurrency-based incentives
Requires adversary control	Provides security by smart contract

Table 4.1: FL issues and blockchain solutions.

Blockchain can be used with FL to provide a decentralised solution, manage incentives and ensure security and privacy in a trustworthy manner. Due to its decentralised nature, blockchain complements both FL and VANETs. Furthermore, smart contracts can enforce security by ensuring that a set of rules is followed [68]. The process of transaction verification in blockchain can also be utilised to validate local models in FL [55]. Table 4.1 summarises the current issues of FL and corresponding solutions provided by blockchain.

4.1.3 FL in Vehicular Networks

Approaches	Limitations	Solutions
Distance / link quality based predictions [27]	Assumptions/ rules are not adaptable to network changes	Local models trained with different networks and the global model can cater network changes
Fuzzy logic [30]		
Machine learning [32] - [33]	Huge data have to be managed centrally	Distributed learning and decentralised storage
Any scheme without incentives [26]	$RLYs$ may act selfishly	Blockchain incentives for motivation

Table 4.2: Multi-hop relay selection limitations and solutions offered by blockchain-based FL.

FL is suggested as a promising technique to securely train intelligent models across smart cars [54] and Unmanned Aerial Vehicles (UAVs) [133]. It has the feature of reducing network latency by dividing training task among network edges. In C-V2X communications, FL is proposed to reduce failure probability by intelligently offloading high computation tasks to nearby base stations [134]. Resource allocation and sharing in C-V2X by FL among nodes has promised better coverage and Quality-of-Service (QoS) in [135]. FL and fog-assisted V2X is presented in [136] to improve driving experience of vehicles by providing user-end services, for example, car sharing, intelligent parking allocation, infotainment, and e-commerce applications. In [137], FL is used to tackle energy transfer issues of electric vehicles at charging stations and has resulted in improved accuracy of energy demand prediction. FL assisted blockchain is proposed in [138] to adjust block arrival rate to reduce communication latency and consensus delay among nodes. Applications of FL in vehicular networks are summarised in [139] and most of the recent applications focus on resource management, performance optimization in computing tasks and user-end services. However, FL can also be promising in message delivery and RLY selection. Table 4.2 lists the limitations in existing multi-hop relay selection schemes and solutions offered by blockchain-based FL.

4.1.4 Contributions

a) Modes of FL

FL can be carried out in two modes: synchronous and asynchronous, as shown in Figure 4.2. In synchronous FL, nodes are given a time limit in which they submit their local models. A global model is formed after a time epoch. In asynchronous FL, nodes can send their models at their own convenient time. A global model is updated each time a new model is received [135]. Synchronous FL promises more accuracy and convergence [54]. However, a node may not be able to upload its local model in a fixed time epoch due to high mobility in a vehicular network, as shown in Figure 4.3 (a). On the other hand, in asynchronous FL in VANET, it is possible that a node loses connection with the aggregator and is unable to receive every update in global model. It may continue training its local model on the basis of an outdated global model, thereby leading to waste of its resources, as shown in Figure 4.3 (b). To increase accuracy and reduce packet loss, a modified synchronous FL can be used in VANET in which the aggregator waits for a certain number of local models to be received instead of a time epoch. This chapter employs modified synchronous FL and waits for a certain number of local models before aggregation.

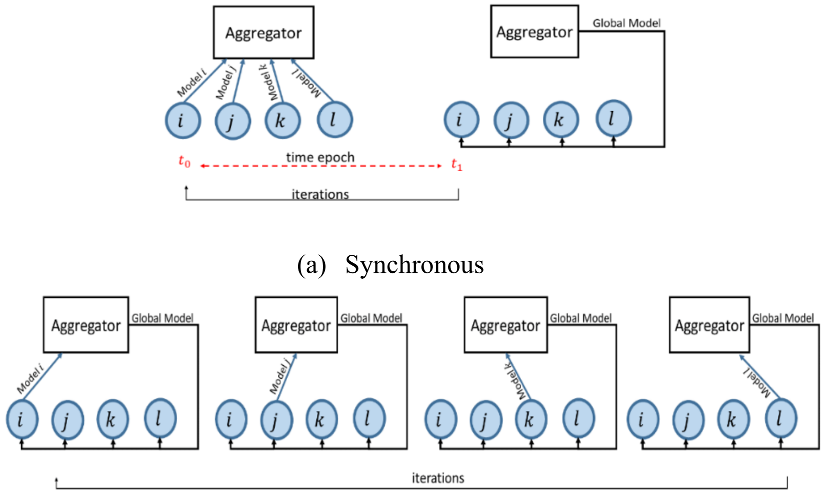

(a) Synchronous

(b) Asynchronous

Figure 4.2: Modes of FL.

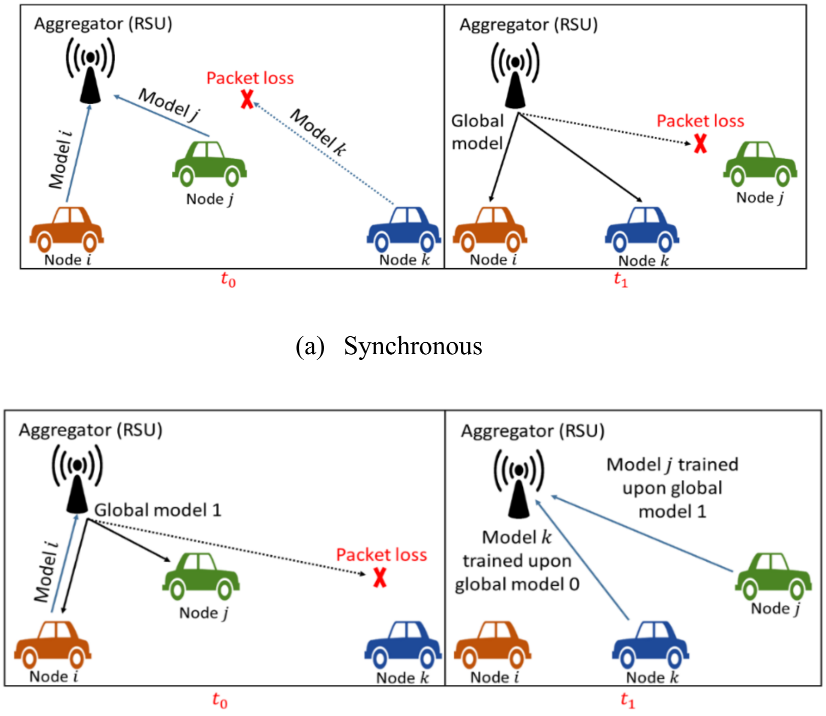

(a) Synchronous

(b) Asynchronous

Figure 4.3: Modes of FL in VANET.

b) Consensus

Selection of an appropriate consensus is one of the challenges of blockchain-enabled FL in VANETs. In [138], the drawback of additional delay due to blockchain management in FL process of vehicular networks is discussed. A possible reason of delay is PoW being used by nodes to record and validate local models. To reduce the delay, DPoS is used as a consensus of blockchain-supported FL in [140]. The proposed approach is faster but decentralization is compromised because only RSUs can generate blocks. In addition, a consensus algorithm in blockchain-enabled FL requires not only time-efficiency but also security against malicious nodes. As a solution, this chapter uses a machine learning based algorithm embedded in smart contract to replace consensus and ensure security against malicious local models.

4.2 Blockchain-based FL for Message Dissemination

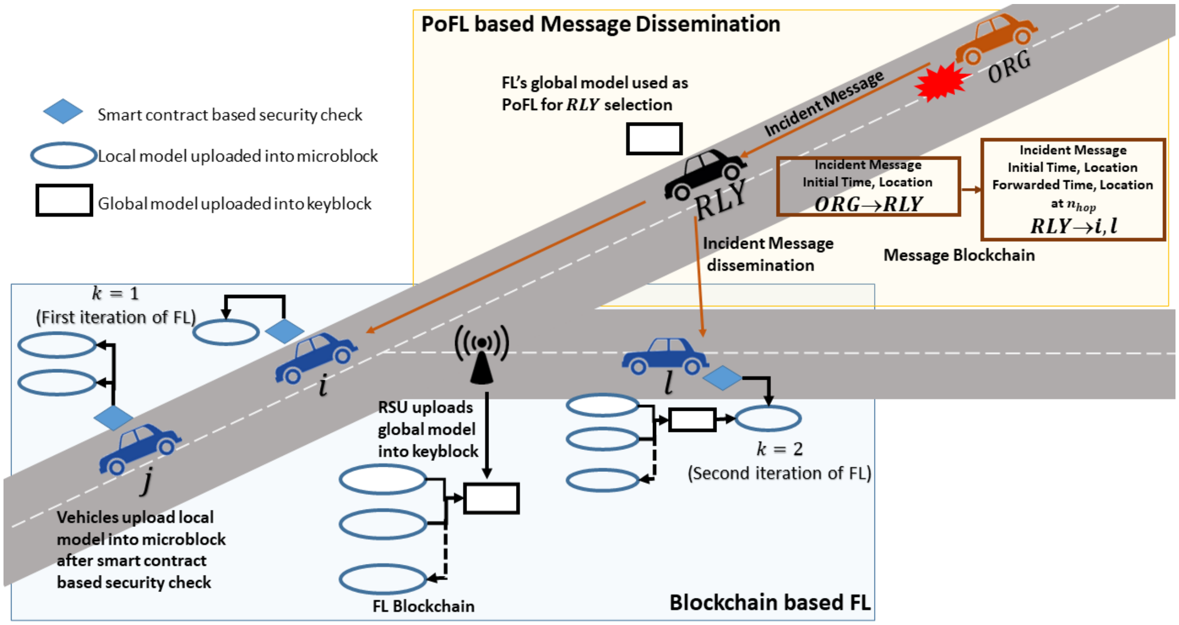
PoFL based Message Dissemination
FL's global model used as PoFL for RLY selection
Incident Message
ORG
RLY
Incident Message Initial Time, Location $ORG \rightarrow RLY$
Incident Message Initial Time, Location Forwarded Time, Location at n_{hop} $RLY \rightarrow i, l$
Incident Message dissemination
Message Blockchain
Smart contract based security check
Local model uploaded into microblock
Global model uploaded into keyblock
$k = 1$ (First iteration of FL)
i
j
l
RSU uploads global model into keyblock
$k = 2$ (Second iteration of FL)
Vehicles upload local model into microblock after smart contract based security check
FL Blockchain
Blockchain based FL

Figure 4.4: Blockchain-based FL and Message Dissemination.

As illustrated in Figure 4.4, the proposed solution consists of a blockchain-based FL process and a solution for multi-hop relay selection. The FL process is aimed to form a global model which is later used as a consensus to select RLY when an incident message is originated by a node. The vehicles act as nodes participating in FL by training local models and RSU performs the role of aggregator. Overall, the proposed approach consists of two major parts:

- *Blockchain-supported FL* where nodes complete an FL process to create a global model for RLY selection.
- *Proof-of-Federated-Learning (PoFL) based blockchain-enabled message dissemination*, where global model produced in the above solution is run by nodes to find their eligibility of becoming RLY.

4.2.1 Blockchain-supported FL

a) *Preliminary elements*

- *Hello packet by designated node:* A CA appoints some designated nodes to regularly originate a Hello packet and share their position to initiate dataset collection by nodes participating in FL. Only the designated nodes are allowed to originate Hello packets. The motivation behind designated nodes is two-fold: first is because they are trusted by CA to honestly send their actual position without any malicious change and second is because the identities of designated nodes are already shared with other nodes, so Hello packet from any other identity is not recognized by the network. Designated vehicles can either be representatives of Central Authority or selected from the existing network based on their reputation.
- *Dataset:* In the proposed solution, dataset collected by node i includes multi-hop relay selection parameters collected as data samples to train local model. After forwarding a Hello packet, dataset collected by node i consists of the following parameters: $d_{i,s}$; distance from sender s (designated node or previous RLY), $dir_{i,s}$; moving direction (either towards or away from sender s), v_i; speed at the time of forwarding message, n_{hop}; hop number, λ_V; traffic density within its transmission range and n_A; number of acknowledgments received as the score of relaying. λ_V in dataset can be pre-specified by CA or estimated by counting average number of nodes sending beacon messages per meter [118]. The process of dataset collection is explained in detail later in this chapter.

b) <u>FL components supported by blockchain</u>

Table 4.3 defines components involved in an FL and supporting elements for each corresponding component in a blockchain-enabled process.

Component of an FL process	**Blockchain Support**
Adversary: The following adversary threats are considered in an FL process: a) Malicious nodes: They may deliberately change or inject false data so that local model is not trained accurately. This phenomenon is also known as poisoning attack [132]. *b)* Selfish nodes: They may not send acknowledgment messages despite receiving forwarded messages. Therefore, n_A cannot be recorded correctly during dataset collection, leading to an inaccurate local model produced by node i.	*Security Check:* It is a machine learning algorithm embedded in smart contract of FL blockchain to detect adversary before a local model is uploaded as a block by node i.
Local Model: Each node i participating in FL trains a Deep Neural Network based local model consisting of 7 hidden layers and 256 neurons in each layer.	*Microblock:* A local model is stored in FL blockchain as a microblock after undergoing a security check. A microblock is added in parallel to other microblocks, all containing hash of previous keyblock.
Global Model: It is an aggregated model of n_{FL} local models, where n_{FL} also refers to the number of nodes participating in FL. The global model is consolidated by RSU in the proposed solution.	*Keyblock:* A global model is stored in FL blockchain by RSU in the form of a keyblock, containing hashes of previous n_{FL} microblocks.

Table 4.3: FL components and corresponding blockchain support.

c) The proposed solution

Algorithm 4.1: Actions by node i to complete blockchain-support FL

```
    Input: Hello packet
    Output: Global model
1.  while $n_{hop} \leq n_{hop}^{max}$ do
2.      Generate random waiting time
3.      while time elapsed ≤ random waiting time do
4.          if Forwarded Hello packet received at $n_{hop}$ then
5.              Break
6.          end if
7.      end while
8.      if Forwarded Hello packet not received at $n_{hop}$ then
9.          Forward Hello packet
10.         Count acknowledgement packets into $n_A$
11.         Record in $d_{i,s}, v_i, dir_{i,s}, \lambda_V, n_A$ in dataset
12.         Break
13.     Else
14.         $n_{hop} = n_{hop} + 1$
15.     end if
16. end while
17. if data size == $s_i$ then
18.     Train local model
19. Else
20.     Go to 1
21. end if
22. while $k \leq k_{max}$ do
23.     Upload local model through smart contract
24.     Receive updated global model
25.     Re-train local model
26.     $k = k + 1$
27. end while
```

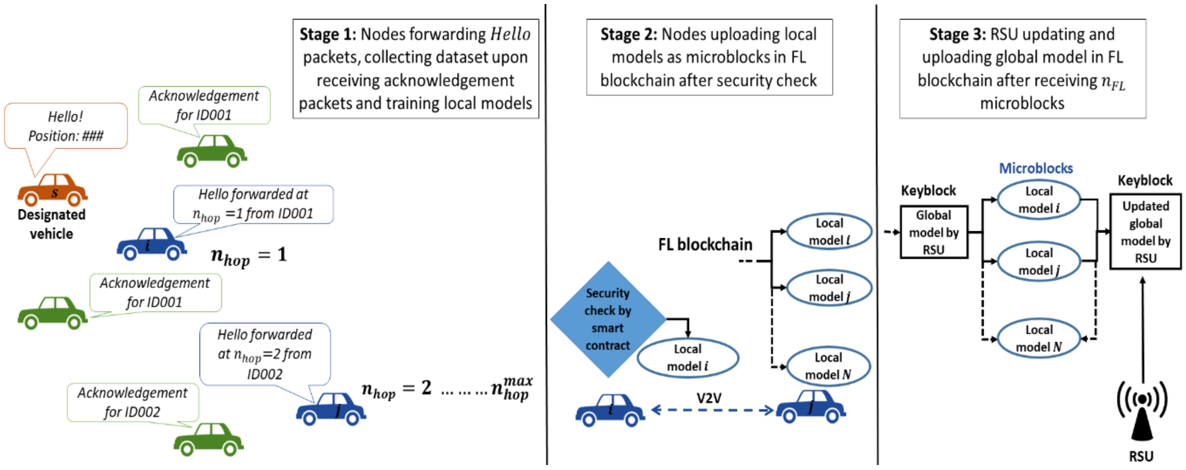
Stage 1: Nodes forwarding *Hello* packets, collecting dataset upon receiving acknowledgement packets and training local models
Stage 2: Nodes uploading local models as microblocks in FL blockchain after security check
Stage 3: RSU updating and uploading global model in FL blockchain after receiving n_{FL} microblocks
Hello! Position: ###
Acknowledgement for ID001
s
Designated vehicle
Hello forwarded at n_{hop} =1 from ID001
i
$n_{hop} = 1$
Acknowledgement for ID001
Hello forwarded at n_{hop}=2 from ID002
Acknowledgement for ID002
j
$n_{hop} = 2$ …… n_{hop}^{max}
FL blockchain
Security check by smart contract
Local model i
Local model i
Local model j
Local model N
i
V2V
j
Keyblock
Global model by RSU
Microblocks
Local model i
Local model j
Local model N
Keyblock
Updated global model by RSU
RSU

Figure 4.5: The proposed stages of blockchain-supported FL.

The proposed blockchain-supported FL consists of three stages, as shown in Figure 4.5, and explained below. The solution is also described in Algorithm 4.1.

- *Stage 1 - Dataset Collection and Local Model Training:* In this stage, nodes collect dataset for training. Upon receiving a Hello packet from a designated node, a node i which aims to collect dataset, generates a random waiting time. When the waiting time is complete, it forwards Hello packet with its encrypted identity. The reason behind a random waiting time is to prevent multiple nodes from transmitting at the same time and avoid packet collision. The nodes which receive the forwarded Hello packet for the first time share their acknowledgment. An acknowledgment packet contains encrypted identity of node i, so that it can collect dataset. A node j, which participates in FL, will broadcast the received Hello packet again after a random waiting time. This process continues up to a specified number of hops, n_{hop}^{max}.
- *Stage 2 - Security Check and FL Blockchain Update:* A node i shares its local model with the network by adding it into FL blockchain as a microblock. It is added after passing a security check performed by the smart contract embedded in FL blockchain. The proposed security check employs a machine learning algorithm called Isolation Forest [141] to detect anomaly in a local model caused by adversary. Isolation Forest is used because it only requires a small number of samples for training. A true sample is provided by the CA for its initial training. Later, it can be used in a fully unsupervised manner to detect anomaly. Moreover,

it is computationally efficient and has low memory requirement [142]. The security check is used in three ways. Firstly, the security check on dataset is conducted by finding anomalies in dataset of each node. Secondly, the security check performs anomaly detection on weights of local models. If a malicious node i deliberately changes its dataset for training its local model but shares a true dataset in smart contract, the adversary attack will be detected by anomaly detection on weights. Thirdly, the security check on both dataset and weights is performed. If local models successfully pass the security check, they are added in FL blockchain in the form of parallel microblocks. The microblock announcement is broadcasted by node i and the receiving nodes will then update their copy of FL blockchain. Nodes can exchange new microblock updates with their neighbours regularly.

- *Stage 3 - Global Model Aggregation by RSU:* Whenever a node i finds an RSU available in its transmission range, it shares its updated copy of FL blockchain. When n_{FL} microblocks are received by RSU in FL blockchain, it aggregates local models into a global model and uploads it into a keyblock. All stages are repeated at each iteration. The goal is to repeat the process up to k_{max} iterations for minimizing global loss function $LF\left(\boldsymbol{w}_G^k\right)$, which is defined as

$$LF\left(\boldsymbol{w}_G^k\right) = \frac{1}{n_{FL}} \sum_{i=1}^{n_{FL}} LF\left(\boldsymbol{w}_i^k\right), \tag{4.1}$$

where $\boldsymbol{w}_G^k$ are weights of global model and $LF\left(\boldsymbol{w}_i^k\right)$ is the loss function of local model by node i and $\boldsymbol{w}_i^k$ are its corresponding weights at k^{th}iteration. Neural networks commonly use Mean Squared Error (MSE) as the loss function [54]. The value of k_{max} is adjusted by CA to achieve the minimum possible or desired $LF(\boldsymbol{w}_G^{k_{max}})$ [130].

4.2.2 PoFL based Blockchain-enabled Message Dissemination

a) <u>*Components*</u>

- *PoFL:* It is the consensus to elect RLY for forwarding an incident message, initiated by ORG. It uses the global model contained in the latest keyblock of FL blockchain, described in above solution. It is run by a smart contract of message blockchain.

- *Message Blockchain:* It contains history of incident messages. When a RLY is elected by PoFL, it adds a block in the message blockchain containing the forwarded incident message. The block also contains time, location and encrypted identity of the RLY which adds the block. The motivation behind message blockchain is to record forwarded incident messages as immutable blocks and avoid discrepancies during incentive distribution among $RLYs$.

b) The proposed solution

Algorithm 4.2: PoFL based message dissemination

```
Input: Incident message, global model
Output: New block announcement in message blockchain
while $n_{hop} \leq n_{hop}^{max}$ do
    Compute score from global model
    timer expiry limit = 1/score
    while time elapsed ≤ timer expiry limit do
        if New block announced then
            Break
        end if
    end while
    if New block not announced then
        Announce block
        Break
    Else
        $n_{hop} = n_{hop} + 1$
    end if
end while
```

When an incident message is initiated by ORG, all receiving nodes attempt to become the RLY by competing through PoFL consensus. Each node i runs PoFL consensus to find its score of being RLY. PoFL is aimed to assign the highest score to the most appropriate RLY. The smart contract starts a timer whose length is inversely proportional to the score of node i. As shown in Figure 4.6, a block is added in the message blockchain and a block announcement with the forwarded incident message is initiated by node i if its timer first expires. In this case, node i is assigned as RLY at $n_{hop} = 1$. All other nodes continue to compete for becoming RLY at further hops until the message is forwarded up to n_{hop}^{max} number of hops. The solution is also described in Algorithm 4.2. The relationship between two solutions is illustrated in Figure 4.7.

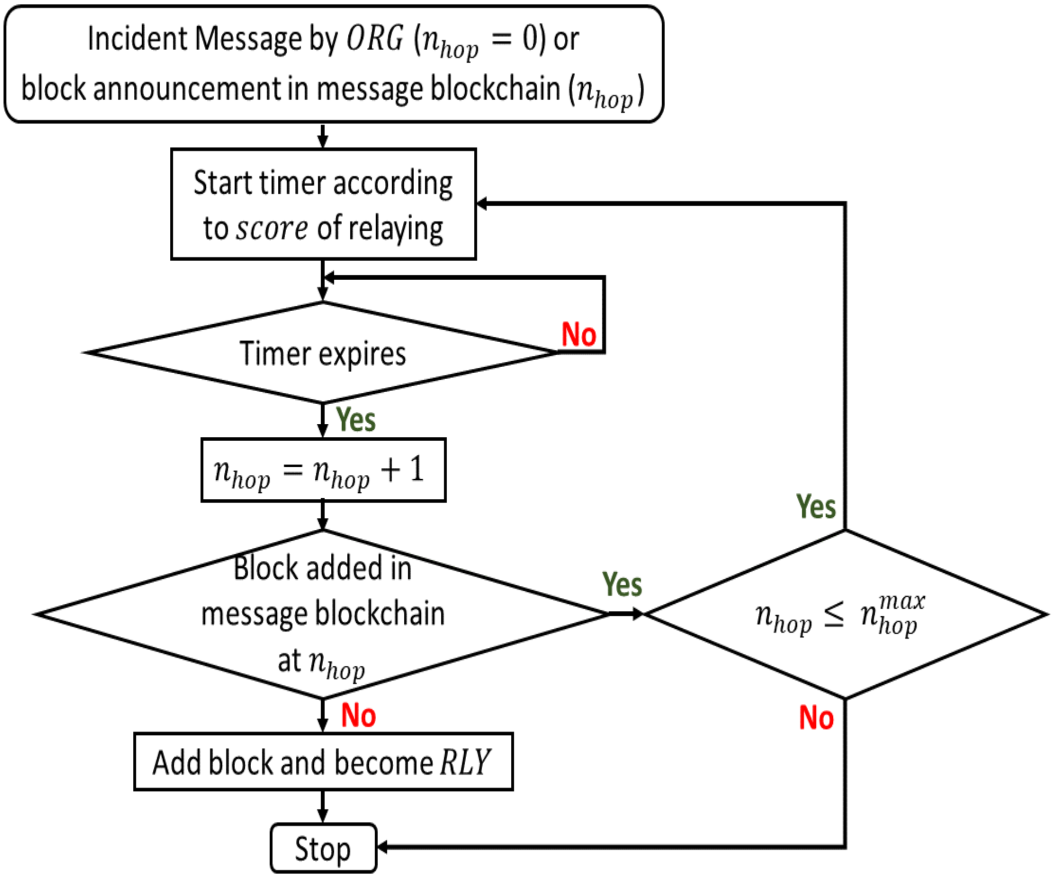
Incident Message by ORG ($n_{hop} = 0$) or block announcement in message blockchain (n_{hop})
Start timer according to $score$ of relaying
Timer expires
No
Yes
$n_{hop} = n_{hop} + 1$
Block added in message blockchain at n_{hop}
Yes
$n_{hop} \leq n_{hop}^{max}$
Yes
No
No
Add block and become RLY
Stop

Figure 4.6: Flowchart of actions by node i according to PoFL based blockchain-enabled message dissemination.

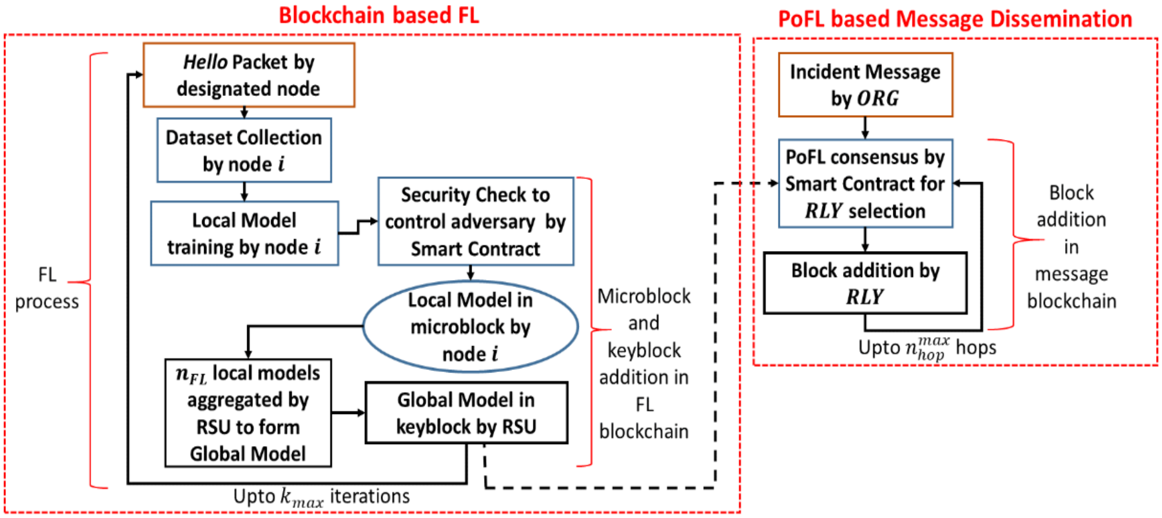
Blockchain based FL
Hello Packet by designated node
Dataset Collection by node i
Local Model training by node i
Security Check to control adversary by Smart Contract
Local Model in microblock by node i
n_{FL} local models aggregated by RSU to form Global Model
Global Model in keyblock by RSU
FL process
Microblock and keyblock addition in FL blockchain
Upto k_{max} iterations
PoFL based Message Dissemination
Incident Message by ORG
PoFL consensus by Smart Contract for RLY selection
Block addition by RLY
Block addition in message blockchain
Upto n_{hop}^{max} hops

Figure 4.7: The flow of steps in blockchain-supported FL and PoFL based message dissemination.

c) *Privacy of FL based message dissemination*

Approach	Position	Speed	Other parameters
Distance / link quality based predications [26] - [27]	✓	✓	×
Fuzzy logic [30]	✓	×	×
Deep learning [33]	✓	✓	Transmission power
PoQF (Chapter 3)	✓	✓	×
PoFL	×	×	×

Table 4.4: Parameter-sharing required from neighbour nodes.

Table 4.4 lists the parameters required to be shared by neighbour nodes in various multi-hop relay selection approaches. The position, speed and heading direction of moving nodes are regularly shared in VANETs using beacon messages and thus create a threat to privacy [143]. The proposed approach does not require such information from all neighbour nodes and can therefore be considered as a privacy-preserving solution. The position and direction of only sender is required for dataset collection in blockchain based FL and for score calculation of relaying in PoFL based message dissemination. However, identities of nodes are kept anonymous using encryption. Disclosure of identities through brute force attack is a possibility but it will not be very effective for the attacker. Due to high time complexity of brute force attack [144], the position, speed and direction of a node will be changed until its identity is disclosed. In case of high probability of brute force attack, a private blockchain with only trusted nodes or timely refreshing of cryptographic identities is recommended [145].

4.3 Theoretical Analysis

4.3.1 Training Capacity of FL

This analysis is aimed to compare the capacity of blockchain to complete one FL iteration in a given amount of time with the same process without blockchain. FL without blockchain is referred to as a centralised approach in which each node i submits its local model directly to RSU instead of uploading it into FL blockchain. As the convergence performance of FL improves with increasing number of local models [146], FL via blockchain is expected to achieve greater accuracy, provided the number of uploaded local models are higher as compared to the process carried out without blockchain within the same time period.

a) *<u>FL with blockchain</u>*

Let TS be a time slot in which a node i is required to upload its local model as microblock in FL blockchain, after it has completed training and passed its local model through security check. Let λ_{MB} be the microblock arrival rate at RSU or throughput in microblocks/s. If microblock arrival is modelled using Poisson distribution as defined in [75], the expected number of nodes able to upload their local models via FL blockchain in TS can be given as [120]

$$E(n_B) = \sum_{l=1}^{\lambda_{MB}TS} l\, e^{-\lambda_{MB}TS} \frac{(\lambda_{MB}TS)^l}{l!}. \tag{4.2}$$

b) *<u>FL without blockchain</u>*

If moving nodes are required to upload their models directly to RSU without blockchain, then it is necessary that either RSU is in their transmission range or they are able to reach towards RSU within TS. Consider a general and dynamic movement of nodes, the position of nodes (vehicles) on road follows Poisson distribution, λ_V nodes/m^2 is assumed as the density of nodes on a two-dimensional road segment with no separation of lanes [117], the expected number of nodes with RSU in their transmission range is

$$E(n_V) = \sum_{l=1}^{\lambda_V \pi R^2} l\, e^{-\lambda_V \pi R^2} \frac{(\lambda_V \pi R^2)^l}{l!}, \tag{4.3}$$

where transmission range is assumed as a uniform circle with radius R. Similarly, the expected number of moving nodes with RSU not currently in their transmission range but can travel to reach RSU within TS is

$$E(n'_V) = \sum_{l=1}^{\frac{TS}{\mu_d - R}\mu_v} l e^{-\frac{TS}{\mu_d - R}\mu_v} \frac{\left(\frac{TS}{\mu_d - R}\mu_v\right)^l}{l!}\ , \tag{4.4}$$

where $\mu_d > R$ is the mean distance of those nodes from RSU which do not have RSU within their transmission range and μ_v is their average speed. Therefore, the expected number of nodes able to upload their local models to RSU without blockchain during TS is

$$E(n_{WB}) = E(n_V) + E(n'_V). \tag{4.5}$$

4.3.2 Incentive Distribution Mechanism and its Analysis

An incentive distribution mechanism to reward nodes contributing in FL and message dissemination is formulated. The feasibility of incentive strategy is analysed by investigating behaviour of $RLYs$ and nodes participating in FL based on their expected utilities through Stackelberg game model.

a) Stackelberg game formulation

The Stackelberg game model consists of three types of players: ORG, RLY participating in message dissemination and node i participating in FL. For each incident message initiated by ORG, there are n_{RLY} number of $RLYs$ which forward the incident message and n_{FL} nodes in the network which train their local models during blockchain based FL. The proposed incentive distribution mechanism is formulated as a two-stage Stackelberg game.

First, at stage 1, ORG pays reward to $RLYs$ for forwarding message. At stage 2, $RLYs$ pay reward to n_{FL} nodes for participating in FL to form a global model of RLY selection. Since, both FL and message dissemination processes are blockchain-based, the contribution of players is stored as immutable timestamped blocks and cannot be altered for cheating. The transactions of incentives are also processed in the form blockchain based virtual currency automatically through smart contracts. As shown in Table 4.5, the rewards to n_{FL} nodes are paid in proportion to the sizes of dataset they have used in training their local models. Assume that the dataset sizes of n_{FL} nodes are $\boldsymbol{s} = \{s_1, s_2, \ldots., s_{n_{FL}}\}$. The utility of each node i participating in FL process is

$$U_i(s_i, I) = n_{FL} I s_i - Cost(s_i), \tag{4.6}$$

where I denotes incentive which is constant for every node i and $Cost(s_i)$ is the computational cost of training a local model on dataset of size s_i and is modelled as a quadratic function, i.e.,

$$Cost(s_i) = \rho_i s_i^2, \tag{4.7}$$

where $\rho_i > 0$ denotes cost co-efficient of node i [147]. The utility of each RLY is

$$U_{RLY}(\boldsymbol{s}, I) = CClog(1 + I) - \sum_{i=1}^{N} I \cdot s_i. \tag{4.8}$$

where $CClog(1 + I)$ is paid by ORG for forwarding the incident message. Here $CC > 0$ and can be assumed as a compensation amount paid to $RLYs$ present in an area affected by an incident or traffic jam caused by ORG.

Player	**Gains**	**Pays**
ORG	None	$n_{RLY} CClog(1 + I)$ to $RLYs$
RLY	$CClog(1 + I)$ from ORG	$\sum_{i=1}^{N} Is_i$ to n_{FL} nodes
Node i	$n_{RLY} Is_i$ from $RLYs$	$\rho_i s_i^2$ to train local model

Table 4.5: Reward gained and payment made by players.

b) Stackelberg game analysis

The proposed incentive distribution mechanism assumes information symmetry, i.e., all players have complete information about s_i.

- *Definition 4.1:* Assume that s_i^* is the optimal data size for each node i and I^* is the optimal incentive amount per data size paid by each RLY to node i, then (s_i^*, I^*) is the Nash equilibrium point which satisfies the following conditions

$$U_i(s_i^*, I^*) \geq U_i(s_i, I^*), \tag{4.9}$$

$$U_{RLY}\,(s_i^*,\, I^*) \;\geq\; U_{RLY}\,(s_i^*,\, I). \tag{4.10}$$

- *Theorem* 4.1*:* There exists a Nash equilibrium point for a node i with U_i defined in (4.9).

  Proof: For a fixed I^*, U_i is

$$U_i(s_i, I^*) = N_{RLY} \cdot I^* \cdot s_i - \rho_i s_i^2. \tag{4.11}$$

  The second order derivative of (4.11) is

$$\frac{\partial^2 U_i(s_i, I^*)}{\partial s_i^2} = -2\rho_i. \tag{4.12}$$

  Since $\rho_i > 0$, the second-order derivative of U_i is negative and $U_i(s_i, I^*)$ is a strictly concave function, which proves the existence of Nash equilibrium. ■

- *Theorem 4.2:* There exists a Nash equilibrium point for RLY with U_{RLY} defined in (4.10).

  Proof: The second order derivative of (4.10) is

$$\frac{\partial^2\, U_{RLY}\,(\boldsymbol{s},\, I)}{\partial\, I^2} \;=\; \frac{-\,CC}{(1+I)^2}\,. \tag{4.13}$$

Since $CC > 0$ and $(1+I)^2 > 0$, the second-order derivative of U_{RLY} is negative and $U_{RLY}(s, I)$ is a strictly concave function, which proves the existence of Nash equilibrium. ■

Based on Theorem 4.1 and Theorem 4.2, it can be stated that the unique Stackelberg Nash equilibrium point of the proposed model exists. CA is responsible to choose values of I and CC such that Nash equilibrium points for all n_{FL} nodes and n_{RLY} $RLYs$ become their best response strategies (i.e., $U_i > 0$ and $U_{RLY} > 0$) and all players are willing to cooperate in the proposed game.

If permissioned blockchain is used, complete information may not be visible to every player and the incentive distribution mechanism will be information asymmetric. In this case, players may predict information using probabilistic assumption [147] or through a machine learning method [148]. Let $\boldsymbol{s} = \{s_1, s_2, \ldots. s_Z\}$ be the n_Z dataset sizes used by nodes and p_z be the probability that a node i uses s_z. (4.10) can be modified as

$$U_{RLY}(\boldsymbol{s}, I) = CClog(1+I) - \sum_{z=1}^{n_Z} p_z\, n_{FL} I s_z, \tag{4.14}$$

Similar to Theorem 4.2, the existence of Nash Equilibrium point can be proved for U_{RLY} defined in (4.14).

4.3.3 Asymptotic Complexities

Consensus	Latency	Communication	Computation
PoS	$\Omega(\kappa)$	$\Theta(1)$	$\Theta(1)$
PoQF	$\kappa O(1)$	$O(n_{mn})$	$\Theta(1)$
PoFL	$\Theta(1)$	$\Theta(1)$	$\Theta(1)$
Blockchain-enabled FL	$\Omega(\kappa)$	$\Omega(n_{FL})$	$n_{FL}\Omega(\kappa)$

Table 4.6: Comparison of asymptotic complexities.

Table 4.6 compares the asymptotic latency, communication and computation complexities of PoS, PoQF, PoFL and the blockchain-based FL process which is used to produce a global model for PoFL. κ denotes consensus parameter and is unique to each algorithm which is the smallest dataset size in blockchain-based FL. The blockchain-based FL process has the highest computation complexity, as its computations depend on the size of dataset and number of vehicles submitting local models. Also, its communication complexity is proportional to the number of nodes participating in FL and its latency depends on the time of training a local model, which is proportional to the dataset size. However, PoFL, resulted from a blockchain-based FL process, outperforms PoS and PoQF because its latency, communication and computation complexities are independent of n_{FL} and κ. It is therefore a highly scalable solution once the FL process is completed.

4.4 Simulated Performance Analysis

4.4.1 Simulation Setup

Parameters	Values	Parameters	Values
Simulation time	300 s	Protocol	IEEE 802.11p
Size of area	2.5 km × 2.5 km	Encryption	SHA-256
DR	6 Mbps	s_i	8000
Mobility model	Krauss	Loss function	MSE
Number of RSUs	1	R	250 m
Number of nodes (vehicles)	100, 200, 300	n_{hop}^{max}	6
k_{max}	100, 110	μ_v	50 km/hr

Table 4.7: Simulation parameters for blockchain-based FL and message dissemination.

The proposed solutions are simulated using OMNeT++, Python and SUMO[2]. Python is employed for carrying out FL using Tensorflow library of machine learning. Python can be embedded into C++ by writing an extension module. Since OMNeT++ is a modular C++ based network simulator, it supports dynamic loading of Python script at run time. Appendix C shows code snippet of OMNeT++ integrating Python. The simulation parameters used are listed in Table 4.7.

[2] Source code is available at https://zenodo.org/record/5575863#.YW2BmOhKiUk.

4.4.2 Loss Function of Global Model

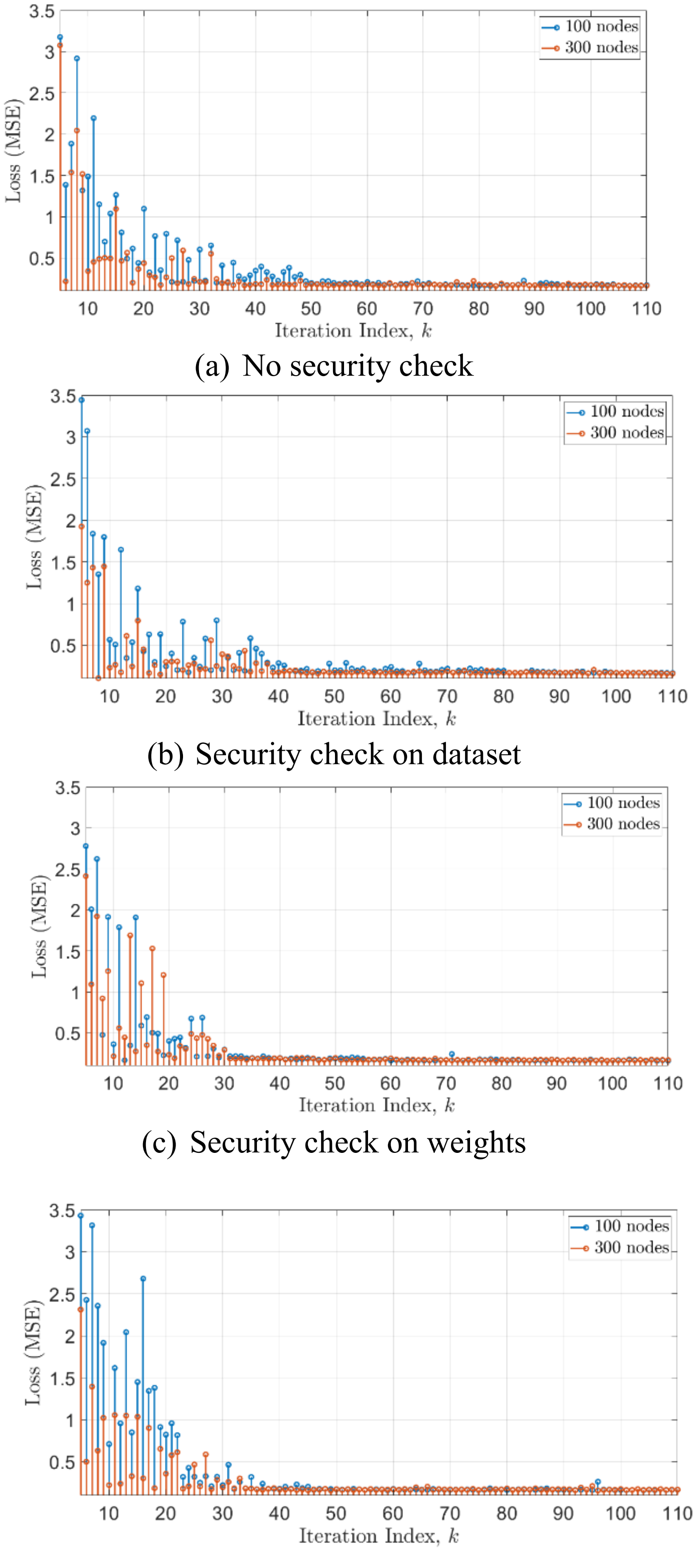

(a) No security check

(b) Security check on dataset

(c) Security check on weights

(d) Security check on both dataset and weights

Figure 4.8: Loss (MSE) of global model with 50% adversary.

Figure 4.8 shows the loss (MSE) of global model with respect to iteration index k, in presence of 50% adversary among the nodes participating in FL, consisting of equal percentage of malicious and selfish nodes. In all cases, the loss converges to its lowest possible value until 100 iterations. However, this convergence is achieved in less number of iterations with 300 nodes as compared to 100 nodes, which means that the maximum accuracy of a global model can be attained faster with greater number of nodes. Figure 4.8 (a) shows the loss when no security check is implemented. The convergence rate is slower without security check and takes more iterations than those with security checks, as shown in Figure 4.8 (b) - (d). It indicates that the increased computation required to implement security check can be compensated with less iterations processed to attain maximum accuracy. Table 4.8 shows loss of global model after 100 iterations with respect to number of nodes participating in FL without any adversary or security check. As shown in Table 4.8, the loss is inversely proportional to both dataset size and number of nodes.

s_i	$n_{FL} = 100$	$n_{FL} = 200$	$n_{FL} = 300$
2000	0.19643	0.18724	0.16541
5000	0.17251	0.17021	0.16313
8000	0.15297	0.15101	0.15085

Table 4.8: Loss (MSE) of global model after 100 iterations.

Figure 4.10 and Figure 4.10 show the loss of global model after 100 iterations of FL in presence of malicious and selfish nodes respectively. The global loss function is the highest if no security check is employed in smart contract of FL blockchain. Security check on weights results in less loss as compared to security check on dataset in presence of malicious nodes and vice-versa in case of selfish nodes. It is because selfish nodes affect only n_A in dataset by not sending acknowledgments and such discrepancy is easily detected if security check is applied on dataset only. On the other hand, malicious nodes can change all parameters in dataset and therefore it is not easy to detect anomaly on such dataset. It shows that security check on weights is more suitable to prevent poisoning attack caused by malicious nodes and security check on dataset is more appropriate to reduce the effect of selfish behaviour. Nevertheless, malicious nodes may submit a true dataset for security check and upload inaccurate local models using a false dataset. Therefore, in this case, only security check on weights can prevent adversary caused by malicious nodes. The loss function is minimum if security check on both dataset and weights is used and is suitable for both malicious and selfish nodes. As a trade-off, increased computation is required to run security check twice.

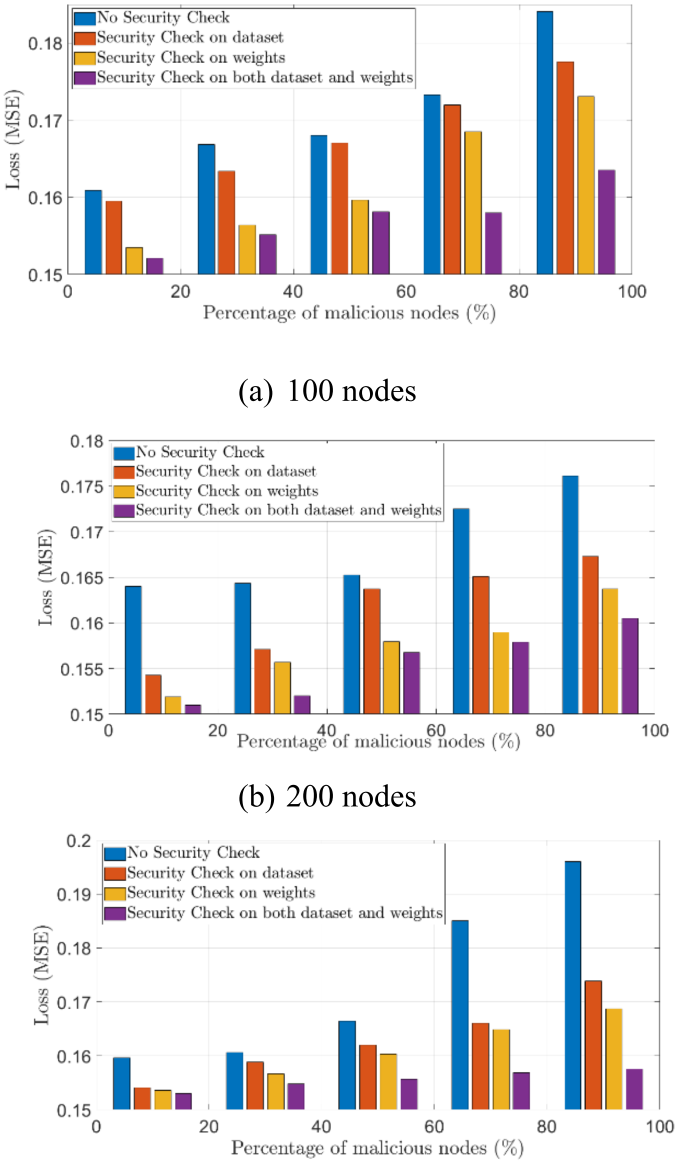

(a) 100 nodes

(b) 200 nodes

(c) 300 nodes

Figure 4.9: Loss (MSE) of global model after 100 iterations with malicious nodes.

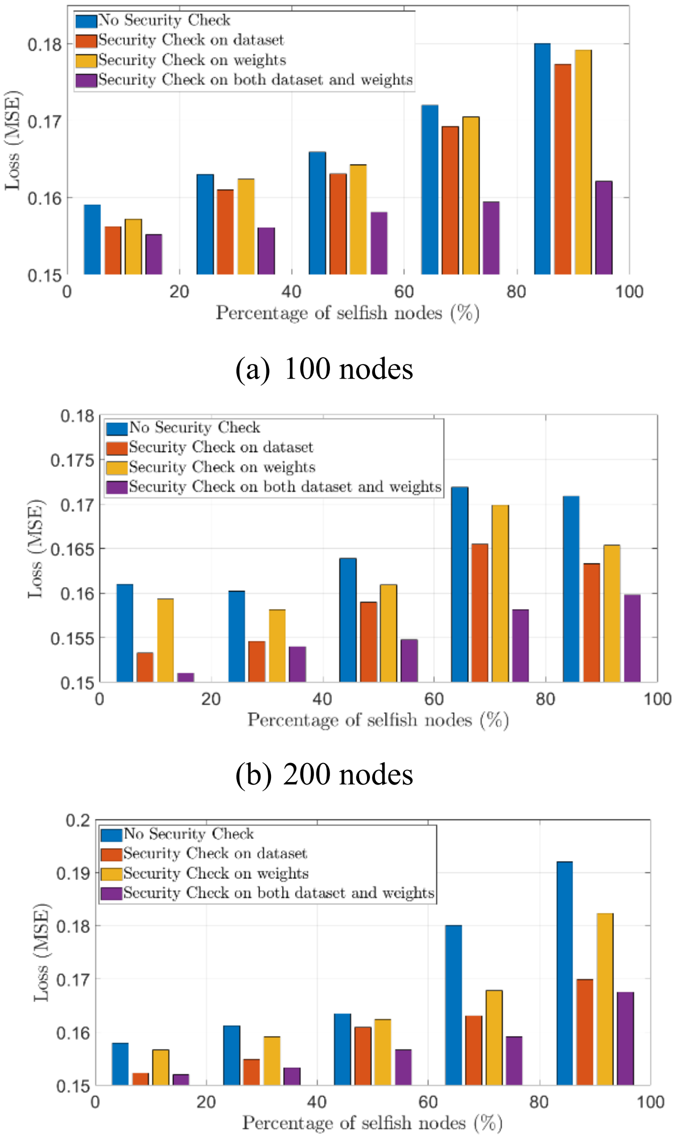

(a) 100 nodes

(b) 200 nodes

(c) 300 nodes

Figure 4.10: Loss (MSE) of global model after 100 iterations with selfish nodes.

4.4.3 Evaluation of Training Capacity of FL with and without Blockchain

Figure 4.11 displays the average number of nodes over 100 simulation runs which uploaded their local models during TS, with and without blockchain at various λ_V. The simulation results are matched with expected values derived in (4.2) and (4.5), confirming theoretical analysis. λ_{MB} and μ_d change with varying λ_V and are listed in Table 4.9. Figure 4.11 shows that blockchain based approach results in average 18 more nodes uploading their local models within same TS compared with the centralised solution in submitting local models directly to RSU without blockchain. This is because a copy of FL blockchain is possessed by each node. A local model by a node i can be entered into FL blockchain without depending upon RSU. Subsequently, RSU is able to receive an updated FL blockchain by another node j, containing local models of both node i and node j. Without blockchain, a node i must travel towards RSU within TS to directly share its local model. In this case, one RSU or small TS may not be sufficient for receiving local models from large number of nodes. Also, as shown in Table 4.9, the loss of global model decreases with rising n_{FL}. It can be concluded that FL blockchain can achieve desired accuracy of a global model faster than FL carried out without blockchain, because FL blockchain enables collection of local models from a greater number of nodes within the same time limit.

λ_V (nodes/m^2)	16	32	48
λ_{MB} (microblocks/s)	2.01	1.99	0.98
μ_d (m)	344	298	276

Table 4.9: λ_{MB} and μ_d with respect to λ_V.

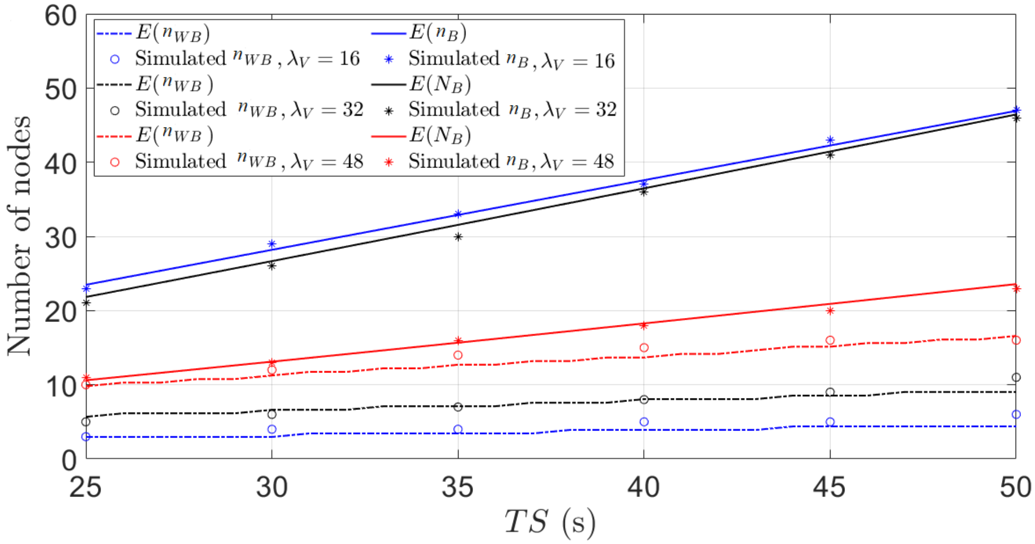

Figure 4.11: Number of nodes uploading local model in TS.

4.4.4 Evaluation of Incentive Distribution Mechanism

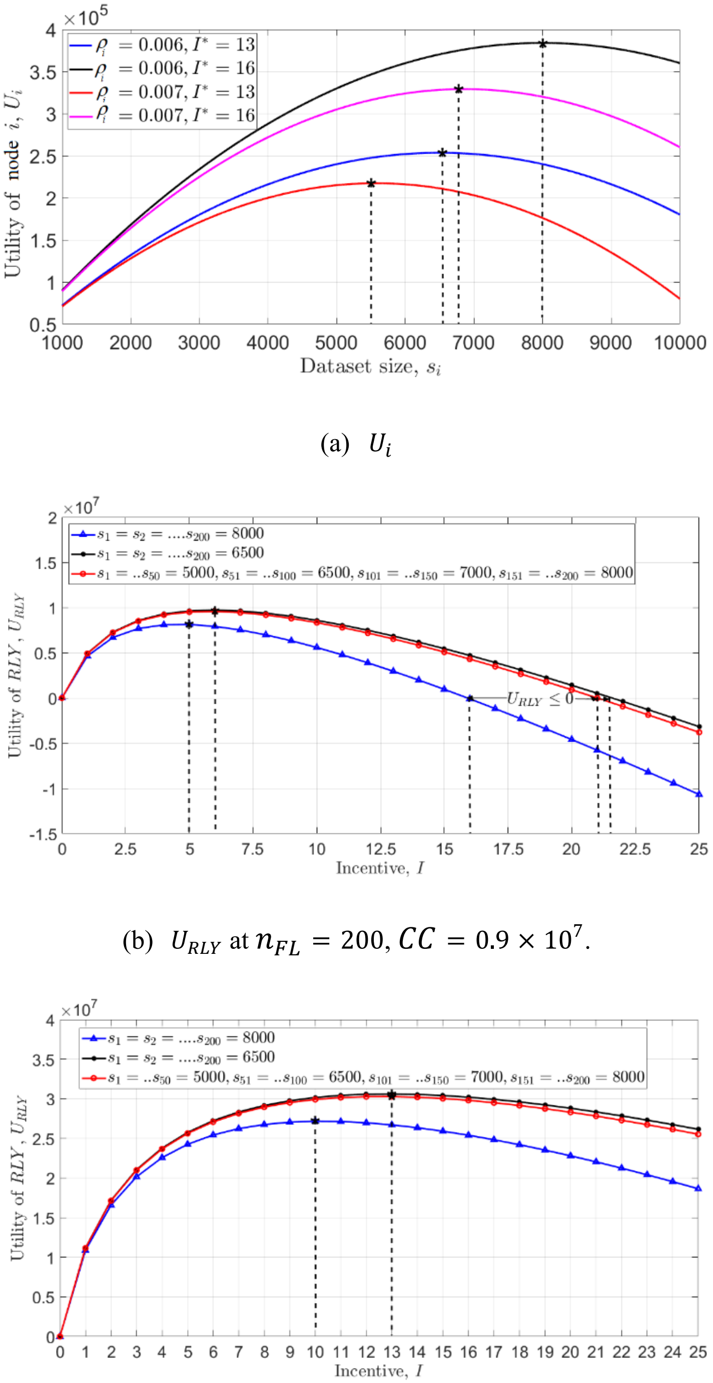

(a) U_i

(b) U_{RLY} at $n_{FL} = 200, CC = 0.9 \times 10^7$.

(c) U_{RLY} at $n_{FL} = 200, CC = 1.8 \times 10^7$.

Figure 4.12: Utility of players in Stackelberg Game with equilibrium points (*).

Figure 4.12 proves Definition 4.1 at equilibrium points at various values of ρ_i, CC and n_{FL}. Figure 4.12 (a) shows the utility of node i, U_i, participating in a blockchain based FL. As shown in Figure 4.12 (a), for a given I^*, there exists only one s_i^* which results in maximum U_i. Figure 4.12 (b) and (c) show U_{RLY} at $n_{FL} = 200$ with varying values of s_i and CC. In each case, an equilibrium point exists where U_{RLY} is maximum for a given I^*. A CA can select the value of I^*, which gives both maximum U_i and U_{RLY}. As shown in Figure 4.12 (b), $U_{RLY} \leq 0$ for certain values of I, which will motivate $RLYs$ to become selfish. An appropriate value of CC can be selected to make $U_{RLY} > 0$ for every value of I, as shown in Figure 4.12 (c). A machine learning model can be used to predict the optimum values of CC and I, according to s_i, which result in best response strategy of $RLYs$. This model can be embedded into smart contract of message blockchain to automate reward distribution independently without CA.

4.4.5 Comparison of PoFL with other Solutions

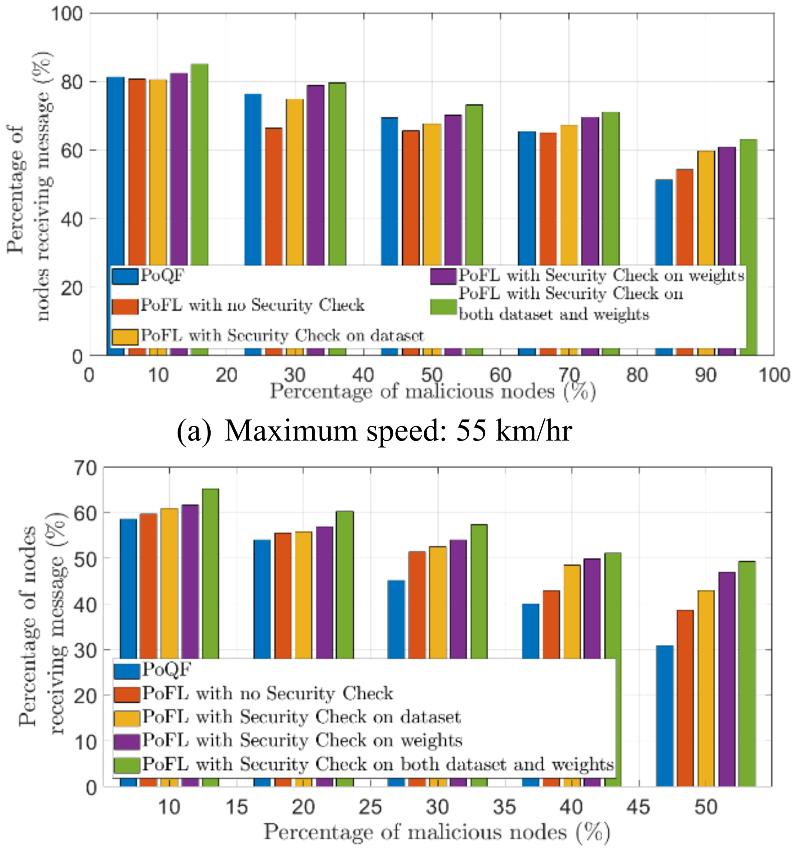

(a) Maximum speed: 55 km/hr

(b) Maximum speed: 110 km/hr

Figure 4.13: Message delivery ratio with 300 nodes.

Figure 4.13 shows message delivery ratio among 300 nodes at varying percentages of malicious nodes in the network as a result of 100 simulation runs. Results are compared with PoQF described in Chapter 3. PoFL outperforms voting based relay selection method and PoQF when security check is applied. However, with low percentage of malicious nodes and maximum speed of 55 km/hr, PoQF results in better message delivery ratio than PoFL when security check on weights is not applied. Nevertheless, PoFL with security check on both dataset and weights always outperforms voting based relay selection and PoQF by an average of 25% and 8.2% increase in message delivery ratio respectively.

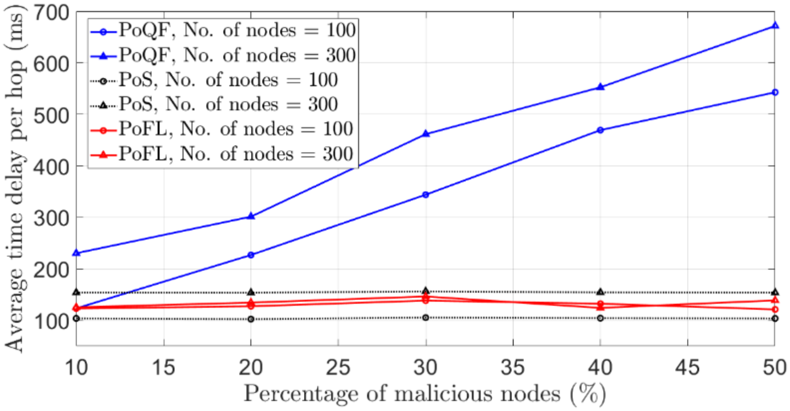

Figure 4.14: Average time delay per hop.

Figure 4.14 shows the average time delay per hop in completing PoFL, PoQF and PoS consensus. PoS is simulated such that it selects RLY on the basis of reputation of node. A random reputation value following uniform distribution, ranging from 0 to 100 is assigned to each node. The average time delay per hop of PoQF rises with increasing number of nodes and percentage of malicious nodes in the network. This is because PoQF waits for a threshold number of votes to determine RLY and the optimum threshold increases with rising number of total nodes and malicious nodes percentage. Time delay of PoS rises with increasing number of nodes due to more time required in accessing large amount of reputation values but it is independent of percentage of malicious nodes. PoFL is run by each node simultaneously and therefore its time delay is independent of both number of nodes and malicious percentage. On an average, PoFL is 65.2% faster than PoQF in relay selection and is more suitable for time-critical emergency situations. As a trade-off, PoQF only involves Quality Factor calculations but PoFL is based on a computationally expensive FL process with multiple iterations. Compared to PoS, PoFL is 15.74% faster when there are 300 nodes but 18.93% slower when there are 100 nodes. This is because PoS consumes time only in accessing the blockchain to find reputation of nodes. The access time increases when there is a large number of nodes registered in a blockchain network. Although PoS with 100 nodes outperforms both PoQF and PoFL, this faster consensus for block verification and addition cannot be run independently for appropriate relay selection, unlike PoQF and PoFL.

4.5 Summary

In this chapter, a decentralised FL based message dissemination, governed by blockchain is introduced. The theoretical and practical performances of uploading local models using blockchain are compared with a centralised approach without blockchain. The proposed FL with blockchain can be considered as a more efficient approach since it results in greater number of uploaded local models within a given time as compared to a solution without blockchain. Smart contract based security checks are proposed to detect adversary, which result in lower MSE in less number of iterations achieved by global model than FL without security check. An incentive distribution mechanism for blockchain based FL is also proposed and analysed using Stackelberg game to determine optimal data size and incentive which result in the best response strategy of players.

The future work can include FL based message validation process before relay selection. To achieve a light-weight solution and reduced computation cost, alternative consensus algorithms can be used to prevent malicious attacks instead of machine learning method embedded in smart contract. For example, a local model may be considered credible if reputation of the trainer exceeds a certain threshold.

Chapter 5 —Blockchain-enabled FD-NOMA based Vehicular Network with Physical Layer Security

In this chapter, a blockchain based vehicular network using FD-NOMA is analysed with physical layer security ensuring a transmission's reliability and secrecy rate. The chapter is divided into three main sections. Background and motivation are discussed in section 5.1. In section 5.2, an FD-NOMA based vehicular network is theoretically analysed for security and privacy of the proposed network against eavesdropping and jamming. We derive the upper bound of blockchain throughput in terms of physical layer characteristics, i.e., SINR and secrecy rate. In section 0, Monte Carlo simulations are presented to validate the theoretical analysis.

5.1 Overview

5.1.1 Introduction

There are several attacks on security and privacy which can affect the performance of vehicular networks. These attacks can be classified on the basis of layer used by an attacker in a communications protocol stack [149]. From physical layer's perspective, a vehicular network may suffer from the following attacks [10], [150]:

a) Jamming Attack

It is caused when an attacker creates interference to disrupt the communications between sender and legitimate receiver. It affects the *availability* attribute of security in a vehicular network.

b) Eavesdropping Attack

It is caused when an eavesdropper intercepts the transmission between sender and legitimate receiver. It affects the *confidentiality* attribute of privacy in a vehicular network.

Security and privacy are usually managed at the upper layers of a communications protocol stack by using various techniques including blockchain and key based encryption [38]. Blockchain has been proven resilient against security attacks, such as application layer attack of repudiation [151], network layer attacks of Denial of Service and Sybil [152]. A permissioned blockchain not only ensures security but also privacy, by allowing only authorized nodes to join and communicate in a network. However, physical layer attacks can severely affect performance of a blockchain-enabled vehicular network. For example, jamming can disrupt block announcement, thereby reducing throughput of blockchain. PLS is another effective approach to protect privacy and maintain secrecy against eavesdropping [153] but may also result in a decreased blockchain throughput.

5.1.2 Motivation

Motivated by the latest advances in blockchain and the importance of security and privacy in vehicular communications, we study the effects of physical layer attacks on blockchain-enabled vehicular network. Additionally, due to increasing number of connected nodes, heterogeneous environment and requirement of high communication rates, FD-NOMA based V2X communications scenario is considered [154]. An FD-NOMA model fulfils the requirements of various QoS and multiple communication rates in V2X systems [155]. It also addresses the issue of low latency in existing Orthogonal Frequency Division Multiple Access based 5G technologies by simultaneous transmission and retrieval of data [156]. It is particularly suggested for V2X applications, e.g., navigation and emergency message dissemination [154]. Its roadmap for V2X based services has already been prepared by technical organizations, such as 3rd Generation Partnership Project [157]. Furthermore, NOMA based techniques can be used to provide security against jamming attack by nullifying co-channel interferences via Successive Interference Cancellation (SIC) [154].

The effect of interference on blockchain throughput is also studied in [120]. SINR is a physical layer parameter and a function of distances between nodes in wireless communications. It can be severely degraded by attackers causing jamming and interference in signal transmission and therefore result in a reduced blockchain throughput. However, FD-NOMA can significantly improve SINR by SIC. Therefore, the performance of FD-NOMA for a secure blockchain based V2X system is worth investigating. Performance of FD-NOMA based V2X systems is analysed in [154] assuming both Rayleigh and Rician channel models. The analysis does not take into account the traffic density, speeds or distances between moving nodes which greatly affect the reliability of signal transmission in V2X systems.

Furthermore, some of the security and privacy requirements of V2X systems may not be met by blockchain alone. For example, if a blockchain uses voting consensus, the votes must also be encrypted in presence of an eavesdropper, which increases computation and communication overheads. Moreover, if all nodes broadcast their votes at the same time, the reliability of a transmission is severely reduced by interference. Therefore, an integrated approach considering both physical layer aspects, e.g., SINR and secrecy rate, and application layer schemes, e.g., blockchain, can be utilized to provide robust security in vehicular networks. However, the feasibility analysis of an integrated approach is required before its practical implementation.

5.2 Analysis of Blockchain-enabled FD-NOMA based Vehicular Network

5.2.1 System Model

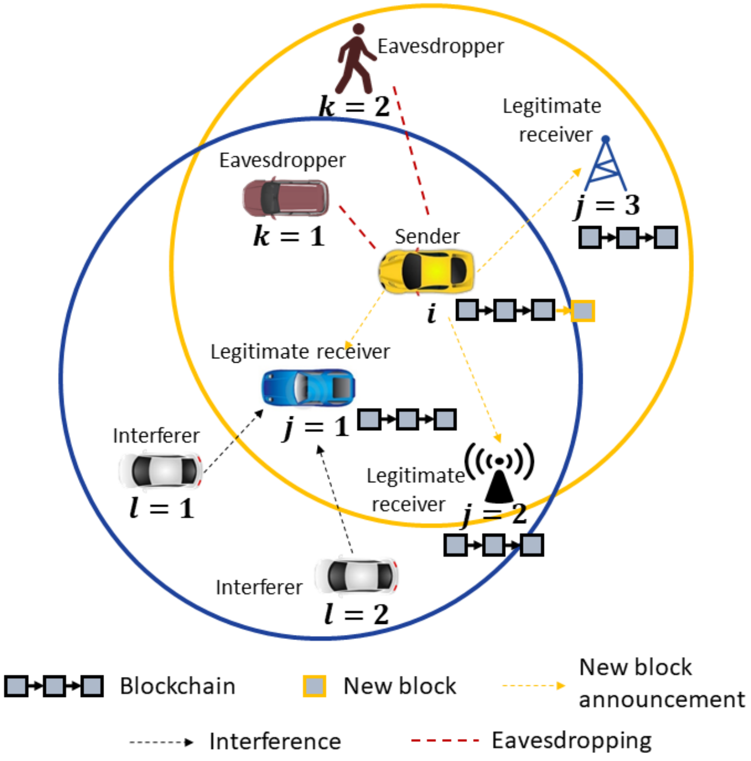

Figure 5.1: The system model.

Figure 5.1 illustrates a V2X network consisting of mobile and stationary nodes including vehicles, pedestrian, RSU, base station etc. forming an FD-NOMA based system. The nodes can be categorised into one of the following: sender, legitimate receiver, interferer and eavesdropper. We assume urban and crowded environment is assumed; hence all communication channels are modelled by Rayleigh fading [158]. The channel matrix from n_s sender nodes to n_r receiver nodes in FD-NOMA based decentralised V2X systems is defined in [154] as

$$\boldsymbol{H} = \begin{bmatrix} h_{1,1} & \cdots & h_{n_s,1} \\ \vdots & \ddots & \vdots \\ h_{1,n_r} & \cdots & h_{n_s,n_r} \end{bmatrix}, \tag{5.1}$$

where $h_{i,j} = \sqrt{g_{i,j} d_{i,j}^{-\alpha}}$ is the channel coefficient between node i and node j and $g_{\,i,j}$ is the channel gain following Rayleigh fading [38]. Assume that all channels are uncorrelated and have increasing order of channel coefficients, i.e., $|h_{1,j}| \leq |h_{2,j}| \leq, \ldots |h_{i,j}| \leq, \ldots |h_{n_s,j}| \; \forall \; i \in [1, n_s], j \in [1, n_r]$. In this case, co-channel interference of j^{th} node is from $(j+1)^{th}$ to n_s^{th} node. Other co-channel interferences are nullified by SIC feature of NOMA [154].

Due to high mobility of nodes in a vehicular network, we take into account the uncertainty of nodes' positions. Therefore, $d_{i,j}$ is assumed as a random variable following exponential distribution. Exponential distribution has been shown as a suitable approximation to model traffic flow condition [159]. The PDF of $d_{i,j}$ is

$$f(d_{i,j}) = \frac{1}{\overline{d_{\imath,\jmath}}} e^{-\frac{d_{i,j}}{\overline{d_{\imath,\jmath}}}}, \tag{5.2}$$

where $\overline{d_{\imath,\jmath}}$ is the average distance between node i and node j. The traffic density in nodes/km can be defined as $1000/\overline{d_{\imath,\jmath}}$ [160].

The performance of a blockchain-enabled wireless network is characterized by two important parameters: data rate and blockchain throughput. Data rate is defined as the amount of transmitted data in a unit time for a network, usually measured in bits per second (bps). Blockchain throughput, λ_B, is the number of blocks validated and generated in a unit time. It is measured in blocks per second (blocks/s). The relationship of data rate DR with blockchain throughput λ_B and block length L is defined in [120] as

$$DR \geq \lambda_B \cdot L. \tag{5.3}$$

5.2.2 SINR

When a signal is received by node j from node i, the instantaneous SINR is defined in [154] as

$$SINR_{i,j} = \frac{P_i \left|h_{i,j}\right|^2}{\sum_{l=j+1}^{n_s} P_l \left|h_{i,j}\right|^2 + \eta P_j + P_{noise}}, \tag{5.4}$$

where ηP_j is the self-interference by FD up-link, $\eta \epsilon [0,1]$ is the coefficient of self-interference, P_{noise} is the noise power of Additive White Gaussian Noise (AWGN), P_i and P_l are the power of signal transmitted by node i and interference node l respectively. The received signal is subjected to only co-channel interference from neighbours of node j after SIC.

In urban and crowded environment, the PDF of $SINR_{i,j}$ is given in [154], [161] as

$$f(SINR_{i,j}) = \frac{1}{\overline{SINR_{\iota,J}}} e^{-\frac{SINR_{i,j}}{\overline{SINR_{\iota,J}}}}, \tag{5.5}$$

where $\overline{SINR_{\iota,J}}$ is the average SINR. It is noted that $SINR_{i,j}$ can be modelled as a random variable following exponential distribution. As shown in (5.4), it depends on $h_{i,j}$, which is a function of $d_{i,j}^{-\alpha}$. Since $d_{i,j}$ is also an exponential variable, as shown in (5.2), Lemma 5.1 and Theorem 5.1 are presented to derive bounds of $\overline{SINR_{\iota,J}}$ as a function of $d_{i,j}$ and n_{itf}^{j}, i.e., the number of interference nodes to receiver j.

- *Lemma 5.1:* $E\left(\frac{1}{d_{i,j}^{-\alpha}}\right) = \overline{d_{\iota,J}}^{\alpha}\left(\Gamma\left(\alpha+1, d_{min}/\overline{d_{\iota,J}}\right) - \Gamma\left(\alpha+1, d_{max}/\overline{d_{\iota,J}}\right)\right)$, where d_{min} is the minimum $d_{i,j}$ and d_{max} is the maximum $d_{i,j}$ up to which a signal can be transmitted.

Proof: Since

$$E(1/X) = \int_{-\infty}^{\infty} x^{-1} f(x)dx, \tag{5.6}$$

let $X = d_{i,j}^{-\alpha}$, then its CDF is

$$\begin{aligned} F_X(x) &= Pr(X \leq x) = Pr\left(d_{i,j}^{-\alpha} \leq x\right) \\ &= Pr\left(d_{i,j} > x^{-\frac{1}{\alpha}}\right) = 1 - F_{d_{i,j}}(x^{-\frac{1}{\alpha}}). \end{aligned} \tag{5.7}$$

PDF of X can be obtained by taking derivative of (5.7), i.e.,

$$f_X(x) = \frac{1}{\alpha} x^{-\frac{1}{\alpha}-1} f_{d_{i,j}}(x^{-\frac{1}{\alpha}}) = \frac{1}{\overline{d_{\iota,\jmath}}\alpha} x^{-\frac{1}{\alpha}-1} e^{-\frac{x^{-\frac{1}{\alpha}}}{\overline{d_{\iota,\jmath}}}}. \tag{5.8}$$

Combining (5.6) and (5.8) gives

$$E(1/X) = \frac{1}{\overline{d_{\iota,\jmath}}\alpha} \int_{d_{max}^{-\alpha}}^{d_{min}^{-\alpha}} x^{-\frac{1}{\alpha}-2} e^{-\frac{x^{-\frac{1}{\alpha}}}{\overline{d_{\iota,\jmath}}}} dx, \tag{5.9}$$

Solving (5.9) gives $E\left(\frac{1}{d_{i,j}^{-\alpha}}\right) = \overline{d_{\iota,\jmath}}^{\alpha} \left(\Gamma\left(\alpha + 1, d_{min}/\overline{d_{\iota,\jmath}}\right) - \Gamma\left(\alpha + 1, d_{max}/\overline{d_{\iota,\jmath}}\right)\right)$. ■

- *Theorem 5.1:* $\frac{1}{\left(n_{itf}^{j} E\left(d_{i,j}^{-\alpha}\right)+P'\right)E\left(\frac{1}{d_{i,j}^{-\alpha}}\right)} \leq \overline{SINR_{\iota,\jmath}} \leq \frac{\overline{d_{\iota,\jmath}}^{-\alpha}}{n_{itf}^{j} d_{max}^{-\alpha}+P'}$,where $E\left(\frac{1}{d_{i,j}^{-\alpha}}\right)$ is

defined in Lemma 5.1, $P' = \frac{\eta P_j + P_{noise}}{Pg}$ and $P = P_i = P_l$, $g = g_{i,j} = g_{l,j} \,\forall\, l \,\epsilon\, n_s$, without loss of generality.

Proof: Assuming $P = P_i = P_l$ and $g = g_{i,j} = g_{l,j} \,\forall\, l \,\epsilon\, n_s$, (5.4) can be rewritten as

$$SINR_{i,j} = \frac{d_{i,j}^{-\alpha}}{n_{itf}^{j} d_{l,j}^{-\alpha} + P'}, \tag{5.10}$$

and therefore,

$$\frac{1}{SINR_{i,j}} = \frac{n_{itf}^{j} d_{l,j}^{-\alpha}}{d_{i,j}^{-\alpha}} + \frac{P'}{d_{i,j}^{-\alpha}}, \tag{5.11}$$

$$E\left(\frac{1}{SINR_{i,j}}\right) = n_{itf}^{j} E\left(\frac{d_{l,j}^{-\alpha}}{d_{i,j}^{-\alpha}}\right) + P' E\left(\frac{1}{d_{i,j}^{-\alpha}}\right). \tag{5.12}$$

Let $E\left(\frac{d_{l,j}^{-\alpha}}{d_{i,j}^{-\alpha}}\right) = E\left(\frac{Y}{X}\right) = E(Y).E\left(\frac{1}{X}\right)$ where $X = d_{i,j}^{-\alpha}$ and $Y = d_{l,j}^{-\alpha}$. Since both $d_{i,j}$ and $d_{l,j}$ represent distance between nodes, $E(Y) = E(X) = \frac{1}{\overline{d_{l,j}}\alpha}\int_{d_{max}^{-\alpha}}^{d_{min}^{-\alpha}} x^{-\frac{1}{\alpha}} e^{-\frac{x^{-\frac{1}{\alpha}}}{\overline{d_{l,j}}}} dx$. According to Jensen's inequality [162], $\frac{1}{E(SINR_{i,j})} \leq E\left(\frac{1}{SINR_{i,j}}\right)$, which follows that $\overline{SINR_{l,j}} \geq \frac{1}{E\left(\frac{1}{SINR_{i,j}}\right)}$. Since $SINR_{i,j}$ is directly proportional to $d_{i,j}^{-\alpha}$, $\overline{SINR_{l,j}} \leq \frac{\overline{d_{l,j}}^{-\alpha}}{n_{itf}^{j} d_{max}^{-\alpha} + P'}$ ■

For a reliable message transmission and successful block generation, it is necessary that $SINR_{i,j}$ exceeds a certain threshold. The probability that $SINR_{i,j}$ exceeds a threshold β_1 can be given by its CDF, i.e.,

$$F_{SINR_{i,j}}(\beta_1) = \int_0^{\beta_1} f(SINR_{i,j}) dSINR_{i,j} = \int_0^{\beta_1} \frac{1}{\overline{SINR_{l,j}}} e^{-\frac{SINR_{i,j}}{\overline{SINR_{l,j}}}} dSINR_{i,j}$$
$$= 1 - e^{-\frac{\beta_1}{\overline{SINR_{l,j}}}}, \tag{5.13}$$

and

$$Pr(SINR_{i,j} \geq \beta_1) = 1 - F_{SINR_{i,j}}(\beta_1) = e^{-\frac{\beta_1}{\overline{SINR_{l,j}}}}. \tag{5.14}$$

Also, $e^{-\frac{\beta_1}{\overline{SINR_{l,j}}^{LB}}} \leq Pr(SINR_{i,j} \geq \beta_1) \leq e^{-\frac{\beta_1}{\overline{SINR_{l,j}}^{UB}}}$. In case of a jamming attack caused by interference, a block can only be generated if it is transmitted successfully to at least one legitimate receiver. Therefore, (5.3) is modified as follows

$$DR \geq \frac{\lambda_B}{Pr(SINR_{i,j} \geq \beta_1)^{UB}} \cdot L. \tag{5.15}$$

5.2.3 Secrecy Rate

If a signal from node i is sent to a legitimate receiver node j but a node k attempts to receive the signal as an eavesdropper, as shown in Figure 5.1, the secrecy rate is defined in [163] as

$$C_{i,j} = \left[C_j - C_k\right]^+, \tag{5.16}$$

where $C_j = log_2\left(1 + SINR_{i,j}\right)$, $C_k = \sum_{k=1}^{n_e} log_2\left(1 + SINR_{i,k}\right)$, n_e is the number of eavesdroppers present in the communication range of node i and $[.]^+$ denotes $max(.,0)$. Using logarithmic property, i.e., $log(a) + log(b) = log(ab)$, C_k can also be represented as $C_k = log_2\phi$, where $\phi = \left(1 + SINR_{i,1}\right)\left(1 + SINR_{i,2}\right) \ldots\ldots \left(1 + SINR_{i,n_e}\right)$.

PLS ensures that a message is transmitted when secrecy rate is greater than a certain threshold β_2. Theorem 5.2 defines the probability of maintaining confidentiality through PLS.

- *Theorem 5.2:*

$$Pr\left(C_{i,j} \geq \beta_2\right) = \begin{cases} \dfrac{\overline{SINR_{\iota,J}}\, e^{\frac{1-2^{\beta_2}}{\overline{\overline{SINR_{\iota,J}}}}}}{2^{\beta_2}\overline{SINR_{\iota,k=1}} + \overline{SINR_{\iota,J}}}, & n_e = 1, \\ \dfrac{\overline{SINR_{\iota,J}}^2 e^{\frac{-2^{\beta_2}}{\overline{\overline{SINR_{\iota,J}}}}} E_1\left(\frac{v_1 v_2}{u}\right) e^{\frac{v_1 v_2}{u}}}{u}, & n_e = 2, \end{cases}$$

where $u = 2^{\beta_2}\overline{SINR_{\iota,J}} \cdot \overline{SINR_{\iota,k=1}} \cdot \overline{SINR_{\iota,k=2}}$, $v_1 = \overline{SINR_{\iota,J}} + 2^{\beta_2}\overline{SINR_{\iota,k=2}}$, $v_2 = v_1 + 2^{\beta_2+1}\overline{SINR_{\iota,k=1}}$ and $E_1(a) = \int_a^\infty \frac{e^{-z}}{z} dz$ is exponential integral.

$Pr\left(C_{i,j} \geq \beta_2\right) \approx 0$ for $n_e > 2$.

Proof: Since $C_{i,j}$ is a function of $SINR_{i,j}$ and $SINR_{i,k}$, $Pr\left(C_{i,j} \geq \beta_2\right)$ is given in [161] as

$$Pr\left(C_{i,j} \geq \beta_2\right) = \int\limits_{SINR_{i,n_e}=0}^{\infty} \cdots \int\limits_{SINR_{i,1}=0}^{\infty} \int\limits_{2^{\beta_2}\phi-1}^{\infty} f\left(SINR_{i,j}\right) f\left(SINR_{i,1}\right) \ldots \\ \ldots f\left(SINR_{i,n_e}\right) dSINR_{i,j} dSINR_{i,1} \ldots dSINR_{i,n_e}. \tag{5.17}$$

When $n_e = 1$, (5.17) reduces to

$$Pr\left(C_{i,j} \geq \beta_2\right) \\ = \int_0^{\infty} \int_{2^{\beta_2}\left(1+SINR_{i,1}\right)-1}^{\infty} f\left(SINR_{i,j}\right) f\left(SINR_{i,1}\right) dSINR_{i,j} dSINR_{i,1}. \tag{5.18}$$

Using $\int_t^{\infty} \frac{1}{a} e^{-\frac{z}{a}} dz = e^{-\frac{t}{a}}$, (5.18) becomes

$$Pr\left(C_{i,j} \geq \beta_2\right) = \frac{1}{\overline{\overline{SINR_{\imath,1}}}} \int_0^{\infty} e^{-\frac{2^{\beta_2}\left(1+SINR_{i,1}\right)-1}{\overline{SINR_{\imath,\jmath}}} - \frac{SINR_{1,i}}{\overline{\overline{SINR_{\imath,1}}}}} dSINR_{i,1}, \tag{5.19}$$

which follows that

$$Pr\left(C_{i,j} \geq \beta_2\right) = \frac{\overline{SINR_{\imath,\jmath}} e^{\frac{1-2^{\beta_2}}{\overline{\overline{SINR_{\imath,\jmath}}}}}}{2^{\beta_2}\overline{SINR_{\imath,1}} + \overline{SINR_{\imath,\jmath}}}. \tag{5.20}$$

For $n_e = 2$, the first two integrals of (5.17) can be solved similarly and it becomes

$$Pr\left(C_{i,j} \geq \beta_2\right) \\ = \frac{1}{\overline{\overline{SINR_{\imath,1}}}} \int_0^{\infty} \frac{\overline{SINR_{\imath,\jmath}} e^{\frac{1-2^{\beta_2}}{\overline{\overline{SINR_{\imath,\jmath}}}}}}{2^{\beta_2}\left(1+SINR_{i,2}\right)\overline{SINR_{\imath,1}} + \overline{SINR_{\imath,\jmath}}} f\left(SINR_{i,2}\right) dSINR_{i,2} \\ = \frac{\overline{SINR_{\imath,\jmath}}^2 e^{\frac{-2^{\beta_2}}{\overline{\overline{SINR_{\imath,\jmath}}}}} E_1\left(\frac{v_1 v_2}{u}\right) e^{\frac{v_1 v_2}{u}}}{u}. \tag{5.21}$$

As (5.21) involves exponential integral, obtaining a closed form equation of $Pr\left(C_{i,j} \leq \beta_2\right)$ for $n_e > 2$ is at least arduous, if not impossible [38], [154]. However, it can be seen that the resulting values of u, v_1 and v_2 after solving (5.17) for $n_e > 2$ will increase and will lead to $Pr\left(C_{i,j} \geq \beta_2\right) \approx 0$. ■

Theorem 5.2 shows that an FD-NOMA transmission without blockchain may not provide secrecy when $n_e > 2$, since $Pr(C_{i,j} \geq \beta_2) \approx o.$ Therefore, privacy preserving measures such as encryption schemes and blockchain are therefore essential in such cases, where confidentiality cannot be protected by PLS alone.

Using $E_1(z)e^z \leq log\left(1+\frac{1}{z}\right)$ [164] and assuming $e^{\frac{1-2^{\beta_2}}{\overline{SINR_{i,j}}^{UB}}} \approx 1$, the upper bound of $Pr(C_{i,j} \geq \beta_2)$ can be defined as

$$Pr(C_{i,j} \geq \beta_2) \leq \begin{cases} \dfrac{\overline{SINR_{i,j}}^{UB}}{2^{\beta_2}\overline{SINR_{i,1}} + \overline{SINR_{i,j}}^{UB}}, & n_e = 1, \\ \dfrac{\overline{SINR_{i,j}}^{UB} log\left(1+\dfrac{u'}{v_1{}'v_2{}'}\right)}{u'}, & n_e = 2, \\ 0, & otherwise, \end{cases} \tag{5.22}$$

where $u' = 2^{\beta_2} \cdot \overline{SINR_{i,1}} \cdot \overline{SINR_{i,2}}$, $v_1{}' = \overline{SINR_{i,j}}^{UB} + 2^{\beta_2}\overline{SINR_{i,1}}$, $v_2{}' = v_1{}' + 2^{\beta_2+1}\overline{SINR_{i,1}}$.

In case of eavesdropping attack, the secrecy rate must be greater than β_2 for every receiver to protect confidentiality. Therefore, for protecting every legitimate receiver from eavesdropping attack on physical layer, (5.3) is modified as follows

$$DR \geq \frac{\lambda_B}{\prod_{j=1}^{n_r} Pr(C_{i,j} \geq \beta_2)^{UB}} \cdot L. \tag{5.23}$$

A sender can probabilistically estimate the presence and location of eavesdropper before transmission through solutions defined in [165] and [166].

5.2.4 Goodput

To analyse the impact of PLS combined with blockchain, we define the term goodput as DR times the ratio of number of blocks successfully and secretly added into the blockchain to the total number of block generation attempts, i.e.,

$$Goodput = DR \cdot \frac{No.\ of\ blocks\ added\ to\ blockchain}{Total\ No.\ of\ block\ generation\ attempts}, \tag{5.24}$$

where $Total\ No. of\ block\ generation\ attempts$ $= No. of\ blocks\ added\ to\ blockchain + Number\ of\ blocks\ lost\ or\ eavesdropped.$

5.3 Simulated Performance Analysis

In this section, simulation results are compared with theoretical analysis presented in Section 5.2. Monte Carlo simulations are conducted on MATLAB. The code for FD-NOMA implementation can be seen in Appendix D. The parameters used in simulations are listed in Table 5.1.

Parameters	**Values**	**Parameters**	**Values**
Iterations	10^5	η	0.1
P_i	20 dBm	P_{noise}	-104 dBm
d_{max}	400 m	d_{min}	10 m
β_1	-15 dB	β_2	0.3 bits/sec/Hz
λ_B	1, 50 blocks/s	L	756 bytes
α	3	n_e	[1, 2]
n_{itf}	[1, 5]	n_r	[2, 5]

Table 5.1: Parameters used in simulation of FD-NOMA based vehicular network.

5.3.1 SINR

Figure 5.2 (a) shows $\overline{SINR_{\iota,J}}$ varying with respect to $\overline{d_{\iota,J}}$ at $n_{itf}^{j} = 1$ and $n_{itf}^{j} = 2$. The simulated $\overline{SINR_{\iota,J}}$ lies within the bounds defined in Theorem 5.1, validating our analysis. It can be seen that $\overline{SINR_{\iota,J}}$ falls with increasing $\overline{d_{\iota,J}}$. The dependence of $\overline{SINR_{\iota,J}}$ on $\overline{d_{\iota,J}}$ is higher when $n_{itf}^{j} = 1$ as compared to $n_{itf}^{j} = 2$. It shows that $\overline{SINR_{\iota,J}}$ can be enhanced by reducing $\overline{d_{\iota,J}}$ only when interference is low. Figure 5.2 (b) shows $Pr\left(SINR_{i,j} \geq \beta_1\right)$ with respect to $\overline{d_{\iota,J}}$. The theoretical result is computed using (5.14). In simulation, $SINR_{i,j} \geq \beta_1$ is counted as a successful transmission for each iteration. The percentage of successful transmissions is plotted as a simulated result in Figure 5.2 (b). It can be seen in that $Pr\left(SINR_{i,j} \geq \beta_1\right)$ falls with increasing $\overline{d_{\imath,\jmath}}$. due to decreasing $SINR_{i,j}$. $Pr\left(SINR_{i,j} \geq \beta_1\right)$ is higher for less n_{itf}^{j}, which depicts the effect of interference. High interference is considered as a collusion of attackers to hinder successful transmission. This is why a high $Pr\left(SINR_{i,j} \geq \beta_1\right)$ is desired for a secure and reliable transmission.

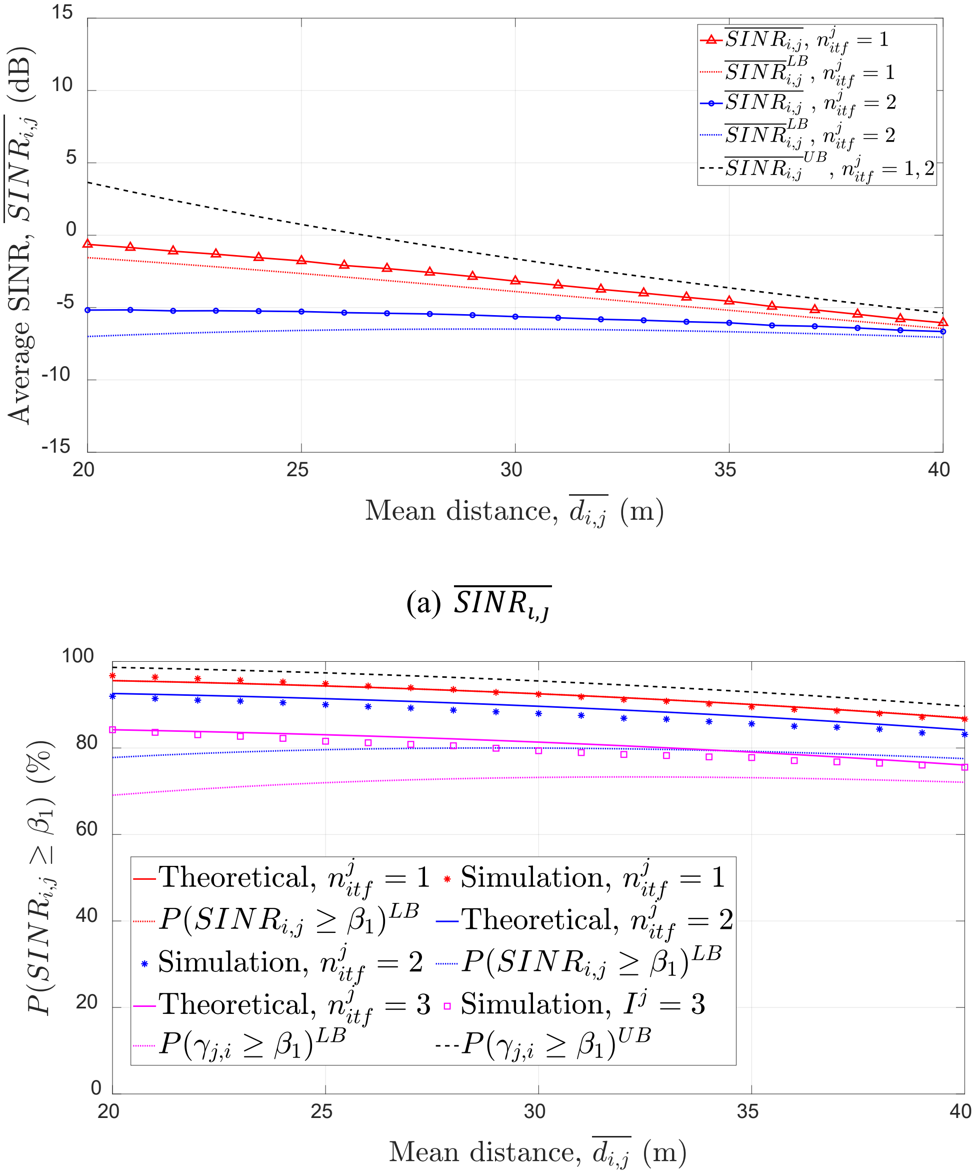

(a) $\overline{SINR_{\imath,\jmath}}$

(b) $Pr\left(SINR_{i,j} \geq \beta_1\right)$

Figure 5.2: $\overline{SINR_{\imath,\jmath}}$ and $Pr\left(SINR_{i,j} \leq \beta_1\right)$ with respect to $\overline{d_{\imath,\jmath}}$.

5.3.2 Secrecy Rate

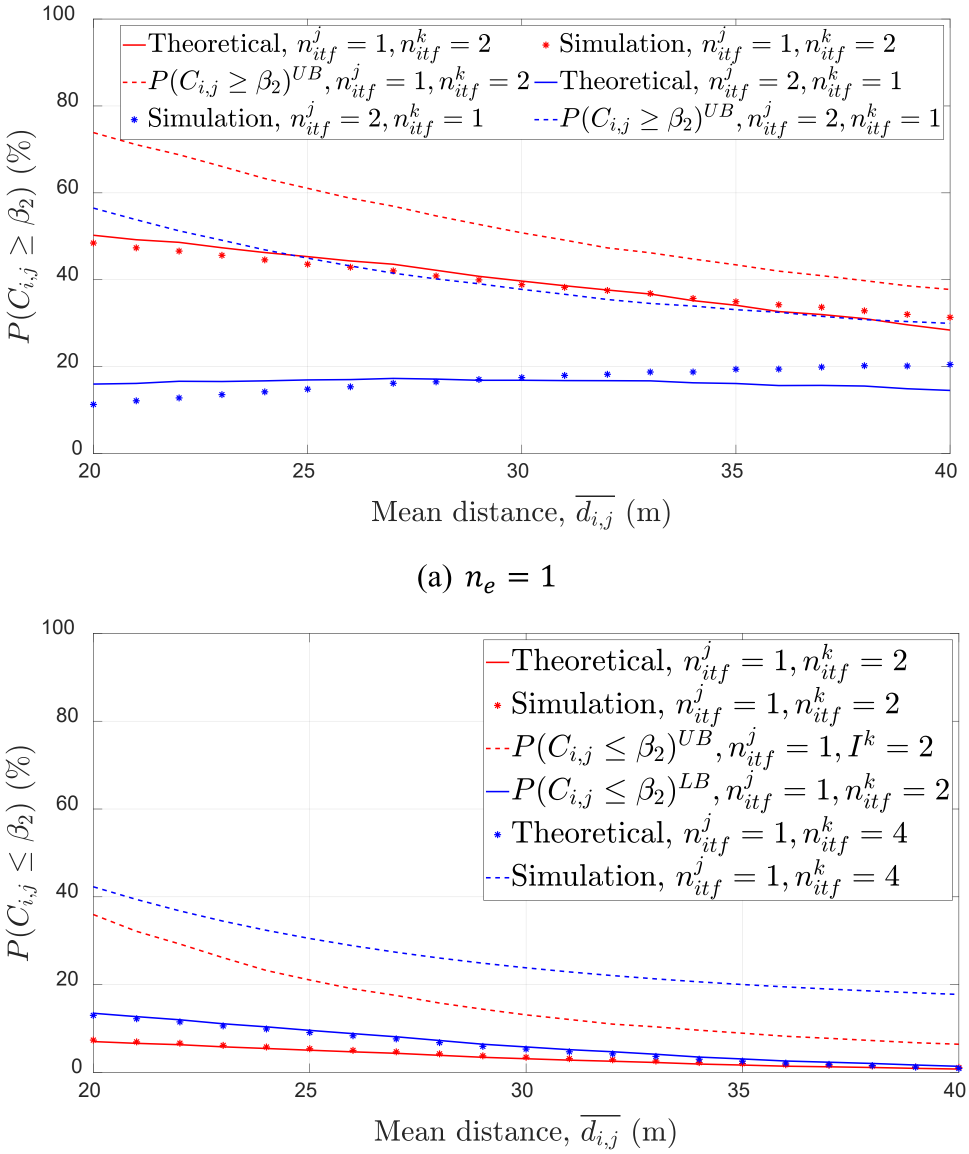

(a) $n_e = 1$

(b) $n_e = 2$

Figure 5.3: $Pr\left(C_{i,j} \geq \beta_2\right)$ with respect to $\overline{d_{\iota,J}}$.

Figure 5.3 shows $Pr\left(C_{i,j} \geq \beta_2\right)$ with $n_e = 1$ and $n_e = 2$. The theoretical result and upper bound are plotted using Theorem 5.2 and (5.22) respectively. Simulations show the percentage of iterations which resulted in $C_{i,j} \geq \beta_2$. $Pr\left(C_{i,j} \geq \beta_2\right)$ reduces with increasing n_e. Figure 5.3 (b) shows that $Pr\left(C_{i,j} \geq \beta_2\right)$ is less than 50% when $n_e = 2$ and $n^j_{itf} = 1$, despite varying values of n^k_{itf}. It reflects that maintaining secrecy is extremely challenging with large number of eavesdroppers. Therefore, cryptographically protected blockchain is an effective solution to ensure confidentiality of a transmission in such case.

5.3.3 Percentage of Success Transmissions

Figure 5.4 shows percentage of success transmissions with respect to $\overline{d_{\imath,\jmath}}$ in presence of jammers and eavesdroppers. A success transmission is counted if $SINR_{i,j} \geq \beta_1$, with jammers only and also if $C_{i,j} \geq \beta_2$, when eavesdroppers are present. As shown in Figure 5.4, success rate is higher with jammers only than with eavesdroppers. Specifically, when $n_e = 2$, the success rate is below 50% for every $\overline{d_{\imath,\jmath}}$. As a PLS approach, a sender must estimate that $C_{i,j} \geq \beta_2$ to protect secrecy of a message. However, it is extremely challenging to attain $C_{i,j} \geq \beta_2$ in presence of large number of eavesdroppers. A cryptographically protected blockchain is an effective solution to ensure confidentiality of a transmission in such case. Therefore, a cross-layer approach combining both PLS and blockchain is promising to provide security against both attacks.

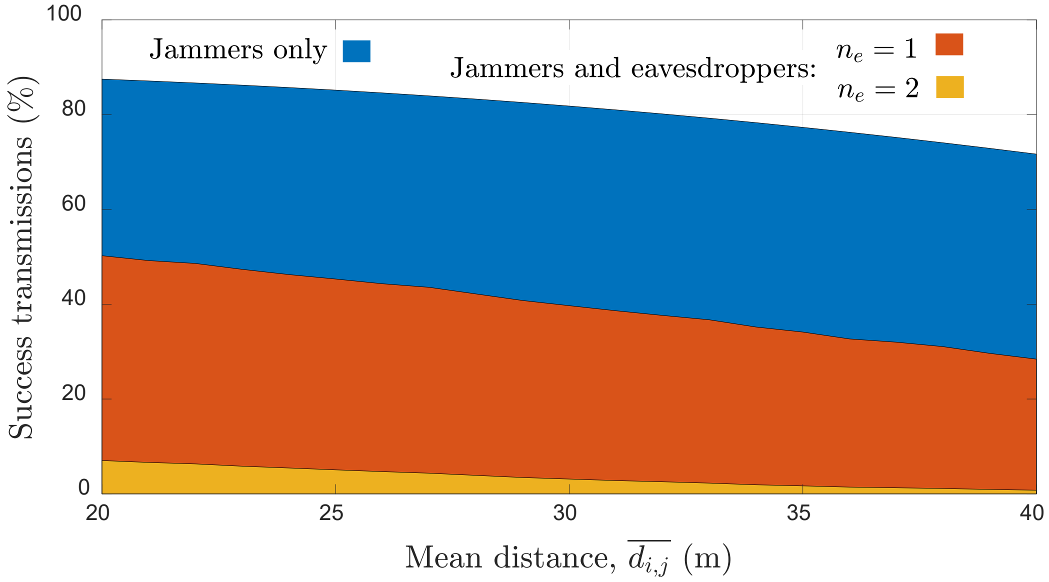

Figure 5.4: Success transmissions in presence of jammer and eavesdroppers, $n_{itf}^{j} = 2, n_{itf}^{k} = 1$.

5.3.4 Minimum Allowable Data rate

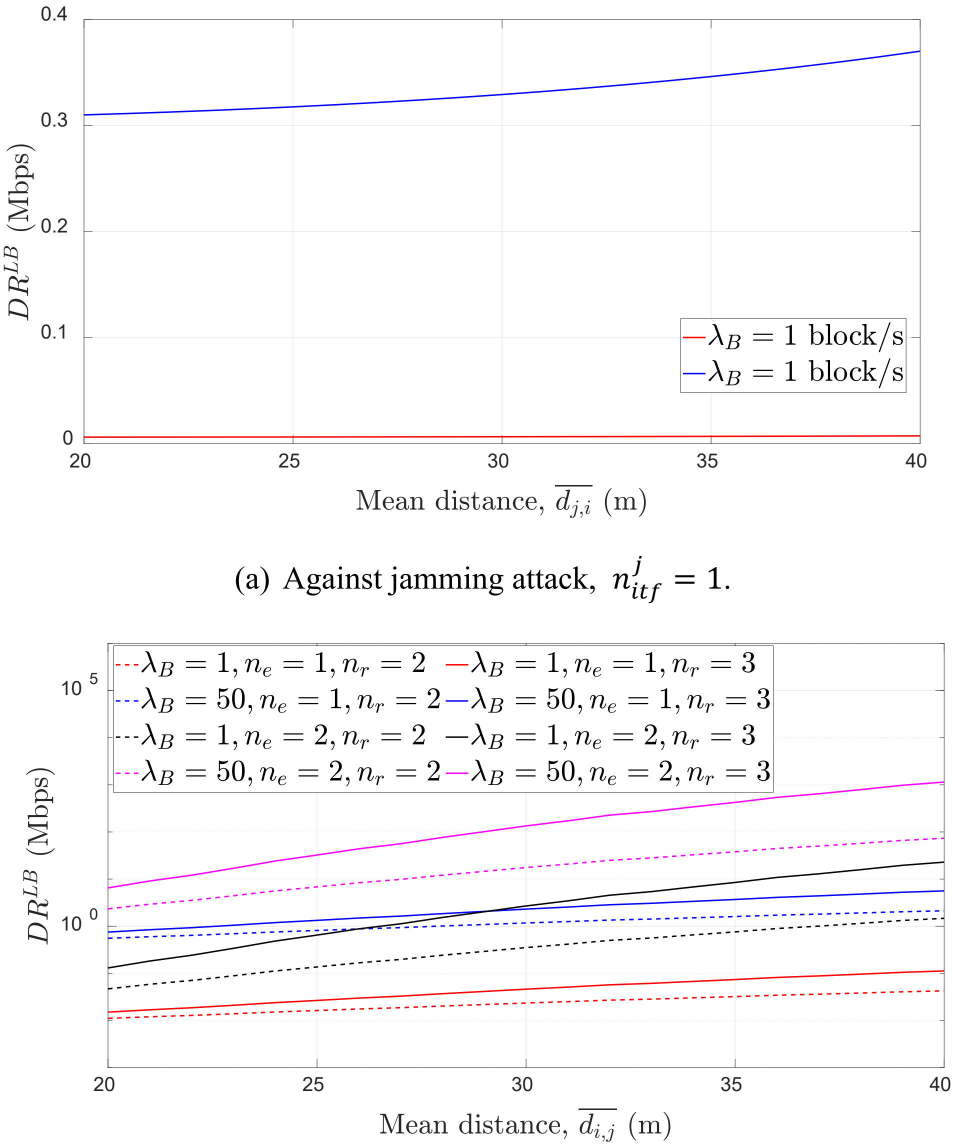

(a) Against jamming attack, $n_{itf}^{j} = 1$.

(b) Against eavesdropping attack, $n_{itf}^{j} = 1, n_{itf}^{k} = 2$.

Figure 5.5: Minimum allowable DR.

Figure 5.5 shows the lower bound of DR, i.e., minimum allowable DR sufficient to support both PLS and blockchain as a combined solution against jamming and eavesdropping according to the relation derived in (5.15) and (5.23) respectively. As shown in Figure 5.5 (a), $DR^{LB} < 0.5$ Mbps for both $\lambda_B = 1$ block /s and $\lambda_B = 50$ block /s, which shows that the proposed approach does not require a very high data rate to provide security against jamming attack. However, in (b), DR^{LB} is rising with increase in n_r, n_e, λ_B or $\overline{d_{\imath,\jmath}}$. Specifically, for certain values of $\overline{d_{\imath,\jmath}}$, when $n_r = 3$, it can be seen that $DR^{LB} > 100$ Mbps. Since IEEE 802.11p supports DR ranging from 3 to 54 Mbps [167], it may not be feasible to implement a secure blockchain-enabled PLS solution when high blockchain throughput is required or large number of receivers are present. An integration of blockchain and PLS can be more effective with 5G or beyond 5G technologies which offer peak data rates in Gbps [168].

5.3.5 Goodput

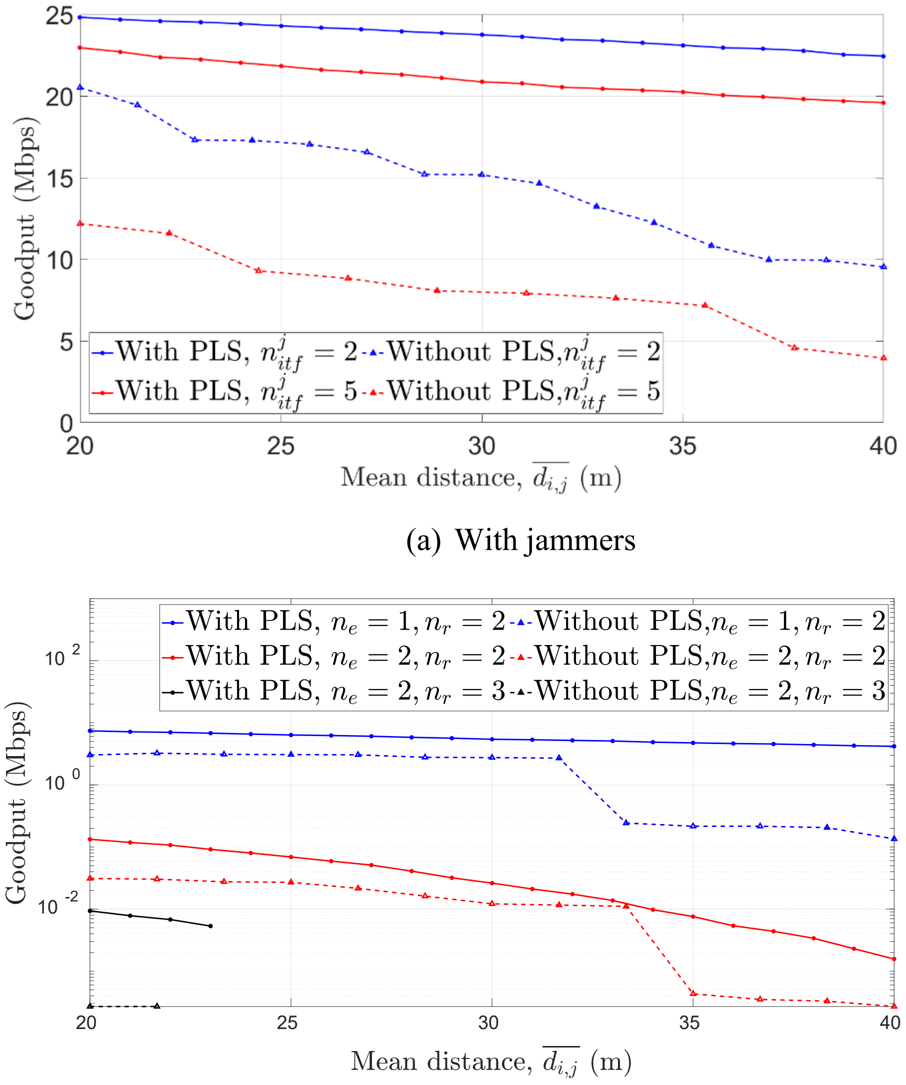

(a) With jammers

(b) With eavesdroppers, $n_{itf}^{j} = 1, n_{itf}^{k} = 2$.

Figure 5.6: Goodput in presence of jammers and eavesdroppers.

Figure 5.6 shows comparison of goodput in a blockchain-based V2X system, with and without PLS, simulated in OMNeT++ at $DR = 27$ Mbps using IEEE 802.11p protocol. Figure 5.6 (a) depicts significant improvement in goodput by using PLS in presence of jammers. Goodput in presence of eavesdroppers is also improved, as shown in Figure 5.6 (b). On an average, there is an increase of 8.2 Mbps in goodput with PLS as compared to the same solution without PLS. However, the goodput falls with increase in $\overline{d_{\iota,J}}$, n_e or n_r in all cases. With $n_e = 2$ and $n_r = 3$, no block is successfully and secretly added into the blockchain after a certain $\overline{d_{\iota,J}}$. It shows that there is no sufficient DR available to support the integrated approach of blockchain and PLS. Nevertheless, strong cryptographic measures in blockchain can still protect confidentiality of eavesdropped blocks.

5.4 Summary

This chapter has analysed FD-NOMA based vehicular network which employs both PLS and blockchain to meet security and privacy requirements in presence of jammers and eavesdroppers. It can be concluded that integration of PLS and blockchain can provide better goodput against both jamming and eavesdropping attacks. However, it requires high DR to support large number of legitimate receivers for protecting privacy in presence of eavesdroppers. DSRC based IEEE 802.11p communications may not provide sufficient DR for feasible integration of PLS and blockchain. Therefore, 5G technologies are recommended for such applications. We plan to further evaluate and collect simulation results to thoroughly analyse the approach in practical scenarios.

Chapter 6 – Conclusions and Future Work

This final chapter concludes the thesis. It is divided into two main sections. Section 6.1 summarises the contributions of the research work. Section 6.2 highlights future research directions.

6.1 Contributions and Conclusions

The main focus of this thesis is to devise solutions for message dissemination in VANETs which can be secured by blockchain. The performance of the solutions is measured in terms of time delay in message validation and dissemination per hop, blockchain throughput, success rate in message delivery and tolerance (i.e., failure in message validation and loss in federated learning) with varying percentage of malicious nodes. In the following subsections, we briefly highlight the important contributions in security, privacy and trust domains of VANETs.

6.1.1 Security

The main contribution of Chapter 3 is to propose solution to support message credibility and availability by a voting-based consensus algorithm, PoQF. It serves the dual purpose of message validation and a competitive relay selection process based on probabilistic prediction of distance and channel quality between transmitter and receiver. It is proposed as a suitable solution to VANETs as it results in 11% and 15% higher security than PoS and PoET, respectively and is 68ms faster than PoET. and . More specifically, the proposed solution includes

- Voting based message validation mechanism
- Quality factor based multi-hop relay selection
- Scalable blockchain and consensus algorithm

Another relay selection algorithm, PoFL is presented in Chapter 4 which is based on blockchain-enabled FL. It results in 65.2% less time delay in message dissemination per hop and 8.2% higher message delivery ratio than PoQF. It uses machine learning enabled smart contract to provide security in presence of both malicious and selfish nodes. The complete solution includes

- Smart contract based security against poisoning attack
- FL based multi-hop relay selection
- Blockchain approach for complementing FL

6.1.2 Privacy

One of the motivations in using FL for message dissemination is to ensure privacy. As concluded in Table 4.4, the proposed PoFL provides better privacy compared to the other relay selection approaches. To further propose solutions for privacy enhancement, PLS integrated with blockchain is studied in Chapter 5. It analyses a blockchain-enabled FD-NOMA based V2X system and evaluates its performance in presence of jamming and eavesdropping attack. The main contributions include

- Evaluating the lower bound of required data rate for FD-NOMA based vehicular network to support both PLS and blockchain in presence of jammers and eavesdroppers
- 8.2 Mbps increase in blockchain's goodput with PLS as compared to without PLS

6.1.3 Trust

For establishing trust in the proposed solutions, incentive mechanisms are designed which motivate nodes to take honest actions as their best response strategy. In both Chapter 3 and Chapter 4, the incentive mechanisms distribute rewards to contributing nodes on the basis of virtual credit CC paid by ORG. CC is proposed to be inversely proportional to Rep_{ORG} to form an integrated strategy of both price-based and reputation-based incentive scheme. The motivation behind CC being paid by ORG is to create a sustainable economic model for promoting safe driving conditions and healthy traffic flow. Ideally, the virtual credit earned and lost in a year will reflect a node's behaviour. A node which is involved in less number of incidents would have spent less credit in originating a message, leaving higher balance remaining in its credit wallet, which can be redeemed into annual road tax. The nodes will therefore be motivated to drive safely to avoid incidents and to earn credit by positive cooperation. For supporting secure annual road tax calculation, the distribution of incentives is proposed to be recorded as immutable blocks in blockchain.

6.2 Future Work

The following subsections discuss potential future research areas which can extend the work presented in this thesis.

6.2.1 Energy Aware, UAV Assisted Blockchain and AI for IoV

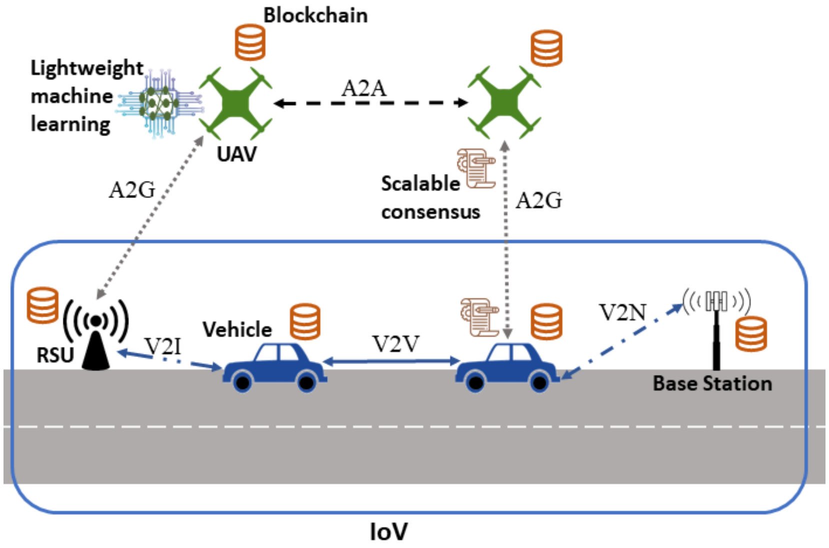

Figure 6.1: Integrated solution of connected UAVs and IoV.

This thesis focuses on message dissemination on road, such as traffic jam or incident. However, timely message dissemination is of crucial importance in case of disasters also. Vehicular infrastructures are often prone to destruction in case of disasters and alternate solutions are therefore required [169]. Recently, UAVs featured with small size, low weight, flexible mobility with aerial capabilities are recommended for mission critical applications such as rescue service in post-disaster situation. UAVs can also assist vehicular networks through Air-to-Air (A2A) and Air-to-Ground (A2G) communications when infrastructure is unavailable or connectivity is poor [169]. Therefore, integration of UAVs and IoV, as shown in Figure 6.1, is a promising solution for enhanced connectivity. Since connected UAVs also form MANETs, their security, trust and privacy challenges are similar to VANETs. Blockchain can be a potential approach to resolve these challenges and ensure decentralisation. Furthermore, AI techniques are integral part for an intelligent and autonomous solution [170]. However, UAVs are low powered devices with limited storage. Both AI and blockchain solutions must be lightweight and compatible with energy and memory requirements of UAVs.

In future work, we plan to propose scalable solutions such as Tiny Machine Learning [171] for UAVs to reduce computational load and memory demands of existing on-device machine learning algorithms. UAVs can be utilised for on-device machine learning and to overcome the existing limitation of FL, i.e., variation in global model's performance in heterogenous networks. Also, we plan to continue our work on devising blockchain consensus with same security as PoW but less computation. A promising alternative to PoW is Riemann Zeta function [172]. We will analyse its suitability for both UAVs and IoV.

6.2.2 Quantum Resistant Cryptography

Blockchain adopts cryptography for producing hash functions and digital signatures to ensure privacy. Analysis of cryptographic schemes used with blockchain is out of the scope of this thesis. However, as a future work, the suitability of a cryptographic scheme with respect to the processing power of nodes and latency requirements of VANET can be studied. The progress in quantum computing has led to the possibility of attacks on cryptographic algorithms used with blockchain [173]. Also, as concluded in Chapter 5, co-existence of PLS and blockchain is not feasible to protect eavesdropping attack with low data rate or large number of eavesdroppers. Therefore, robust cryptographic schemes are required to preserve privacy. We plan to explore robust but computationally simple quantum-resistant cryptographic schemes, such as lattice-based schemes [174] and chameleon hashes [175], which can be used with blockchain and VANETs.

6.2.3 Network Layer Aspects of Blockchain

This thesis proposes implementation of blockchain on application layer. Additionally, some MAC layer and physical layer aspects are employed to analyse blockchain throughput in Chapter 3 and Chapter 5 respectively. However, blockchain is one of the potential solutions to enhance network layer security as well, which are not explored in this thesis. The network layer features of blockchain, such as Denial-of-Service resistance is analysed in [176]. In [177], network layer is used in heterogenous IoT environment to select a consensus algorithm on the basis of network topology, number of nodes and communication throughput. Furthermore, an efficient technique to enhance network layer trust, i.e., Named Data Networking can be supported by blockchain for better security [178]. A prospect future work lies in investigating blockchain-based solutions to enhance network layer security in IoV.

6.2.4 Alternatives to Linear Distributed Ledger

The high probability of fork occurrence in blockchain of vehicular networks is discussed in Chapter 2. In Chapter 3 and Chapter 4, the hierarchical structure of blockchain consisting of horizontal keyblocks and parallel microblocks is proposed as a solution. However, synchronisation issues may still arise due to dynamicity in vehicular networks. Future research can explore other alternatives to linear ledger. One of the potential techniques is Directed Acylic Graph (DAG) [75], in which a new block is not necessarily linked with its latest predecessor but could be connected to any of the previous blocks. Tangle and Hashgraph are two DAG based approaches under research as a substitute to traditional distributed ledger [179]. A suitable solution for multi-hop message dissemination among vehicle nodes can be made using Monoxide blockchain [180], which consists of zones of blocks instead of one single blockchain and relays transaction from one zone to another, similar to relaying a message from one hop to another.

Bibliography

[1] O. Kaiwartya, A. H. Abdullah, Y. Cao, A. Altameem, M. Prasad, C.-T. Lin and X. Liu, “Internet of Vehicles: Motivation, Layered Architecture, Network Model, Challenges, and Future Aspects,” *IEEE Access,* vol. 4, pp. 5356-5373, September 2016.

[2] A. Aldegheishem, H. Yasmeen, H. Maryam, M. Shah, A. Mehmood, N. Alrajeh and H. Song, “Smart road traffic accidents reduction strategy based on intelligent transportation systems (tars),” *Sensors,* vol. 18, no. 7, pp. 1983-2006, July 2018.

[3] R. Chen, W.-L. Jin and A. Regan, “Broadcasting safety information in vehicular networks: issues and approaches,” *IEEE Network,* vol. 24, no. 1, pp. 20-25, February 2010.

[4] M. B. Mollah, J. Zhao, D. Niyato, Y. L. Guan, C. Yuen, S. Sun, K. Y. Lam and L. H. Koh, “Blockchain for the Internet of Vehicles Towards Intelligent Transportation Systems: A Survey,” *IEEE Internet of Things Journal,* vol. 8, no. 6, pp. 4157-4185, March 2021.

[5] S. Nakamoto, “Bitcoin: A Peer-to-Peer Electronic Cash System,” 2008. [Online]. Available: https://bitcoin.org/bitcoin.pdf. [Accessed 23 May 2021].

[6] S. Bano, A. Sonnino, M. Al-Bassam, S. Azouvi, P. McCorry, S. Meiklejohn and G. Danezis, “SoK: Consensus in the Age of Blockchains,” in *Proc. of 1st ACM Conference on Advances in Financial Technologies*, Zurich, Switzerland, October 2019.

[7] J. Kang, Z. Xiong, D. Niyato, D. Ye, D. I. Kim and Z. Jun, “Toward Secure Blockchain-Enabled Internet of Vehicles: Optimizing Consensus Management Using Reputation and Contract Theory,” *IEEE Transactions on Vehicular Technology,* vol. 68, no. 3, pp. 2906-2920, January 2019.

[8] M. Zaki, “Cellular V2X is gaining momentum,” September 2016. [Online]. Available: https://www.qualcomm.com/news/onq/2016/09/27/cellular-v2x-gaining-momentum. [Accessed 27 September 2021].

[9] A. R. Khan, M. F. Jamlos, N. Osman, M. I. Ishak, F. Dzaharudin and Y. K. Yeow, “DSRC Technology in Vehicle-to-Vehicle (V2V) and Vehicle-to-Infrastructure (V2I) IoT System for Intelligent Transportation System (ITS): A Review,” in *Recent Trends in Mechatronics Towards Industry 4.0.*

Lecture Notes in Electrical Engineering, vol. 730, A. F. A. Nasir, A. N. Ibrahim, I. Ishak, N. M. Yahya, M. A. Zakaria and A. P. P. A. Majeed, Eds., Singapore, Springer, July 2021, pp. 97-106.

[10] Z. Lu, G. Qu and Z. Liu, "A Survey on Recent Advances in Vehicular Network Security, Trust, and Privacy," *IEEE Transactions on Intelligent Transportation Systems,* vol. 20, no. 2, pp. 760-776, February 2019.

[11] *IEEE Standard for Information Technology—Telecommunications and information exchange between systems—Local and metropolitan area networks—Specific requirements—Part 11: Wireless LAN Medium Access Control (MAC) and Physical Layer (PHY) specifications,* IEEE Standard 802.11, 2010.

[12] Y. L. Morgan, "Notes on DSRC & WAVE Standards Suite: Its Architecture, Design, and Characteristics," *IEEE Communications Surveys and Tutorial,* vol. 12, no. 4, pp. 504 - 518, May 2010.

[13] H. Hasrouny, A. E. Samhat, C. Bassil and A. Laouiti, "VANet security challenges and solutions: A survey," *Vehicular Communications,* vol. 7, pp. 7-20, January 2017.

[14] S. Nobahary, H. G. Garakani, A. Khademzadeh and A. M. Rahmani, "Selfish node detection based on hierarchical game theory in IoT," *EURASIP Journal on Wireless Communications and Networking,* vol. 1, pp. 1-19, December 2019.

[15] A. Baiocchi and I. Turcanu, "A Model for the Optimization of Beacon Message Age-of-Information in a VANET," in *Proc. of the 29th International Teletraffic Congress*, Genoa, Italy, September 2017.

[16] V. Ortega, F. Bouchmal and J. F. Monserrat, "Trusted 5G vehicular networks: Blockchains and content-centric networking," *IEEE Vehicular Technology Magazine,* vol. 13, no. 12, pp. 121-127, April 2018.

[17] T. Gazdar, A. Belghith and H. Abutair, "An enhanced distributed trust computing protocol for VANETs," *IEEE Access,* vol. 6, pp. 380-392, October 2017.

[18] J. Cui, X. Zhang, H. Zhong, Z. Ying and L. Liu, "RSMA: Reputation System-Based Lightweight Message Authentication Framework and Protocol for 5G-Enabled Vehicular Networks," *IEEE Internet of Things Journal,* vol. 6, no. 4, pp. 6417-6428, August 2019.

[19] R. Sugumar, . A. Rengarajan and C. Jayakumar , “Trust based authentication technique for cluster based vehicular ad hoc networks (VANET),” *Wireless Networks,* vol. 24, p. 373–382, February 2018.

[20] X. Wang, Z. Ning, M. Zhou, X. Hu, L. Wang, Y. Zhang, F. R. Yu and B. Hu, “Privacy-Preserving Content Dissemination for Vehicular Social Networks: Challenges and Solutions,” *IEEE Communications Surveys and Tutorials,* vol. 21, no. 2, pp. 1314-1345, May 2019.

[21] A. Tajeddine, A. Kayssi and A. Chehab, “A Privacy-Preserving Trust Model for VANETs,” in *Proc. of 10th IEEE International Conference on Computer and Information Technology*, Bradford, UK, June - July 2010.

[22] A. Yáñez, S. Céspedes and J. Rubio-Loyola, “CaSSaM: Context-aware system for safety messages dissemination in VANETs,” in *Proc. of Colombian Conference on Communications and Computing*, Medellin, Colombia, May 2018.

[23] G. Martuscelli, A. Boukerche, L. Foschini and P. Bellavista, “V2V protocols for traffic congestion discovery along routes of interest in VANETs: a quantitative study,” *Wireless Communications and Mobile Computing,* vol. 16, no. 17, pp. 2907-2923, December 2016.

[24] P. Cataldi and J. Harri, “User/operator utility-based infrastructure deployment strategies for vehicular networks,” in *Proc. of Vehicular Technology Conference*, San Francisco, CA, USA, September 2011.

[25] A. Yasser, M. Elzorkany and N. A. Kader, “Vehicle to Vehicle Implementation in Developing Countries,” in *Proc. of International Conference on Advanced Intelligent Systems and Informatics*, Cairo, Egypt, August 2017.

[26] D. Cao, B. Zheng, B. JI, Z. Lei and C. Feng, “A robust distance-based relay selection for message dissemination in vehicular network,” *Wireless Networks,* vol. 26, pp. 1755-1771, October 2018.

[27] N. Li, J.-F. Martínez-Ortega, V. H. Díaz and J. A. S. Fernandez, “Probability Prediction-Based Reliable and Efficient Opportunistic Routing Algorithm for VANETs,” *IEEE/ACM Transactions on Networking,* vol. 26, no. 4, pp. 1933-1947, July 2018.

[28] M. A. Gawas, P. Hurkat, V. Goyal and L. J. Gudino, “Cross layer approach for efficient dissemination of emergency messages in VANETs,” in *Proc. of Ninth International Conference on Ubiquitous and Future Networks (ICUFN)*, Milan, Italy, July 2017.

[29] C. I. Paredes, M. A. Mezher, M. A. Igartua and J. Forné, “Game-Theoretical Design of an Adaptive Distributed Dissemination Protocol for VANETs,” *Sensors,* vol. 18, no. 1, p. 294, January 2018.

[30] A. Hawbani, E. Torbosh, X. Wang, P. Sincak, L. Zhao and A. Al-Dubai, “Fuzzy based distributed protocol for vehicle to vehicle communication,” *IEEE Transactions on Fuzzy Systems,* vol. 29, no. 3, pp. 612-626, Marchi 2021.

[31] C. Wu, S. Ohzahata, Y. Ji and T. Kato, “Joint fuzzy relays and networkcoding-Based Forwarding for Multihop Broadcasting in VANETs,” *IEEE Transactions on Intelligent Transportation Systems,* vol. 16, no. 3, pp. 1415 - 1427, November 2014.

[32] M. E. Morocho-Cayamcela, H. Lee and W. Lim, “Machine Learning to Improve Multi-Hop Searching and Extended Wireless Reachability in V2X,” *IEEE Communications Letter,* vol. 24, no. 7, pp. 1477 - 1481, July 2020.

[33] A. Mchergui, T. Moulahi and S. Nasri, “Relay Selection Based on Deep Learning for Broadcasting in VANET,” in *Proc. of 15th International Wireless Communications & Mobile Computing Conference (IWCMC)*, Tangier, Morocco, June 2019.

[34] X. Zhang, A. Kunz and S. Schröder, “Overview of 5G security in 3GPP,” Helsinki, Finland, September 2017.

[35] A. R. Prasad, S. Arumugam, S. B and A. Zugenmaier, “3GPP 5G Security,” *Journal of ICT Standardization,* vol. 6, no. 1, 2, pp. 137 - 158, May 2018.

[36] R. Al-ani, B. Zhou, Q. Shi and A. Sagheer, “A Survey on Secure Safety Applications in VANET,” in *Proc. of 0th International Conference on High Performance Computing and Communications, 16th International Conference on Smart City, 4th International Conference on Data Science and Systems (HPCC/SmartCity/DSS)*, Exeter, UK, June, 2018.

[37] L. Li, J. Liu, L. Cheng, W. Wang and S. Qiu, “Creditcoin: A privacy-preserving blockchain-based incentive announcement network for communications of smart vehicles,” *IEEE Transactions on Intelligent Transportation Systems,* vol. 19, no. 7, pp. 2204-2220, January 2018.

[38] A. U. Makarfi, K. M. Rabie, O. Kaiwartya, K. Adhikari and G. Nauryzbayev, “Toward Physical-Layer Security for Internet of Vehicles: Interference-Aware Modeling,” *IEEE Internet of Things Journal,* vol. 8, no. 1, pp. 443-457, January 2021.

[39] C. Bajracharya, "Performance Evaluation for Secure Communications in Mobile Internet of Vehicles With Joint Reactive Jamming and Eavesdropping Attacks," *IEEE Transactions on Intelligent Transportation Systems,* vol. Early Access, July 2021.

[40] H. Janzadeh, K. Fayazbakhsh, M. Dehghan and M. S. Fallah, "A secure credit-based cooperation stimulating mechanism for MANETs using hash chains," *Future Generation Computer Systems,* vol. 25, no. 8, pp. 926-934, September 2008.

[41] J. Crowcroft, R. Gibbens, F. Kelly and S. Östring, "Modelling incentives for collaboration in mobile ad hoc networks," *Performance Evaluation,* vol. 57, no. 4, pp. 427-439, August 2004.

[42] M. T. Refaei, L. A. DaSilva, M. Eltoweissy and T. Nadeem, "Adaptation of reputation management systems to dynamic network conditions in ad hoc networks," *IEEE Transactions on Computers,* vol. 59, no. 5, pp. 707-719, February 2010.

[43] P. Dewan, P. Dasgupta and A. Bhattacharya, "On using reputations in ad hoc networks to counter malicious nodes," in *Proc. of 10th International Conference on Parallel and Distributed Systems*, Newport Beach, CA, USA, July 2004.

[44] V. Srivastava, J. Neel, A. B. MacKenzie, R. Menon, L. A. DaSilva, J. E. Hicks, J. H. Reed and R. P. Gilles, "Using game theory to analyze wireless ad hoc networks," *IEEE Communications Surveys & Tutorials,* vol. 7, no. 4, pp. 46-56, October 2005.

[45] Z. Li and H. Shen, "Game-theoretic analysis of cooperation incentive strategies in mobile ad hoc networks," *IEEE Transactions on Mobile Computing,* vol. 11, no. 8, pp. 1287-1303, July 2011.

[46] L. Kulkarni, J. Bakal and U. Shrawankar, "Energy based incentive scheme for secure opportunistic routing in vehicular delay tolerant networks," *Computing ,* vol. 102, no. 1, pp. 201-219, June 2019.

[47] N. Haddadou, A. Rachedi and Y. Ghamri-Doudane, "Trust and exclusion in Vehicular Ad Hoc Networks: An economic incentive model based approach," in *Proc. of the Computing, Communications and IT Applications Conference (ComComAp)*, Hong Kong, China, April, 2013.

[48] A. Jesudoss, K. S. Raja and A. Sulaiman, "Stimulating truth-telling and cooperation among nodes n VANETs through payment and punishment scheme," *Ad Hoc Networks,* vol. 24, no. A, pp. 250-263, January 2015.

[49] A. Kazmi, M. A. Khan and M. U. Akram, "DeVANET: decentralized software-defined VANET architecture," in *Proc. of International Conference on Cloud Engineering Workshop*, Berlin, Germany, April 2016.

[50] C. Zhang, K. Chen, X. Zeng and X. Xue, "Misbehavior Detection Based on Support Vector and Dempster-Shafer Theory of," vol. 6, pp. 59860-59870, October 2018.

[51] A. S. Rahman, H. Tout, C. Talhi and A. Mourad, "Internet of Things Intrusion Detection: Centralized, On-Device, or Federated Learning?," *IEEE Network,* vol. 34, no. 6, pp. 310-317, November/December 2020.

[52] S. Dhar, J. Guo, J. (. Liu, S. Tripathi, U. Kurup and M. Shah, "A Survey of On-Device Machine Learning: An Algorithms and Learning Theory Perspective," *ACM Transactions on Internet of Things,* vol. 2, no. 3, pp. 1-49, July 2021.

[53] A. A. Diro and N. Chilamkurti, "Distributed attack detection scheme using deep learning approach for Internet of Things," *Future Generation Computer Systems,* vol. 82, pp. 761-768, May 2018.

[54] W. Y. B. Lim, N. C. Luong, D. T. Hoang, Y. Jiao and Y. C. Liang, "Federated Learning in Mobile Edge Networks: A Comprehensive Survey," *IEEE Communications Surveys & Tutorials,* vol. 22, no. 3, pp. 2031-2063, April 2020.

[55] Y. Lu, X. HUang, K. Zhang, S. Maharjan and Y. Zhang, "Communication-Efficient Federated Learning and Permissioned Blockchain for Digital Twin Edge Networks," *IEEE Internet of Things Journal,* vol. 8, no. 4, pp. 2276-2288, August 2020.

[56] Z. Zheng, S. Xie, H. Dai, X. Chen and H. Wang, "An Overview of Blockchain Technology: Architecture, Consensus, and Future Trends," in *Proc. of IEEE International Congress on Big Data (BigData Congress)*, Honolulu, HI USA, June 2017.

[57] W. Gao, W. G. Hatcher and W. Yu, "A Survey of Blockchain: Techniques, Applications, and Challenges," in *Proc. of 27th International Conference on Computer Communication and Networks (ICCCN)*, Hangzhou, China, July/ August 2018.

[58] B. Biais, C. Bisière, M. Bouvard and C. Casamatta, "The Blockchain Folk Theorem," *The Review of FInancial Studies,* vol. 32, no. 5, pp. 1662 - 1715, May 2019.

[59] C. Decker and R. Wattenhofer, “Information propagation in the Bitcoin network,” in *Proc. of IEEE P2P*, Trento, Italy, September 2013.

[60] P. K. Sharma, S. Y. Moon and J. H. Park, “Block-VN: A Distributed Blockchain Based Vehicular Network Architecture in Smart City,” *Journal of Information Processing Systems,* vol. 13, no. 1, pp. 184-195, February 2017.

[61] B. Leiding, P. Memarmoshrefi and D. Hogrefe, “Self-managed and blockchain-based vehicular ad-hoc networks,” in *Proc. of ACM International Joint Conference on Pervasive and Ubiquitous Computing: Adjunct*, Heidelberg, Germany, September 2016.

[62] L. Campanile, M. Iacono, F. Marulli and M. Mastroianni, “Designing a GDPR compliant blockchain-based IoV distributed information tracking system,” *Information Processing and Management,* vol. 58, no. 3, p. 102511, May 2021.

[63] R. Garrard and S. Fielke, “Blockchain for trustworthy provenances: A case study in the Australian aquaculture industry,” *Technology in Society,* vol. 62, p. 101298, August 2020.

[64] L. Liu and M. Loper, “Trust as a Service: Building and Managing Trust in the Internet of Things,” in *Proc. of IEEE International Symposium on Technologies for Homeland Security (HST)*, Woburn, MA, USA, October 2018.

[65] M. D. Pierro, “What Is the Blockchain?,” *Computing in Science and Engineering,* vol. 19, no. 5, pp. 92-95, September 2017.

[66] G. Zyskind, O. Nathan and A. '. Pentland, “Decentralizing Privacy: Using Blockchain to Protect Personal Data,” in *Proc. of IEEE Security and Privacy Workshop*, San Jose, CA, USA, May 2015.

[67] G. G. Dagher, J. Mohler, M. Milojkovic and P. B. Marella, “Ancile: Privacy-preserving framework for access control and interoperability of electronic health records using blockchain technology,” *Sustainable Cities and Society,* vol. 39, pp. 283-297, May 2018.

[68] K. Christidis and M. Devetsikiotis, “Blockchains and Smart Contracts for the Internet of Things,” *IEEE Access,* vol. 4, pp. 2292-2303, May 2016.

[69] A. Iqbal, A. S. Rajasekaran, G. S. Nikhil and M. Azees, “A Secure and Decentralized Blockchain Based EV Energy Trading Model Using Smart

Contract in V2G Network," *IEEE Access,* vol. 9, pp. 75761-75777, May 2021.

[70] Z. Su, Y. Wang, Q. Xu, M. Fei, Y.-C. Tian and N. Zhang, "A Secure Charging Scheme for Electric Vehicles With Smart Communities in Energy Blockchain," *IEEE Internet of Things Journal,* vol. 6, no. 3, pp. 4601-4613, September 2018.

[71] K. Zhang, Y. Mao, S. Leng, Y. He, S. Maharjan, S. Gjessing, Y. Zhang and D. H. K. Tsang, "Optimal Charging Schemes for Electric Vehicles in Smart Grid: A Contract Theoretic Approach," *IEEE Transactions on Intelligent Transportation Systems,* vol. 19, no. 9, pp. 3046-3058, August 2018.

[72] D. Ghosh, "How the Byzantine General Sacked the Castle: A Look Into Blockchain," 5 April 2016. [Online]. Available: https://medium.com/@DebrajG/how-the-byzantine-general-sacked-the-castle-a-look-into-blockchain-370fe637502c. [Accessed 23 May 2021].

[73] F. Tschorsch and B. Scheuermann, "Bitcoin and Beyond: A Technical Survey on Decentralized Digital Currencies," *IEEE Communications Survey,* vol. 18, no. 3, March 2016.

[74] S. Poledna, Fault-Tolerant Real-Time Systems: The Problem of Replica Determinism, vol. 345, The Springer International Series in Engineering and Computer Science, November 2007.

[75] V. Bagaria, S. Kannan, D. Tse, G. Fanti and P. Viswanath, "Prism: Deconstructing the Blockchain to Approach Physical Limits," in *Proc. of ACM SIGSAC Conference on Computer and Communications Security*, London, UK, November 2019.

[76] S. Zoican, M. Vochin, R. Zoichan and D. Galatchi, "Blockchain and Consensus Algorithms in Internet of Things," in *Proc. of International Symposium on Electronics and Telecommunications (ISETC)*, Timisoara, Romania, November 2018.

[77] A. Baliga, "Understanding Blockchain Consensus Models," Persistent Systems Ltd., April 2017.

[78] L. Chen, L. Xu, N. Shah, Z. Gao, Y. Lu and W. Shi, "On Security Analysis of Proof-of-Elapsed-Time (PoET)," in *Stabilization, Safety, and Security of Distributed Systems (Lecture Notes in Computer Science)*, vol. 10616, Cham, Switzerland: Springer, October 2017, pp. 282-297.

[79] Y. Wang, S. Cai, C. Lin, Z. Chen, Z. Gao and C. Zhou, "Study of Blockchains's Consensus Mechanism Based on Credit," *IEEE Access,* vol. 7, pp. 10224 - 10231, January 2019.

[80] L. S. Sankar, M. Sindhu and M. Sethumadhavan, "Survey of consensus protocols on blockchain applications," Coimbatore, India, January 2017.

[81] A. Miller, "Permissioned and permissionless blockchains," in *Blockchain for Distributed Systems Security*, S. Shetty, C. A. Kamhoua and L. L. Njilla, Eds., IEEE Computer Society, IEEE Press, WIley, March 2019, pp. 193-204.

[82] W. Wang, D. T. Hoang, P. Hu, Z. Xiong, D. Niyato, P. Wang, Y. Wen and D. I. Kim, "A survey on consensus mechanisms and mining strategy management in blockchain networks," *IEEE Access,* pp. 22328-22370, January 2019.

[83] S. Bano, M. Al-Bassam and G. Danezis, "The Road to Scalable Blockchain Designs," *USENIX Login Magazine,* vol. 42, no. 4, pp. 31-36, December 2017.

[84] D. Mingxiao, M. Xiaofeng, Z. Zhe, W. Xiangwei and C. Qijun, "A review on consensus algorithm of blockchain," in *Proc. of IEEE International Conference on Systems, Man, and Cybernetics (SMC)*, Banff, AB, Canada, October 2017.

[85] W. Dong, Y. Li, R. Hou, X. Lv, H. Li and B. Sun, "A Blockchain-Based Hierarchical Reputation Management Scheme in Vehicular Network," in *Proc. of IEEE Global Communications Conference (GLOBECOM)*, Waikoloa, HI, USA, December 2019.

[86] Z. Yang, K. Zheng, K. Yang and V. C. M. Leung, "A blockchain-based reputation system for data credibility assessment in vehicular networks," in *Proc. of 28th annual international symposium on personal, indoor, and mobile radio communications*, Montreal, QC, Canada, October 2017.

[87] S. Zou, J. Xi, S. Wang, Y. Lu and G. Xu, "Reportcoin: A Novel Blockchain-Based Incentive Anonymous Reporting System," *IEEE Access,* vol. 7, pp. 65544-65559, May 2019.

[88] Z. Lu, Q. Wang, G. Qu and Z. Liu, "Bars: a blockchain-based anonymous reputation system for trust management in vanets," in *Proc. of 17th International Conference On Trust, Security And Privacy In Computing And Communications/12th International Conference On Big Data Science And Engineering*, New York, NY, USA, August 2018.

[89] A. Dorri, M. Steger, S. S. Kanhere and R. Jurdak, "BlockChain: A Distributed Solution to Automotive Security and Privacy," *IEEE Communications Magazine,* vol. 55, no. 12, pp. 119-125, December 2017.

[90] D. Yang, S. Yoo, I. Doh and K. Chae, "Selective blockchain system for secure and efficient D2D communication," *Journal of Network and Computer Applications,* vol. 173, p. 102817, January 2021.

[91] R. Dennis and G. Owen, "Rep on the block: A next generation reputation system based on the blockchain," in *Proc. of 10th International Conference for Internet Technology and Secured Transactions (ICITST)*, London, UK, December 2015.

[92] Z. Yang, K. Yang, L. Lei, K. Zheng and V. C. Leung, "Blockchain-based decentralized trust management in vehicular networks," *IEEE Internet of Things Journal,* vol. 6, no. 2, pp. 1495-1505, May 2018.

[93] Y. Ren, Y. Liu, S. Ji, A. K. Sangaiah and J. Wang, "Incentive Mechanism of Data Storage Based on Blockchain for Wireless Sensor Networks," *Mobile Information Systems,* August 2018.

[94] X. Zhang and X. Chen, "Data Security Sharing and Storage Based on a Consortium Blockchain in a Vehicular Ad-hoc Network," *IEEE Access,* vol. 7, pp. 58241-58254, January 2019.

[95] X. Zhang and D. Wang, "Adaptive Traffic Signal Control Mechanism for Intelligent Transportation Based on a Consortium Blockchain," *IEEE Access,* vol. 7, pp. 97281-97295, July 2019.

[96] Y.-T. Yang, L.-D. Chou, C.-W. Tseng, F.-H. Tseng and C.-C. Liu, "Blockchain-Based Traffic Event Validation and Trust Verification for VANETs," *IEEE Access,* vol. 7, pp. 30868 - 30877, March 2019.

[97] M. Kadadha and H. Otrok, "A blockchain-enabled relay selection for QoS-OLSR in urban VANET: A Stackelberg game model," *Ad Hoc Networks,* vol. 117, no. 2021, p. 102502, April 2021.

[98] S. S. Manvi and S. Tangade, "A survey on authentication schemes in VANETs for secured communication," *Vehicular Communications,* vol. 9, pp. 19-30, March 2017.

[99] H. Tan and I. Chung, "Secure Authentication and Key Management With Blockchain in VANETs," *IEEE Access,* vol. 8, pp. 2482-2498, December 2019.

[100] N. Lasla, M. Younis, W. Znaidi and D. B. Arbia, “Efficient Distributed Admission and Revocation Using Blockchain for Cooperative ITS,” in *Proc. of 9th IFIP International Conference on New Technologies, Mobility and Security (NTMS)*, Paris, France, February 2018.

[101] A. Lei, H. Cruickshank, Y. Cao, P. Asuquo, C. P. A. Ogah and Z. Sun, “Blockchain-Based Dynamic Key Management for Heterogeneous Intelligent Transportation Systems,” *IEEE Internet of Things Journal,* vol. 4, no. 6, pp. 1832-1843, August 2017.

[102] M. Brandenburger, C. Cachin, R. Kapitza and A. Sorniotti, “Trusted Computing Meets Blockchain: Rollback Attacks and a Solution for Hyperledger Fabric,” in *Proc. of 38th Symposium on Reliable Distributed Systems (SRDS)*, Lyon, France, October 2019.

[103] Y. Qi, M. S. Hossain, J. Nie and X. Li, “Privacy-preserving blockchain-based federated learning for traffic flow prediction,” *Future Generation Computer Systems,* vol. 117, pp. 328-337, April 2021.

[104] R. Dennis and G. Owen, “Rep on the roll: a peer to peer reputation system based on a rolling blockchain,” *International Journal for Digital Society,,* vol. 7, no. 1, pp. 1123-1134, March 2016.

[105] W. Wang, D. Niyato, P. Wang and A. Leshem, “Decentralized Caching for Content Delivery Based on Blockchain: A Game Theoretic Perspective,” in *Proc. of IEEE International Conference on Communications (ICC)*, Kansas City, MO, USA, May 2018.

[106] N. Xu, K. Han, S. Tang, S. Xu, F. Li and J. Zhang, “Privacy-Preserving Auction-based Incentive Mechanism for Mobile Crowdsensing Systems,” in *Proc. of IEEE 22nd International Conference on Computer Supported Cooperative Work in Design (CSCWD)*, Nanjing, China, May 2018.

[107] Y. He, H. Li, X. Cheng, Y. Liu, C. Yang and L. Sun, “A Blockchain Based Truthful Incentive Mechanism for Distributed P2P Applications,” *IEEE Access,* vol. 6, pp. 27324-27335, April 2018.

[108] Q. Zhang, Y. Leng and L. Fan, “Blockchain-based P2P file sharing incentive,” IACR Cryptology ePrint Archive, Lyon, Frace, Rep. 1152, November 2018.

[109] H. Ichikawa and A. Kobayashi, “Messaging Protocol for Relaying Messages between Participants with Autonomous Distributed Blockchain Propagation,” Aomori, Japan, November 2017.

[110] A. S. Khan, K. Balan, Y. Javed, S. Tarmizi and J. Abdullah, “Secure Trust-Based Blockchain Architecture to Prevent Attacks in VANET,” *Sensors,* vol. 19, no. 22, p. 4954, November 2019.

[111] R. Shrestha, R. Bajracharya, A. P. Shrestha and S. Y. Nam, “A new type of blockchain for secure message exchange in VANET,” *Digital Communications and Networks,* vol. 6, no. 2, pp. 177-186, May 2020.

[112] M. Cebe, E. Erdin, K. Akkaya, H. Aksu and S. Uluagac, “Block4Forensic: An Integrated Lightweight Blockchain Framework for Forensics Applications of Connected Vehicles,” *IEEE Communications Magazine,* vol. 56, no. 10, pp. 50-57, October 2018.

[113] W. Hu, Y. Hu, W. Yao and H. Li, “A blockchain-based Byzantine consensus algorithm for information authentication of the Internet of vehicles,” *IEEE Access,* vol. 7, pp. 139703-139711, September 2019.

[114] F. Dressler, P. Handle and C. Sommer, “Towards a vehicular cloud-using parked vehicles as a temporary network and storage infrastructure,” in *Proc. of ACM international workshop on Wireless and mobile technologies for smart cities*, Philadelphia, USA, August 2014.

[115] M. Haenggi, “Twelve reasons not to route over many short hops,” in *Proc. of IEEE 60th Vehicular Technology Conference*, Los Angeles, CA, USA, September 2004.

[116] Y. Yokoya, Y. Asano and N. Uchida, “Qualitative change of traffic flow induced by driver response,” in *Proc. of IEEE International Conference on Systems, Man and Cybernetics*, Singapore, October 2008.

[117] S. Kim, “Impacts of mobility on performance of blockchain in VANET,” *IEEE Access,* vol. 7, pp. 68646-68655, May 2019.

[118] R. Stanica, E. Chaput and A.-L. Beylot, “Local density estimation for contention window adaptation in vehicular networks,” in *Proc. of IEEE 22nd International Symposium on Personal, Indoor and Mobile Radio Communications*, Toronto, ON, Canada, September 2011.

[119] C. Yeshwanth, P. A. Sooraj, V. Sudhakaran and V. Raveendran, “Estimation of intersection traffic density on decentralized architectures with deep networks,” in *International Smart Cities Conference (ISC2)*, Wuxi, China, September 2017.

[120] Y. Sun, L. Zhang, F. Gang, B. Yang, B. Cao and M. A. Imran, “Blockchain-Enabled Wireless Internet of Things: Performance Analysis and Optimal

Communication Node Deployment," vol. 6, no. 3, pp. 5791 -5802, March 2019.

[121] M. Mitzenmacher and E. Upfal, Probability and Computing: Randomized Algorithms and Probabilistic Analysis, Cambridge University Press, January 2005.

[122] D. Tian, J. Zhuo, M. Chen, Z. Sheng, Q. Ni and V. C. Leung, "Cooperative Content Transmission for Vehicular Ad Hoc Networks using Robust Optimization," in *Proc. of IEEE Conference on Computer Communications*, Honolulu, HI, USA, April 2018.

[123] A. Durand, E. Ben-Hamida, D. Leporini and G. Memmi, "Asymptotic Performance Analysis of Blockchain Protocols," February 2019. [Online]. Available: https://arxiv.org/abs/1902.04363. [Accessed 16 6 2021].

[124] H. Watanabe, S. Fujimura, A. Nakadaira, Y. Miyazaki, A. Akutsu and J. Kishigami, "Blockchain contract: Securing a blockchain applied to smart contracts," in *Proc. of IEEE International Conference on Consumer Electronics (ICCE)*, Las Vegas, NV, USA, January 2016.

[125] V. Buterin, D. Reijsbergen, S. Leonardos and G. Piliouras, "Incentives in Ethereum's hybrid Casper protocol," *International Journal of Network Management,* vol. 30, no. 5, p. 2098, February 2020.

[126] B. Choi, J.-y. Sohn, D.-J. Han and J. Moon, "Scalable network-coded PBFT consensus algorithm," in *Proc. of IEEE International Symposium on Information Theory (ISIT)*, Paris, France, July 2019.

[127] M. F. Feteiha and M. H. Ahmed, "Multihop Best-Relay Selection for Vehicular Communication Over Highways Traffic," *IEEE Transactions on Vehicular Technology,* vol. 67, no. 10, pp. 9845-9855, October 2018.

[128] W. K. Lai, M.-T. Lin and Y.-H. Yang, "A Machine Learning System for Routing Decision-Making in Urban Vehicular Ad Hoc Networks," *International Journal of Distributed Sensor Networks,* vol. 11, no. 3, p. 374391, March 2015.

[129] W. He, G. Yan and L. D. Xu, "Developing Vehicular Data Cloud Services in the IoT Environment," *IEEE Transactions on Industrial Informatics,* vol. 10, no. 2, pp. 1587-1595, January 2014.

[130] H. B. McMahan, E. Moore, D. Ramage, S. Hampson and B. A. y. Arcas, "Communication-Efficient Learning of Deep Networks from Decentralized

Data," in *Proc. of 20th International Conference on Artificial Intelligence and Statistics*, Fort Lauderdale, FL, USA, April 2017.

[131] T. Li, S. Hu, A. Beirami and V. Smi, "Ditto: Fair and Robust Federated Learning Through Personalization," in *Proc. of 38th International Conference on Machine Learning*, Virtual Event, July 2021.

[132] J. Kang, Z. Xiong, D. Niyato, S. Xie and J. Zhang, "Incentive Mechanism for Reliable Federated Learning: A Joint Optimization Approach to Combining Reputation and Contract Theory," *IEEE Internet of Things Journal,* vol. 6, no. 6, pp. 10700-10714, September 2019.

[133] K. Yang, Y. Shi, Y. Zhou, Z. Yang, L. Fu and W. Chen, "Federated Machine Learning for Intelligent IoT via Reconfigurable Intelligent Surface," *IEEE Network,* vol. 34, no. 5, pp. 16-22, September 2020.

[134] K. Xiong, S. Leng, C. Huang, C. Yuen and Y. L. Guan, "Intelligent Task Offloading for Heterogeneous V2X Communications," *IEEE Transactions on Intelligent Transportation Systems,* vol. 22, no. 4, pp. 2226-2238, August 2020.

[135] S. Samarakoon, M. Bennis, W. Saad and M. Debbah, "Distributed Federated Learning for Ultra-Reliable Low-Latency Vehicular Communications," *IEEE Transactions on Communications,* vol. 68, no. 2, pp. 1146-1159, November 2019.

[136] M. Rihan, M. Elwekeil, Y. Yang, L. Huang, C. Xu and M. M. Selim, "Deep-VFog: When Artificial Intelligence Meets Fog Computing in V2X," *IEEE Systems Journal,* pp. 1-14, August 2020.

[137] Y. M. Saputra, D. T. Hoang, D. N. Nguyen, E. Dutkiewicz, M. D. Mueck and S. Srikanteswara, "Energy Demand Prediction with Federated Learning for Electric Vehicle Networks," in *Proc. of IEEE Global Communications Conference (GLOBECOM)*, Waikoloa, HI, USA, December 2019.

[138] S. R. Pokhrel and J. Choi, "Federated Learning With Blockchain for Autonomous Vehicles: Analysis and Design Challenges," *IEEE Transactions on Communications,* vol. 68, no. 8, pp. 4734-4746, April 2020.

[139] K. Tan, D. Bremner, J. L. Kernec and M. Imran, "Federated Machine Learning in Vehicular Networks: A summary of Recent Applications," in *Proc. of International Conference on UK-China Emerging Technologies (UCET)*, Galsgow, UK, August 2020.

[140] Y. Hu, X. Huang, K. Zhang, S. Maharjan and Y. Zhang, "Blockchain Empowered Asynchronous Federated Learning for Secure Data Sharing in

Internet of Vehicles," *IEEE Transactions on Vehicular Technology,* vol. 68, no. 4, pp. 4298-4311, April 2020.

[141] F. T. Liu, K. M. Ting and Z.-H. Zhou, "Isolation Forest," in *Proc. of 8th IEEE International Conference on Data Mining*, Pisa, Italy, December 2008.

[142] G. A. Susto, A. Beghi and S. McLoone, "Anomaly detection through on-line isolation Forest: An application to plasma etching," in *Proc. of 28th Annual SEMI Advanced Semiconductor Manufacturing Conference (ASMC)*, Saratoga Springs, NY, USA, May 2017.

[143] K. Emara, "Safety-Aware Location Privacy in VANET: Evaluation and Comparison," *IEEE Transactions on Vehicular Technology,* vol. 66, no. 12, pp. 10718-10731, December 2017.

[144] J. Zhou, J. Sun, P. Cong, Z. Liu, X. Zhou, T. Wei and S. Hu, "Security-Critical Energy-Aware Task Scheduling for Heterogeneous Real-Time MPSoCs in IoT," *IEEE Transactions on Services Computing,* vol. 13, no. 4, pp. 745 - 758, July - August 2020.

[145] A. W. Roscoe, "Temporal signature in the blockchain," [Online]. Available: https://blockchain.univ.ox.ac.uk/wp-content/uploads/2021/05/Bill-Roscoe-Temporal-Signature.pdf. [Accessed 24 March 2022].

[146] K. Wei, J. Li, M. Ding, C. Ma, H. H. Yang, F. Farokhi, S. JIn, T. Q. S. Quek and H. V. Poor, "Federated Learning With Differential Privacy: Algorithms," *IEEE Transactions on Information Forensics and Security,* vol. 15, pp. 3454-3469, April 2020.

[147] Z. Hou, H. Chen, Y. Li and B. Vucetic, "Incentive Mechanism Design for Wireless Energy Harvesting-Based Internet of Things," *IEEE Internet of Things Journal,* vol. 5, no. 4, pp. 2620-2632, December 2017.

[148] F. Li, H. Yao, J. Du, C. Jiang and Y. Qian, "Stackelberg Game-Based Computation Offloading in Social and Cognitive Industrial Internet of Things," *IEEE Transactions on Industrial Informatics,* vol. 16, no. 8, pp. 5444-5455, December 2019.

[149] B. Mokhtar and M. Azab, "Survey on Security Issues in Vehicular Ad Hoc Networks," *Alexandria Engineering Journal,* vol. 54, no. 4, pp. 1115-1126, December 2015.

[150] B. M. ElHalawany, A. A. A. El-Banna and K. Wu, “Physical-Layer Security and Privacy for Vehicle-to-Everything,” *IEEE Communications Magazine,* vol. 57, no. 10, pp. 84-90, October 2019.

[151] M. U. Aftab, M. Hussain, A. Lindgren and A. Ghafoor, “Towards A Distributed Ledger Based Verifiable Trusted Protocol For VANET,” in *Proc. of International Conference on Digital Futures and Transformative Technologies*, Islamabad, Pakistan, May 2021.

[152] M. Baza, A. Sherif, M. M. E. A. Mahmoud, S. Bakiras, W. Alasmary, M. Abdallah and X. Lin, “Privacy-Preserving Blockchain-Based Energy Trading Schemes for Electric Vehicles,” *IEEE Transactions on Vehicular Technology,* vol. 70, no. 9, pp. 9369-9384, July 2021.

[153] Y. Ai, M. Cheffena, A. Mathur and H. Lei, “On Physical Layer Security of Double Rayleigh Fading Channels for Vehicular Communications,” *IEEE Wireless Communications Letters,* vol. 7, no. 6, pp. 1038-1041, July 2018.

[154] D. Zhang, Y. Liu, L. Dai, A. K. Bashir, A. Nallanathan and B. Shim, “Performance Analysis of FD-NOMA-Based Decentralized V2X Systems,” *IEEE Transactions on Communications,* vol. 67, no. 7, pp. 5024-5036, March 2019.

[155] Q. Chen, H. Jiang and G. Yu, “Service Oriented Resource Management in Spatial Reuse-Based C-V2X Networks,” *IEEE Wireless Communications Letters,* vol. 9, no. 1, pp. 91-94, September 2019.

[156] X. Yue, Y. Liu, S. Kang, A. Nallanathan and Z. Ding, “Exploiting Full/Half-Duplex User Relaying in NOMA Systems,” *IEEE Transactions on Communications,* vol. 66, no. 2, pp. 560-575, February 2018.

[157] C. Lai, R. Lu, D. Zheng and X. Shen, “Security and Privacy Challenges in 5G-Enabled Vehicular Networks,” *IEEE Network,* vol. 34, no. 2, pp. 37-45, March/ April 2020.

[158] N.-P. Nguyen, T. Q. Duong, H. Q. Ngo, . Z. Hadzi-Velkov and L. Shu, “Secure 5G Wireless Communications: A Joint Relay Selection and Wireless Power Transfer Approach,” *IEEE Access,* vol. 4, pp. 3349-3359, June 2016.

[159] A. D. May, Traffic Flow Fundamentals., Englewood Cliffs, NJ, USA:: Prentice Hall, 1990.

[160] K. Abboud and W. Zhuang, “Stochastic Analysis of a Single-Hop Communication Link in Vehicular Ad Hoc Networks,” *IEEE Transactions*

on Intelligent Transportation Systems, vol. 15, no. 5, p. 2297=2307, October 2014.

[161] V. U. Prabhu and M. R. D. Rodrigues, "On Wireless Channels With M-Antenna Eavesdroppers: Characterization of the Outage Probability and ε-Outage Secrecy Capacity," *IEEE Transactions on Information Forensics and Security,* vol. 6, no. 3, pp. 853-860, September 2011.

[162] R. Durrett, Probability: theory and examples, Cambridge University Press, 2020.

[163] L. Wei, Y. Chen, D. Zheng and B. Jiao, "Secure performance analysis and optimization for FD-NOMA vehicular communications," *China Communications,* vol. 17, no. 11, pp. 29-41, November 2020.

[164] H. Alzer, "On some inequalities for the incomplete gamma function," *Mathematics of Computation,* vol. 66, no. 218, pp. 771-778, April 1997.

[165] Y. Tian, Y. Huo, C. Hu, Q. Gao and T. Jing, "A Location Prediction-based Physical Layer Security Scheme for Suspicious Eavesdroppers," in *Wireless Algorithms, Systems, and Applications*, L. Ma, A. Khreishah, Y. Zhang and M. Yan, Eds., Springer, Cham, May 2017, pp. 854 - 859.

[166] Y. Huo, Y. Tian, C. Hu and Q. Gao, "A Location Prediction-Based Helper Selection Scheme for Suspicious Eavesdroppers," *Wireless Communications and Mobile Computing,* p. December 2017.

[167] M. N. Tahir and M. Katz, "Performance evaluation of IEEE 802.11 p, LTE and 5G in connected vehicles for cooperative awareness," *Engineering Reports,* vol. Early View, October 2021.

[168] B. M. Eldowek, N. A. E.-S. Bauomy, E.-S. M. El-Rabaie, S. M. Abd El-Atty and F. E. A. El-Samie, "A survey of 5G millimeter wave, massive multiple-input multiple-output, and vehicle-to-vehicle channel measurements and models," *International Journal of Communication Systems,* vol. 34, no. 16, p. e4830, September 2021.

[169] Z. Su, Y. Wang, Q. Xu and N. Zhang, "LVBS: Lightweight Vehicular Blockchain for Secure Data Sharing in Disaster Rescue," *IEEE Transactions on Dependable and Secure Computing (Early Access),* March 2020.

[170] M. Aloqaily, I. Al Ridhawi and M. Guizani, "Energy-Aware Blockchain and Federated Learning-Supported Vehicular Networks," *IEEE Transactions on Intelligent Transportation Systems (Early Access),* pp. 1-12, August 2021.

[171] S. Disaboto and M. Roveri, “Incremental On-device Tiny Machine Learning,” in *Proc. of the 2nd International Workshop on Challenges in Artificial Intelligence and Machine Learning for Internet of Things*, Virtual Event, Japan, November 2020.

[172] S. King, “Primecoin: Cryptocurrency with Prime Number Proof-of-Work,” July 2013. [Online]. Available: https://primecoin.io/bin/primecoin-paper.pdf. [Accessed 22 October 2021].

[173] T. M. Fernandez-Carams and P. Fraga-Lamas, “Towards Post-Quantum Blockchain: A Review on Blockchain Cryptography Resistant to Quantum Computing Attacks,” *IEEE Access,* vol. 8, pp. 21091-21116, January 2020.

[174] E. Alkim, L. Ducas and T. Pöppelmann, “Post-quantum Key Exchange—A New Hope,” in *Proc. of the 25th USENIX Security Symposium*, Austin, Tx, Auguust, 2016.

[175] C. Wu, L. Ke and Y. Du, “Quantum resistant key-exposure free chameleon hash and applications in redactable blockchain,” *Information Sciences,* vol. 548, pp. 438-449, October 2020.

[176] T. Neudecker and H. Hartenstein, “Network Layer Aspects of Permissionless Blockchains,” *IEEE Communications Surveys & Tutorials,* vol. 21, no. 1, pp. 838-857, September 2018.

[177] P. Foytik, S. Shetty, S. P. Gochhayat , E. Herath and D. Tosh, “A blockchain simulator for evaluating consensus algorithms in diverse networking environments,” in *Proc. of Spring Simulator Conference*, Virginia, US, May 2020.

[178] K. Lei, Q. Zhang, J. Lou, B. Bai and K. Xu, “Securing ICN-Based UAV Ad Hoc Networks with Blockchain,” *IEEE Communications Magazine,* vol. 57, no. 6, pp. 26-32, June 2019.

[179] B. Cao, Y. Li, L. Zhang, S. Mumtaz, Z. Zhou and M. Peng, “When Internet of Things Meets Blockchain: Challenges in Distributed Consensus,” *IEEE Network,* vol. 33, no. 6, pp. 133-139, November - December 2019.

[180] J. Wang and H. Wang, “Monoxide: Scale Out Blockchain with Asynchronous Consensus Zones,” in *Proc. of 16th USENIX Symposium on Networked Systems Design and Implementation*, Boston, MA, USA, February 2019.

[181] A. Varga, “OMNeT++,” in *Modeling and Tools for Network Simulation*, Berlin, Heidelberg, Springer, 2010, pp. 35 - 39.

[182] “Crypto++® Library 8.6,” [Online]. Available: https://cryptopp.com/. [Accessed 26 March 2022].

[183] “Traffic Simulation with SUMO – Simulation of Urban Mobility,” in *Fundamentals of Traffic Simulation*, vol. 145, New York, Springer, 2010, pp. 269-293.

[184] C. Sommer, R. German and F. Dressler, “Bidirectionally Coupled Network and Road Traffic Simulation for Improved IVC Analysis,” *IEEE Transactions on Mobile Computing,* vol. 10, no. 1, January 2011.

[185] M. Abadi, P. Barham, J. Chen, Z. Chen, A. Davis, J. Dean, M. Devin, S. Ghemawat, G. Irving, M. Isard, M. Kudlur, J. Levenberg, R. Monga, S. Moore, D. G. Murray, B. Steiner, P. Tucker, V. Vasudevan, P. Warden, M. Wicke, Y. Yu, X. Zheng and G. Brain, “TensorFlow: A System for Large-Scale Machine Learning,” in *Proc. of 12th USENIX Symposium on Operating Systems Design and Implementation*, Savannah, GA, USA, November 2016.

[186] “Python.h,” [Online]. Available: https://github.com/python/cpython/blob/main/Include/Python.h. [Accessed 26 March 2022].

[187] O. S. Badarneh, P. C. Sofotasios, S. Muhaidat, S. L. Cotton, K. M. Rabie and N. Aldhahir, “Achievable Physical-Layer Security Over Composite Fading Channels,” *IEEE Access,* vol. 8, pp. 195772 - 195787, October 2020.

[188] A. U. Makarfi, K. M. Rabie, O. Kaiwartya, K. Adhikari, G. Nauryzbaye, X. Li and R. Kharel, “Toward Physical-Layer Security for Internet of Vehicles: Interference-Aware Modeling,” *IEEE Internet of Things Journal,* vol. 8, no. 1, pp. 443 - 457, July 2020.

Appendix A

Simulation Tools

Table A.1 lists the simulation tools used to validate results of the proposed solutions described in Chapter 3, Chapter 4 and Chapter 5. Each simulation tool is described below.

Chapter	Simulation Tools
Chapter 3	OMNeT++, VeINS, SUMO
Chapter 4	OMNeT++, VeINS, SUMO, Tensorflow (Python)
Chapter 5	OMNeT++, VeINS, SUMO, MATLAB

Table A.1: Simulation tools used for each of the proposed solution.

A.1 OMNeT++

OMNeT++ is a modular, C++ based framework primarily used for simulating communication networks [181]. It includes an integrated development and graphical runtime environment. It is an open-source tool available at https://www.omnetpp.org. The specific simulation parameters used to run Veins for each of the proposed solutions are listed in Simulated Performance Analysis section of each Chapter. The general parameters used in every solution are shown in Table A.2. The SHA-256 algorithm for generating cyptogrpahic blocks in OMNeT++ is supported by Crypto++ library [182].

Parameters	Values	Parameters	Values
Protocol	IEEE 802.11p	Encryption	SHA-256
Mobility model	Krauss	L	756 bytes
Beacon frequency	0.1 s	n_{hop}^{max}	6
α	3	R	250 m

Table A.2: Simulation Parameters.

A.2 Simulation of Urban Mobility (SUMO)

SUMO is a road traffic simulator which offers a socket-based interface to interact with external applications such as OMNeT++ [183]. It can be accessed as open-source at https://www.eclipse.org/sumo/. It allows to load maps, design routes, control speed limits and distances among nodes. Figure A.1 shows the simulation map of University of Sussex campus obtained from https://www.openstreetmap.org and used in experiments of the proposed solution.

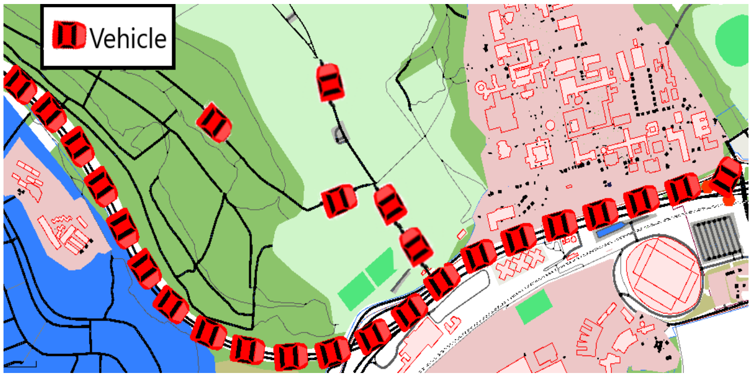

Figure A.1: Simulation map of University of Sussex campus.

A.3 Vehicles in Network Simulation (VeINS)

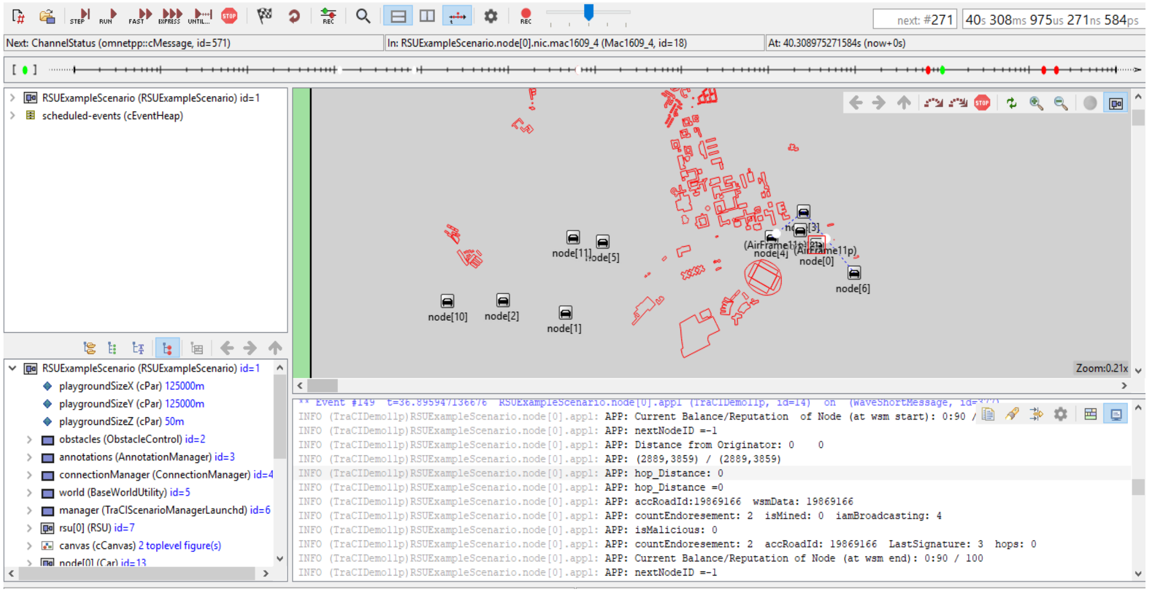

next: #271   40s 308ms 975us 271ns 584ps

Next: ChannelStatus (omnetpp::cMessage, id=571)   In: RSUExampleScenario.node[0].nic.mac1609_4 (Mac1609_4, id=18)   At: 40.308975271584s (now+0s)

RSUExampleScenario (RSUExampleScenario) id=1
scheduled-events (cEventHeap)

RSUExampleScenario (RSUExampleScenario) id=1
- playgroundSizeX (cPar) 125000m
- playgroundSizeY (cPar) 125000m
- playgroundSizeZ (cPar) 50m
- obstacles (ObstacleControl) id=2
- annotations (AnnotationManager) id=3
- connectionManager (ConnectionManager) id=4
- world (BaseWorldUtility) id=5
- manager (TraCIScenarioManagerLaunchd) id=6
- rsu[0] (RSU) id=7
- canvas (cCanvas) 2 toplevel figure(s)
- node[0] (Car) id=13

```
** Event #149  t=36.895947136676  RSUExampleScenario.node[0].appl (TraCIDemo11p, id=14)  on  (WaveShortMessage, id=
INFO (TraCIDemo11p)RSUExampleScenario.node[0].appl: APP: Current Balance/Reputation  of Node (at wsm start): 0:90 /
INFO (TraCIDemo11p)RSUExampleScenario.node[0].appl: APP: nextNodeID =-1
INFO (TraCIDemo11p)RSUExampleScenario.node[0].appl: APP: Distance from Originator: 0    0
INFO (TraCIDemo11p)RSUExampleScenario.node[0].appl: APP: (2889,3859) / (2889,3859)
INFO (TraCIDemo11p)RSUExampleScenario.node[0].appl: APP: hop_Distance: 0
INFO (TraCIDemo11p)RSUExampleScenario.node[0].appl: APP: hop_Distance =0
INFO (TraCIDemo11p)RSUExampleScenario.node[0].appl: APP: accRoadId:19869166  wsmData: 19869166
INFO (TraCIDemo11p)RSUExampleScenario.node[0].appl: APP: countEndoresement: 2  isMined: 0  iamBroadcasting: 4
INFO (TraCIDemo11p)RSUExampleScenario.node[0].appl: APP: isMalicious: 0
INFO (TraCIDemo11p)RSUExampleScenario.node[0].appl: APP: countEndoresement: 2  accRoadId: 19869166  LastSignature: 3  hops: 0
INFO (TraCIDemo11p)RSUExampleScenario.node[0].appl: APP: Current Balance/Reputation of Node (at wsm end): 0:90 / 100
INFO (TraCIDemo11p)RSUExampleScenario.node[0].appl: APP: nextNodeID =-1
```

Figure A.2: Screenshot of Veins running in OMNeT++.

VeINS is also an open-source framework for running vehicular network simulations in OMNeT++ integrated with SUMO [184]. The original VeINS setup simulates an accident upon which the oncoming nodes receive a message. It can be accessed at https://veins.car2x.org. Figure A.2 shows the Graphical User Interface (GUI) of VeINS running in OMNeT++.

A.4 Tensorflow (Python)

Tensorflow is an open-source library offering training and inference of deep neural networks [185]. It is available at www.tensorflow.org. It supports multiple languages including C++ and Python. The proposed solution of FL described in Chapter 4 is implemented using Tensorflow in Python. For PoFL based message dissemination, the execution of global model is simulated by calling Python function in OMNeT++, supported by Python.h library [186].

A.5 MATLAB

MATLAB is a software package which allows to develop algorithms and models mostly used for mathematical computations and iterative analysis. It is commonly used by researchers for PLS analysis [187] - [188]. Many special mathematical computations, such as gamma function $\Gamma(.)$ and exponential integral $E_1(.)$are available as built-in functions in MATLAB.

Appendix B

Code of blockchain implementation in OMNET++

```
//Define_Module(Block);

Block::Block(dataStruct transactionData){
    Amount = transactionData.Amount;
    Comment = transactionData.Comment;
    transactionIndex = 0;
    Payer = transactionData.Payer;
    Recver = transactionData.Recver;
    sPrevHash = "None";
    sCurrentHash = _CalculateHash();
};

std::string Block::GetHash(){
    return sPrevHash;
};

inline std::string Block::_CalculateHash() const {
    std::stringstream ss;
    ss << Amount << Comment << transactionIndex << Payer << Recver <<
sPrevHash;

    return sha256(ss.str());
};
```

Appendix C

Code Snippet of OMNeT++ integrating Python program

```
CPyObject pModule=PyImport_Import(pName);
PyObject *arg;
PyObject *result;
      if (pModule)
     {
          CPyObject pFunc= PyObject_GetAttrString(pModule, "getModel");
           if(pFunc && PyCallable_Check(pFunc))
           {
            arg=Py_BuildValue("(i,i,d,d,d)",hop+1,d_is,speed_data,dir,g
            ammai);
            result=PyObject_CallObject(pFunc, arg);
            score=PyFloat_AsDouble(result);
          }
      }
```

Appendix D

MATLAB Code for FD-NOMA

```
clc;
clear all;
for it=1:100000

%======================================================================
%           Full Duplex Non Orthogonal Multiple Access (NOMA) Simulation
%       Version 1: Encode only: Transmitter side,
%======================================================================
%       Contact: Ferheen Ayaz (f.ayaz@sussex.ac.uk)
%======================================================================
% n0.0f bits for transmit signal: 4 bits only - REMOVE '/25' for 100 bits
% as original SMT/TNY codes;
        TxBits_n = 100/25;
% distance from Sender i to Receiver j1, Receiver j2,Receiver j3,
Receiverj4
% Assuming maximum distance as 1000, minimum distance as 4, for
attenuation calculation purposes
        Dstjj1 = (1000-4).*rand + 4;
        Dstjj2 = (1000-4).*rand + 4;
        Dstjj3 = (1000-4).*rand + 4;
        Dstjj4 = (1000-4).*rand + 4;
        MaxDsttoveh = 1000;
        Dst=[Dstji Dstj1 Dstj2 Dstj3 Dstj4];
        Dst=sort(Dst);
        %Arranging for SIC
        Dstj1=Dst(4);
        Dstj2=Dst(3);
        Dstj3=Dst(2);
        Dstj4=Dst(1);

%Tx Power P=Pi=Pl
        TotPwrS_00 = 0.100;
        Pwrj1 = 0.100;
        Pwrj2 = 0.100;
        Pwrj3 = 0.100;
        Pwrj4=0.100;
        eta=0.1; %Self-interference co-efficient
         alpha=-3; %Path loss

%======================================================================
    %%%Create random binary messages/signals from Sender
%======================================================================
% signal of 'n' bits from Sender
% signal of 'n' bits from j2 as interference
% signal of 'n' bits from j3 as interference
% signal of 'n' bits from j4 as interference
% jth vehicle receives interference from j+1th user
% Correct (actual) binary messages of 'TxBits_n' bits length:
% equal probability of 0 and 1 in every bit;
%   'rand'  generates numbers in [0 to 1], uniformally distributed;
%   Mean is 0.5
%
        Sgni = rand(1,TxBits_n) > 0.5;
        Sgnj1 = rand(1,TxBits_n) > 0.5;
        Sgnj2 = rand(1,TxBits_n) > 0.5;

        Sgnj3 = rand(1,TxBits_n) > 0.5;
        Sgnj4 = rand(1,TxBits_n) > 0.5;
%======================================================================
    %%%Superposition Encoding
%======================================================================
        Enc_Xi = sqrt(TotPwrS_00)*Sgni;
        Enc_Xj1 = sqrt(Pwrj1)*Sgnj1;
        Enc_Xj2 = sqrt(Pwrj2)*Sgnj2;
        Enc_Xj3 = sqrt(Pwrj3)*Sgnj3;
        Enc_Xj4 = sqrt(Pwrj4)*Sgnj4;

%======================================================================
    %%%Received signals for all vehicles
%======================================================================
% Adding Gaussian Noise: use 'randn' instead of 'rand':
```

```
%     'randn' generates numbers in [-Inf,+Inf], normally distributed
(Gaussian);
%   Mean is zero, but with strong concetration in [-1 to +1];
%   'rand'  generates numbers in [0 to 1], uniformally distributed;
%   Mean is 0.5
% Noise


        Noisej1 = randn(1,TxBits_n)/NoiseReduc_0;
        Noisej2 = randn(1,TxBits_n)/NoiseReduc_0;
        Noisej3 = randn(1,TxBits_n)/NoiseReduc_0;
        Noisej4 = randn(1,TxBits_n)/NoiseReduc_0;

% Channel Coefficient
          hj1= sqrt((Dstj1.^(-1.*alpha)).*
        (randn(1,TxBits_n)+1i*randn(1,TxBits_n));
         hj2= sqrt((Dstj2.^(-1.*alpha)).*
        (randn(1,TxBits_n)+1i*randn(1,TxBits_n));
        hj3= sqrt((Dstj3.^(-1.*alpha)).*
        (randn(1,TxBits_n)+1i*randn(1,TxBits_n));
         hj4= sqrt((Dstj4.^(-1.*alpha)).*
        (randn(1,TxBits_n)+1i*randn(1,TxBits_n));


%======================================================================
    %%%Signal received by each vehicle
%======================================================================
RxSgnj5 = Enc_Xi.*hji + Noisej1 + (Enc_X1.*hj1)+ (Enc_X2.*hj2)+
(Enc_X3.*hj3) + (Enc_X4.*hj4)+ (Enc_X5.*hj5) +SI;
        RxSgnj4 = Enc_Xi.*hji + Noise + (Enc_X1.*hj1)+ (Enc_X2.*hj2)+
(Enc_X3.*hj3) + (Enc_X4.*hj4) +SI;
        RxSgnj3 = Enc_Xi.*hji + Noisej2 + (Enc_X1.*hj1)+ (Enc_X2.*hj2)+
(Enc_X3.*hj3) +SI;
        RxSgnj2 = Enc_Xi.*hji + Noisej3 + (Enc_X2.*hj2)+
(Enc_X1.*hj1)+SI;
        RxSgnj1 = Enc_Xi.*hji + Noisej4 + (Enc_X1.*hj1)+SI;
%======================================================================
```